INEautc
Tracking Number AUTC
No s#
Under

Performance Analysis of the Dowling Multi-lane Roundabouts in Anchorage, Alaska

By
Ming Lee
Alaska University Transportation Center
Institute of Northern Engineering
University of Alaska Fairbanks

June 30, 2010

Table of Contents

List of Tables

List of Figures

SUMMARY

The first multi-lane roundabouts in Alaska were constructed in 2004 at the ramp terminals of the Dowling/New Seward Highway interchange in Anchorage. The Dowling roundabouts are currently operating at capacity for a short period of time during the evening peak hours. The Dowling Road roundabouts offer a unique opportunity for traffic engineers to study the operating capacity of multi-lane roundabouts in the US. In addition, the safety performance of these multi-lane roundabouts has not been examined either. This study was designed to measure the operating performance and safety performance of the multi-lane roundabouts. We studied the operation of the roundabouts in both summer and winter operating conditions.

The data collection effort was initiated in the winter of 2008. The winter roundabout operation was video-taped on Wednesday, Dec. 17th, Thursday, Dec. 18th, and Friday, Dec. 19th in 2008. Data collection for the summer evening peak hours was completed on Tuesday, May 12th; Wednesday, May 13th; and Thursday, May 14th in 2009.

After data collection, turning movements as well as queue length and delay at the roundabouts during both the winter and summer peak hours were counted from the video records. The turning movement data were analyzed using software RODEL and SIDRA. The field-measured delay and queue length were compared to the numbers predicted by the two software packages and other available roundabout design guides.

Based on the data extracted from the video records, we found that the extended queue on the EB approach of the west roundabout was a result of the unbalanced flow pattern at the roundabouts, in which the EB entering flow rate was substantially higher than the other three entrance approaches. The unbalanced flow pattern also created a high circulating flow in front of the NB approach of the east roundabout. The high circulating flow for the NB approach explains why this approach of the east roundabout had low capacity and high delay and queue values.

After comparing our field data with those from roundabouts in the UK, Germany, and Australia, we found that the performance of the Dowling roundabout in terms of entry flow and circulating flow are slightly lower than those in the UK and Australia. But, the Dowling numbers are slightly higher than those from Germany. In the future, applying the Dowling data using the Germany models may be tested to see if the model produce better results than those used in the UK and Australia.

We then analyzed the data with RODEL and SIDRA. It is noted that our RODEL and SIDRA models were un-calibrated. The purpose of the analysis is to investigate how well RODEL and SIDRA can predict, in the project planning stage, the eventual field conditions. The results of our analysis show that the un-calibrated RODEL and SIDRA models both overestimate the capacities for the queued approaches. RODEL's capacity estimates are closer to the field measurements than SIDRA's.

For queue length and delay estimation, version 1.0 of RODEL can not model the queue length and delay of roundabouts in presence of right-turn channels. When only the delay and queue caused by the entering flow (without the right turn movements) are considered, RODEL overestimated delays and queue lengths for most approaches. SIDRA's estimation of queue length and delay appears to be more reasonable than RODEL's. However, when compared with field values, SIDRA underestimates the delay and queue length for the two roundabouts.

To find out potential measures for the reduction of the queue and delay at the EB approach of the west roundabout, we designed a series of VISSIM simulation runs to study how much reduction in vehicle flow on the EB entrance approach will result in an acceptable level of delay and queue on this approach. The simulation results show that a reduction of the EB upstream flow at 70% of the original flow can result in an acceptable level of delay and queue length at the EB approach of the west roundabout.

We also simulated the effect of No Turn On Red (NTOR) from the NB Old Seward Highway to EB Dowling Road. The results of the simulation show that NTOR does not appear to be an effective measure to reduce the queue length and delay at the EB approach of the west roundabout. The minimal amount of delay reduction can not justify for the large amount of increase in delay that the NB right turn movement at the Old Seward/Dowling would suffer, if turning on red from this approach were to be prohibited.

A separate investigation effort intended for the analysis of drivers' yielding behavior (i.e., yielding to pedestrians) was also carried out. Drivers' responses to investigators acting as pedestrians at the crosswalks of the Dowling multi-lane roundabouts during summer evening peak hours were video-taped. Although we carried out the plan as intended, the traffic condition was different from what we expected. Our investigation ended after involving in a near collision.

Based on our experience in the field, we found that the high traffic volume combined with long vehicle queue and delays at the entrance created realistic risk for pedestrians crossing the roundabouts during the peak traffic conditions (i.e., 15 to 20 minutes during the evening peak hour). We found that drivers would slow down for pedestrians who had already on the crosswalk in motion. But, very rarely would drivers react to pedestrians who stood still by the side of the road. We recommend that an emphasis be placed on designing exit lanes to facilitate active yielding for pedestrians in the design of roundabouts in the future.

Finally, vehicular accident records before and after the roundabout installation at the study site were retrieved for analysis. Based on the crash statistics of the SB terminal and the NB terminal from 1998 to 2007, we found that there were more events in every crash category (i.e., Property damage only, minor injury, and major injury) after the roundabouts were in operation. But, we also found that the crash rates had been decreasing every year after 2004, suggesting that drivers were learning to safely negotiate the roundabouts. Because we have only three years of data after the roundabout

operation, we need to wait for a few more years before a fair assessment of roundabout crash rate in comparison with traffic signals can be made.

1 INTRODUCTION

1.1 Problem Statement

The first multi-lane roundabouts in Alaska began operation in 2004 at the ramp terminals of the Dowling Road and New Seward Highway interchange in Anchorage (Figure 1). The roundabouts were intended to provide a solution to ease traffic problems that Anchorage commuters had faced at the location. It was estimated that the project saves approximately $1 million in reduced construction costs and associated electricity costs of typical signalized intersections.

Figure 1 East Dowling Road Roundabouts (Source: Google Maps®)

Currently, during most of the day, the Dowling roundabouts is operating smoothly without delay at the entrance. However, for approximately 15 to 20 minutes during the evening peak hour (i.e., from 5 to 6 pm), the roundabouts are operating at capacity with queues of more than 5 vehicles on three (i.e., eastbound, southbound, and northbound) of the four entrance approaches during the entire capacity-saturated period. On the eastbound entrance approach, the queue can reach for over 1,600 feet, occasionally blocking the upstream signalized intersection between the Old Seward Highway and East Dowling Road (see Figure 2 and **Figure** 3). The extended queues prompted the Alaska Department of Transportation and Public Facilities (AK DOT & PF) to initiate this research effort to investigate the performance of the Dowling roundabouts.

Figure 2 Picture showing the queue on the eastbound entrance approach (The camera is approximately 1,200 feet from the entrance of the west roundabout)

Figure 3 Picture showing the queue from the eastbound entrance approach blocking the upstream intersection at Old Seward Highway/E. Dowling Road

The National Cooperative Highway Research Program (NCHRP) in 2007 published a report (Report 572) on roundabout performance and safety analysis in the US. The report noted that there had been a lack of data from capacity-saturated multilane roundabouts in the US for performance analysis. The Dowling Road roundabouts, completed after the data collection effort for the NCHRP research, offer the much needed opportunity for traffic engineers to study the performance of multi-lane roundabouts in the US, and to see how the performance measurements predicted by software applications compare to the results in the field. The results of such an analysis can assist the Alaska Department of Transportation and Public Facilities (AKDOT & PF) in determining whether, where and how to construct additional multi-lane roundabouts in the future.

1.2 Study Objectives

The followings are the original objectives defined by the traffic engineers of the AKDOT & PF for this project.

1. Obtain video records of the roundabouts operating at peak traffic conditions in summer and winter
2. Count turning movements of the roundabouts during the evening peak hour
3. Measure average speed at various points at the roundabouts
4. Measure the length of each stopped and rolling queues at the roundabouts
5. Obtain roundabout geometric data from as built drawings
6. Analyze the turning movements with two existing software SIDRA and RODEL
7. Compare the software prediction with the field-measured speed and queue length
8. Analyze the differences between summer and winter roundabout operations
9. Analyze pedestrian safety at the roundabouts
10. Analyze vehicular safety at the roundabouts

1.3 Research Plan

It was originally proposed to first video tape the roundabout operation during the evening peak hours on three weekdays in the summer of 2008. After the collection and analysis of the summer data, the same effort would be repeated again on three weekdays in winter. However, due to delay in project initiation, fund for the project work was not available until the end of summer 2008, when it was too late to collect the summer data. Instead, the data collection effort was initiated in the winter of 2008. The winter roundabout operation was video-taped on Wednesday, Dec. 17th, Thursday, Dec. 18th, and Friday, Dec. 19th in 2008. Data collection for the summer evening peak hours was completed on Tuesday, May 12th; Wednesday, May 13th; and Thursday, May 14th in 2009.

After data collection, turning movements as well as queue length and delay at the roundabouts during both the winter and summer peak hours were counted from the video records. The turning movement data were analyzed using software RODEL and SIDRA. The field-measured delay and queue length were compared to the numbers predicted by the two software packages and other available roundabout design guides.

A separate investigation effort intended for the analysis of drivers' yielding behavior (i.e., yielding to pedestrians) was also carried out. Drivers' responses to investigators acting as pedestrians at the crosswalks of the Dowling multi-lane roundabouts during summer evening peak hours were video-taped and analyzed.

Finally, vehicular accident records before and after the roundabout installation at the study site were retrieved for analysis.

2 Data Collection

Prior to the actual field data collection in the winter of 2008, preliminary research on data collection equipments led to the decision that pole-mounted video camera systems were to be used to automatically record and count the turning movements at the roundabouts. A purchase order was indeed issued by the University of Alaska Fairbanks (UAF) to purchase the pole-mounted automatic traffic counter made by the company Mio Vision. However, the company insisted that a standard liability requirement requested by UAF be waived. After consulting with the legal experts of the UAF purchasing office, the purchase order was withdrawn, because the consequences of waiving the liability were deemed too significant in the event of a pole failure. It was then determined that regular digital camcorders mounted on high grounds were to be used to record the turning movements.

2.1 Winter Data Collection

Winter roundabout operation was video-taped on Dec. 17th (Wednesday), Dec. 18th (Thursday), and Dec. 19th (Friday) in 2008. Six Camcorders were instrumented. The camcorder locations are shown in Figure 4. Camcorder A and C were mounted at vantage points (i.e., on the high ground by the Seward Highway) to record all of the circulating and entering vehicles at both roundabouts. Four camcorders (B, D, E, and F) were mounted at the individual queued approaches to record the back of queue. The queued approaches were: 1) the North Bound (NB) approach of the east roundabout; 2) the South Bound (SB) approach of the west roundabout; and 3) the East Bound (EB) approach of the west roundabout. Because of the very long queues at the EB approach of the west roundabout, two camcorders (E and F) were mounted on the roadside of East Dowling Road trying to capture the back of queue.

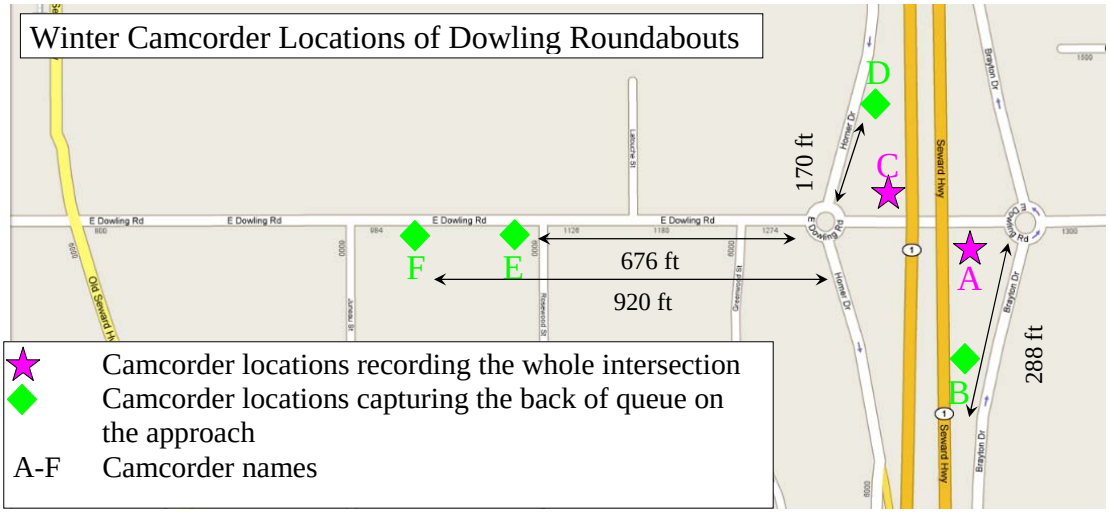

Figure 4 Locations of camcorders used for data collection in winter

2.2 Summer Data Collection

After examining the videos of the winter data, the results showed that the turning movements at both roundabouts were fully captured, because cameras A and C were mounted at vantage points of approximately 15 to 20 feet above ground. For the EB entrance approach, the total queue length in winter occasionally exceeded 1,400 feet from the roundabout entrance. When the EB queue extended beyond the location of camera F, the camera was turned backwards to capture the end of queue. Although the approximate length of the EB queue in feet can be estimated from the markers placed by the side of the road, the extensive length of the queue and the poor lighting conditions in winter made counting exact number of vehicles in the queue difficult. The similar situation also occurred to the NB entrance approach. After analyzing the winter data, the deficiency of the data collection scheme was noted and additional cameras were instrumented for data collection in the summer.

The data collection scheme for the summer is shown in Figure 5. Camcorders A and B mounted on the high ground recorded all of the circulating and entering vehicles of both roundabouts. Camcorders C, D and E were set to record the back of queues on the NB approach of the west roundabout. Camcorders F, G and H were set for the back of queues on the SB approach of the east roundabout. Eight camcorders (I, J, K, L, M, N, O, and P) were used for the back of queues on the west approach of the west roundabout. In addition, camcorder Q was mounted in the southeast corner of the west upstream signalized intersection of E Dowling Road and Old Seward Highway. It recorded the turning movements at the signalized intersection.

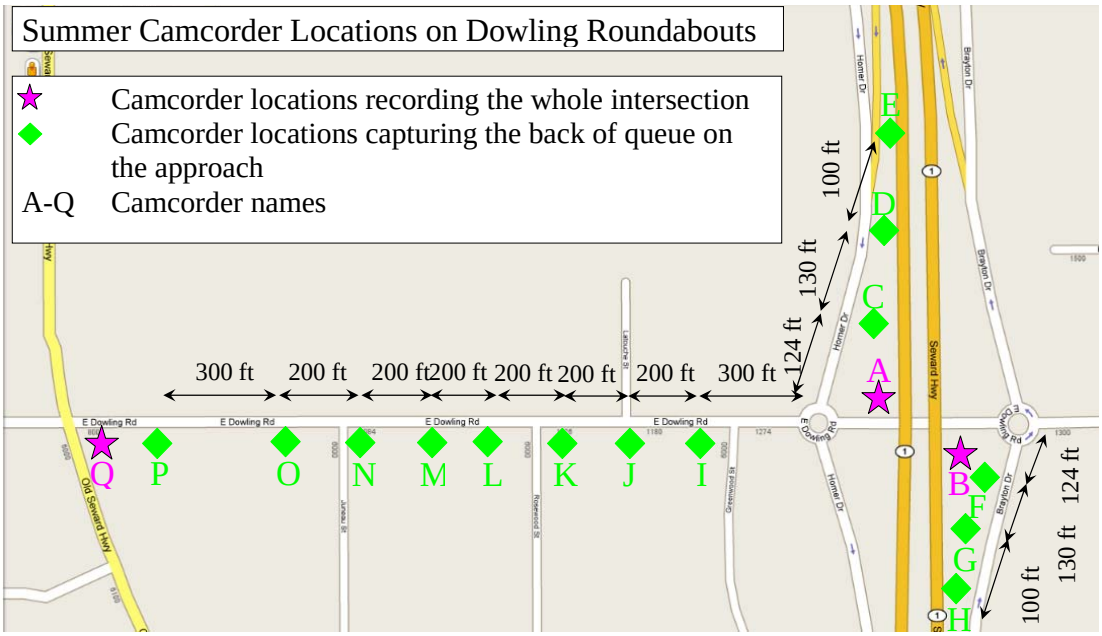

Figure 5 Locations of camcorders used for data collection in the summer

3 DATA EXTRACTION

Data required for roundabout performance analysis were extracted from the video records and other supplemental data such as the actual design plan from AK DOT & PF and the aerial photos from Google Maps. The extracted data can be divided into three categories: geometry data, flow rate data, and queue and delay data.

Because the purpose of the analysis is to study roundabout capacity, delay and queue formation, flow rate data used for the analysis were based on the days on which the queue duration and the maximum queue length were the longest. That is, we analyzed the data collected on Dec. 18th, 2008, on which the maximum queue length was the longest of all three winter data collection days. Similarly, we used data from May 13th, 2009 for the summer data analysis.

3.1 Geometric Data

Geometric data critical to roundabout performance analysis include lane configuration, entry width, approach half width, effective flare length, inscribed circle diameter, entry angle and entry radius (see Figure 6 for an illustration of the variables). It is noted that the original design AutoCAD drawing obtained from AK DOT & PF shows significant difference from the current layout of the roundabouts in the field. The values for the geometric variables used in the analysis were determined by overlaying the design plan AutoCAD drawing with the aerial photos from Google Maps at the same scale. The measurements of the geometric variables were then taken from the overlaid map based on the actual pavement markings and delineators identified in the aerial photos.

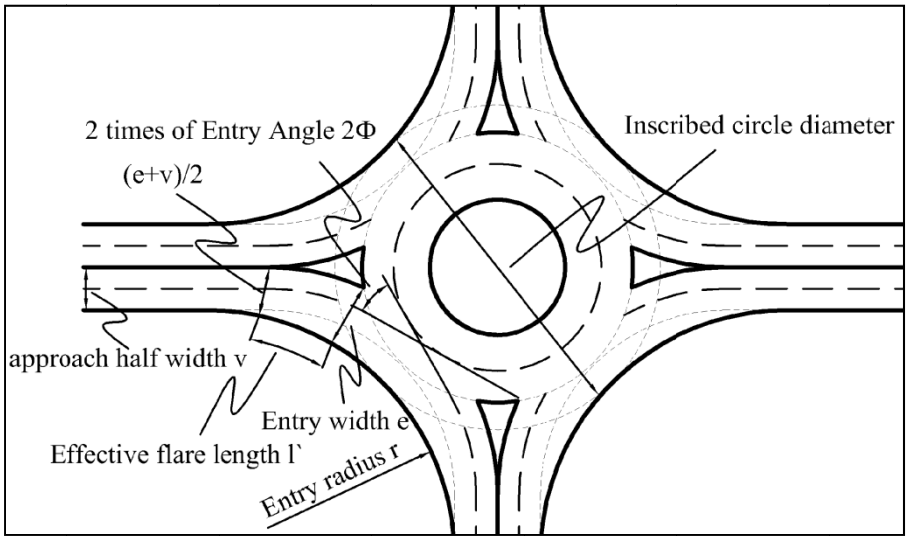

Figure 6 Illustration of roundabout geometric variables

Figure 7 and Figure 8 show the effective geometry of the roundabouts. **Table** 1 summarizes the values of the geometric variables.

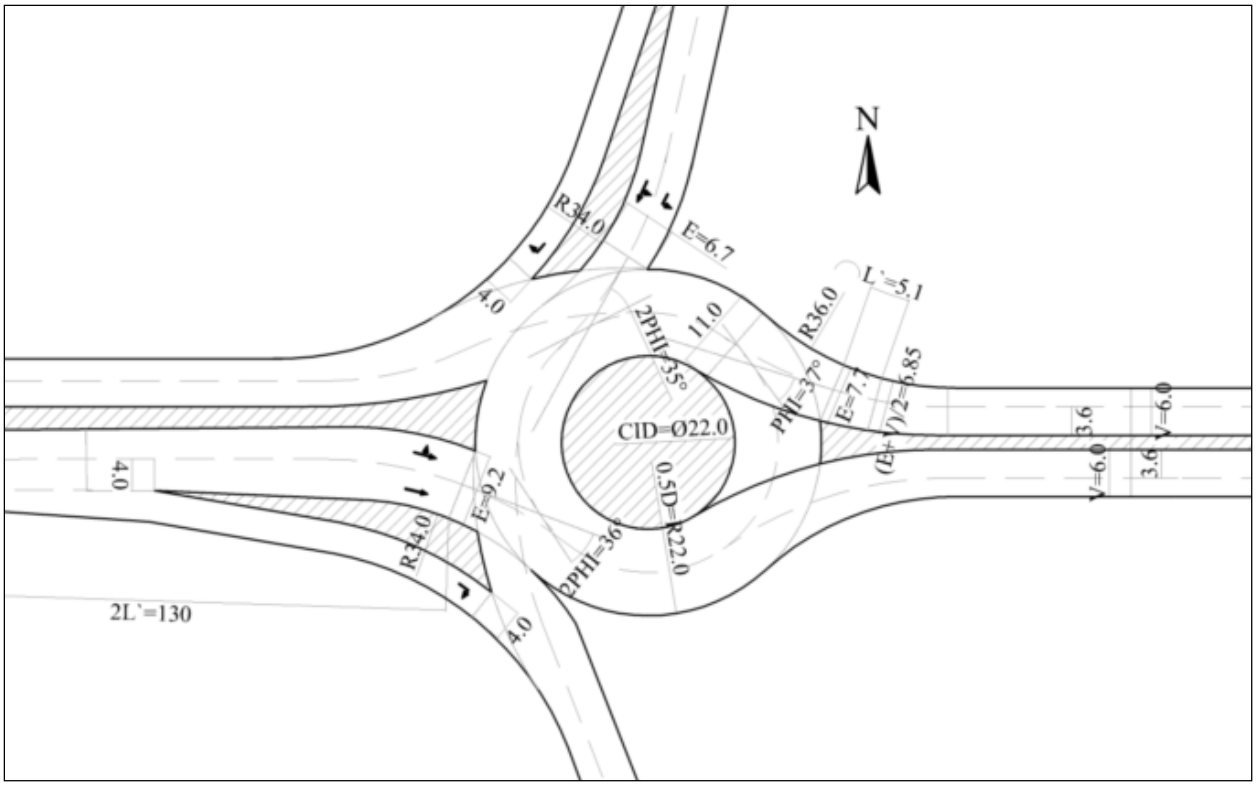

Figure 7 Effective geometry of the west roundabout

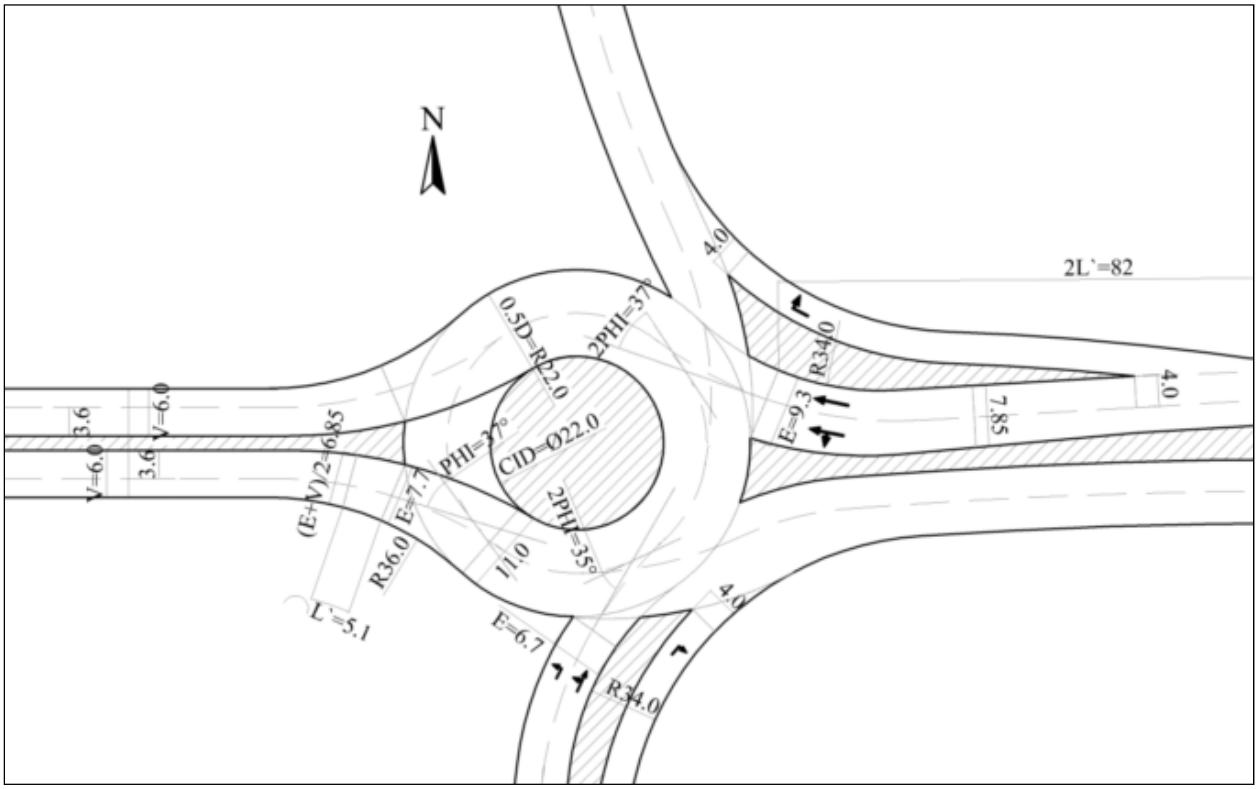

Figure 8 Effective geometry of the east roundabout

Table 1 Effective geometric measurement of the Dowling roundabouts

			West Roundabout			East Roundabout		
EFFECTIVE GEOMETRY	ABBREVIATION	UNITS	WB	SB	EB	EB	NB	WB
Entry width	E	meters	7.8	6.7	9.2	7.7	6.7	9.3
Flare Length	L`	meters	5.2	0	65	5.1	0	41
Half width	V	meters	6	6.7	6.4	6	6.7	6.4
Entry radius	R	meters	36	34	34	36	34	34
Entry angle	PHI	degrees	37	17.5	26.5	37	17.5	18.5
Diameter	D	meters	44	44	44	44	44	44

3.2 Flow Rate Data

Flow rate data (i.e., number of vehicles per analysis time period) used for the analysis include turning movements, entering flow rate, circulating flow rate, and approach capacity. Turning movements include all movements at the two roundabouts, including the right turn movements that bypass the roundabouts through right turn channels. The entering flow rates are the movements that actually enter the inside circles of the roundabouts per analysis period. The approach capacity is the entering flow rate when there are persistent queues of more than 5 vehicles on each lane of the approach during an entire analysis time period. The circulating flow rates in front of the approach are the sum of flow rates passing the approach from upstream approaches.

According to field observation, only three approaches in the two Dowling Roundabouts had persistent queues in both winter and summer. They are the EB and SB approaches of the west roundabout, and the NB approach of the east roundabout. We measured the capacity of an approach by counting the entering flow in each one-minute period, when the queues on the approach are more than 5 vehicles during the entire minute. For each individual minute that had queues greater than 5 vehicles on each lane, we also measured the circulating flow (i.e., number of vehicles passing in front of the approach).

The results of turning movement measurement are presented in Table 2.

Table 2 Turning Movements Data

Winter (December 18, 2008)				
West Roundabout				
Entering Approach	**Right Turn**	**Through**	**Left Turn**	**Total**
WB	0	495	180	675
SB	110	143	640	893
EB	189	922	0	1111
Total				**2679**
East Roundabout				
Entering Approach	**Right Turn**	**Through**	**Left Turn**	**Total**
EB	0	1305	257	1562
NB	212	119	194	525
WB	199	481	0	680
Total				**2767**
Summer (May 13, 2009)				
West Roundabout				
Entering Approach	**Right Turn**	**Through**	**Left Turn**	**Total**
WB	0	581	217	798
SB	116	146	733	995
EB	214	966	0	1180
Total				**2973**
East Roundabout				
Entering Approach	**Right Turn**	**Through**	**Left Turn**	**Total**
EB	0	1370	3029	1699
NB	194	108	236	538
WB	195	562	0	757
Total				**2994**

Table 2 shows that the EB entrance approach of the west roundabout had the highest volume of all three entrance approaches at this roundabout. The high volume on the EB approach of the west roundabout explains why the EB queue is the longest of all three queued approaches. In addition, we also found that the total movements at both the roundabouts in the summer were higher than those in winter. The higher total numbers of movements in summer explains why we observed longer queues on the EB approach of the west roundabout in summer than winter.

3.2.1 Demand Flow Rate Data

To gain insights to the timing of queue formation at the roundabout entrances, we performed an analysis of the demand flow rates at the three queued entrances. Demand flow rate is approach-based and is defined as the number of vehicles that entered the roundabout in a 5-minute period plus the number of vehicles in the queue waiting to enter from the approach at the end of the period. With the demand flow rates, we can assess the temporal distribution of vehicle arrival during the peak hour. **Table** 3 and**Table 4** show the five-minute demand flow rates at the two roundabouts in summer. The shaded cells of the tables identify the peak 15-minute periods at the roundabouts.

Table 3 Summer (May 13th) Five Minute Demand Flow Rates at the West Roundabout

Direction	SB Demand Flow			EB Demand Flow			WB Demand Flow		
Time (pm)	Entering (Turning movements)	Queue	SB Total	Entering (Turning movements)	Queue	EB Total	Entering (Turning movements)	Grand Total	Percentage
5:00	86	10	96	91	43	134	80	310	**8.48%**
5:05	109	3	112	108	68	176	56	344	**9.41%**
5:10	85	25	110	113	75	188	90	388	**10.62%**
5:15	104	10	114	71	94	165	67	346	**9.47%**
5:20	105	2	107	85	72	157	69	333	**9.11%**
5:25	81	2	83	110	69	179	57	319	**8.73%**
5:30	75	1	76	120	55	175	61	312	**8.54%**
5:35	90	3	93	91	79	170	61	324	**8.87%**
5:40	70	1	71	115	36	151	63	285	**7.80%**
5:45	78	1	79	101	6	107	67	253	**6.92%**
5:50	56	4	60	84	14	98	59	217	**5.94%**
5:55	56	1	57	91	7	98	68	223	**6.10%**
Total	**995**	**63**	**1058**	**1180**	**618**	**1798**	**798**	**3654**	**100.00%**
									Peak Hour Factor =0.84

Table 4 Summer (May 13th) Five Minute Demand Flow Rates at the East Roundabout

Direction	NB Demand Flow			WB Demand Flow			EB Demand Flow		
Time (pm)	Entering (Turning movements)	Queue	NB Total	Entering (Turning movements)	Queue	WB Total	Entering (Turning movements)	Grand Total	Percentage
5:00	50	4	54	77	2	79	120	253	**8.30%**
5:05	28	11	39	56	0	56	160	255	**8.36%**
5:10	59	1	60	73	2	75	146	281	**9.22%**
5:15	46	2	48	74	1	75	144	267	**8.76%**
5:20	36	7	43	56	3	59	148	250	**8.20%**
5:25	43	7	50	59	0	59	159	268	**8.79%**
5:30	44	8	52	60	0	60	142	254	**8.33%**
5:35	42	3	45	62	0	62	125	232	**7.61%**
5:40	45	9	54	59	0	59	151	264	**8.66%**
5:45	46	6	52	60	0	60	153	265	**8.69%**
5:50	66	2	68	48	3	51	111	230	**7.54%**
5:55	41	3	44	68	1	69	117	230	**7.54%**
Total	546	63	609	752	12	764	1676	3049	**100.00%**
									Peak Hour Factor =0.95

The 15-minute peak traffic occurred from 5:05 to 5:20 pm at both roundabouts. At the west roundabout the peaking is more pronounced in that approximately 30% of the hourly demand flow occurred during the peak 15-minutes, while the same peak 15-minute accounts for approximately 26% of the total demand flow at the east roundabout.

3.2.2 Capacity vs. Conflicting Flow

Capacity and conflicting flow measurements are presented in **Figure** 9 to 14. Note that the number of data points on each figure depends on the number of minutes in which the queues on the approach were persistently more than 5 vehicles during the entire minute.

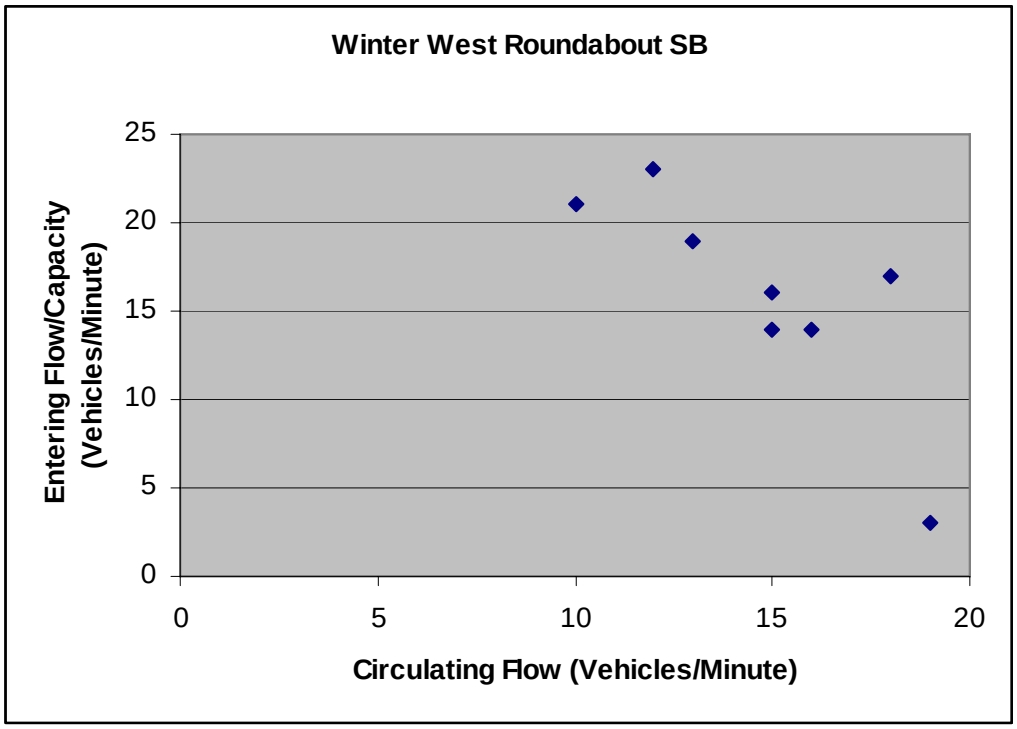

Figure 9 Winter Capacity and Circulating Flow for the SB approach of the West Roundabout

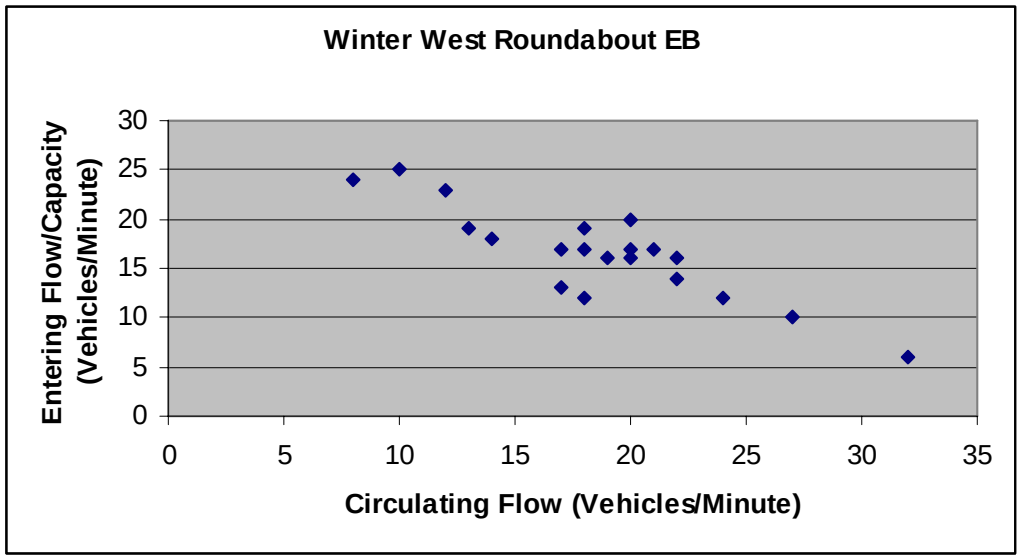

Figure 10 Winter Capacity and Circulating Flow for the EB approach of the West Roundabout

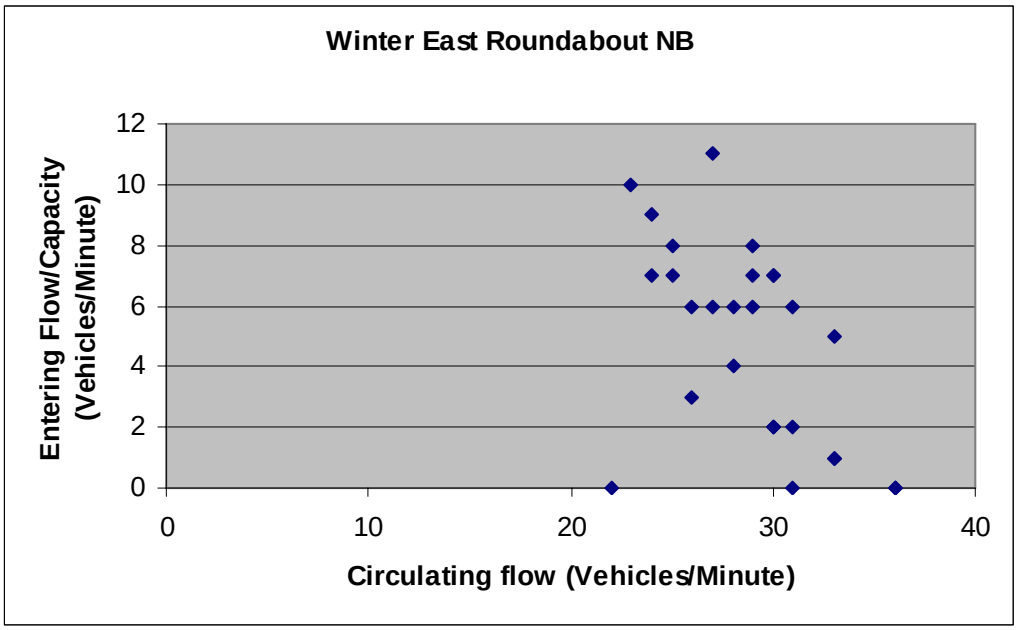

Figure 11 Winter Capacity and Circulating Flow for the NB approach of the East Roundabout

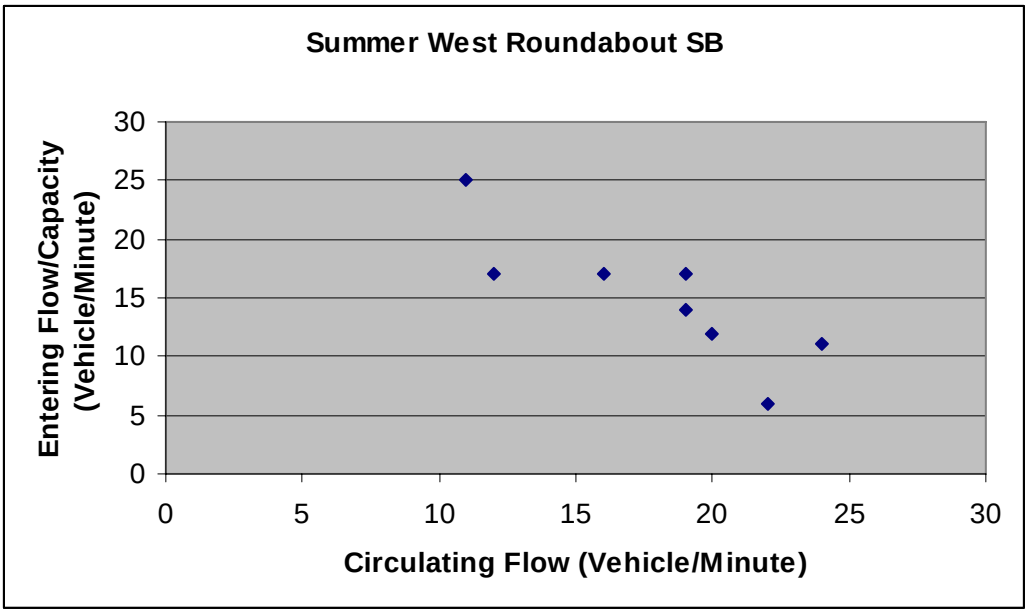

Figure 12 Summer Capacity and Circulating Flow for the SB approach of the West Roundabout

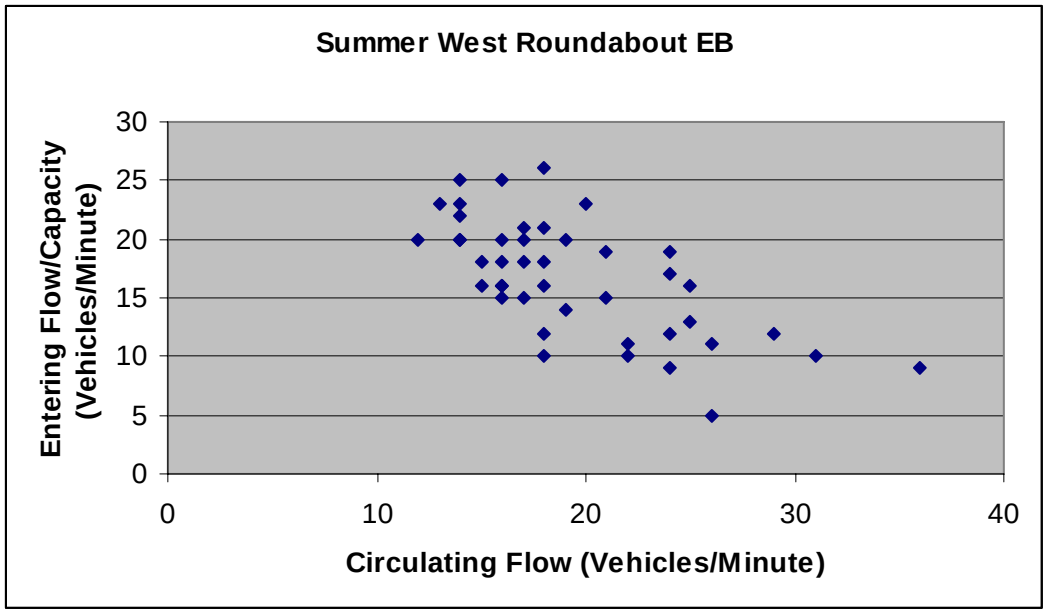

Figure 13 Summer Capacity and Circulating Flow for the EB approach of the West Roundabout

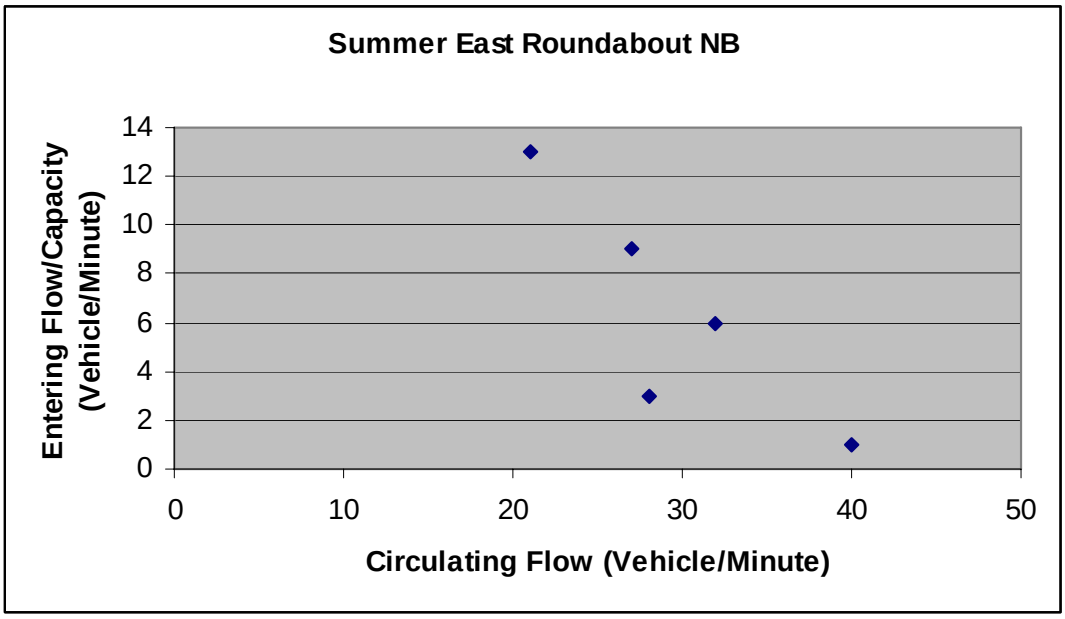

Figure 14 Summer Capacity and Circulating Flow for the NB approach of the East Roundabout

Figures 9 to 14 show that the EB entrance approach of the west roundabout in both the winter and summer had the most minutes with queues longer than 5 vehicles. However, the EB approach did not necessarily have high circulating flow. Most of the queues on the EB entrance approach faced circulating flows in the range between 10 and 20 vehicles per minutes. The finding suggested that the queue on the EB approach is related to high

demand flow rate (i.e., see the turning movement flows in **Table** 2) rather than circulating flow rate.

The NB entrance of the east roundabout faced the higher circulating flow than the EB and SB approaches of the west roundabout. In both winter and summer, the NB entrance never had circulating flow lower than 20 vehicles per minute. The high circulating flow in front of the NB entrance reduced the number of acceptable gaps for the queued vehicles, resulting in lower entering flow/capacity than the other two entrance approaches.

Another interesting pattern of the circulating flow and capacity relationship is that the NB approach had more minutes with queues of more than 5 vehicles in winter than summer. In winter, we observed 4 minutes in which no queued vehicle was able to enter the roundabout from the NB entrance approach. In summer, only 5 individual minutes had queues of at least 5 vehicles. Based on the field observation, the difference in the number of capacity-saturated minutes between winter and summer was likely due to the lighting and driving condition in winter. In winter, there is no daylight at 5 pm and the pavement condition is less favorable than summer. These winter driving conditions (i.e., short sight distance and long headway between vehicles) appeared to have made drivers' average acceptable gap larger than that in the summer. Thus, the NB queues dissipated slower in winter than in summer.

3.3 Queue and Delay Data

Queue and delay data include field-measured queue length in vehicles and delay in seconds. Delay is the difference between the travel time that a vehicle traverses a certain distance in a queued condition and the travel time over the same distance in a free flow condition. To measure the field delay, a vehicle on each lane of a queued approach was randomly sampled for each minute during the evening peak hour (i.e., 5 to 6 pm). The actual travel time of this sampled vehicle from a point behind the back of the queue to its entering the roundabout (i.e., rear bumper leaving the yield line) was measured. The assumption of traveling at the speed limit was used to calculate the free flow travel time over the same distance. With the delay in seconds measured for all randomly sampled vehicles, the average delay and maximum delay over the 60 minute period were calculated.

The queue length was measured at the time when a randomly sampled vehicle arrived at the back of the queue. Table 5 summarizes the field-measured delay and queue length. The average delay per queued vehicle was derived by dividing the total delay in seconds with total number of queued vehicles. Note that the WB approach of the east roundabout never had queue of more than 5 vehicles during any minute of the evening peak hour.

The approach based measurements in Table 5 were created for comparison with RODEL outputs, which are approached-based (the comparison is presented in a later section). The approach-based average delay is the average of the left lane value and right lane values. The approach-based maximum delay is the maximum between the left lane value

and the right lane value. The average queue of an approach is the sum of the average queue length of the left and right lanes. The maximum queue length of an approach is the sum or the maximum length of the left and right lanes.

Table 5 Field-**Measured Delay and Queue Length**

Season	Roundabout	Approach	Measurement	Lane-based measurement		Approach-based measurement
				Left lane	Right lane	
Winter	West	SB	Ave Delay (sec)	17	18	17.5
			Max Delay (sec)	88	83	88
			Ave Queue (veh)	2	3	5
			Max Queue (veh)	10	11	21
			Average Delay per Queued Vehicle (sec/veh)	7.32	6.96	7.13
	West	EB	Ave Delay (sec)	51	35	43
			Max Delay (sec)	171	113	171
			Ave Queue (veh)	8	7	15
			Max Queue (veh)	22	22	44
			Average Delay per Queued Vehicle (sec/veh)	6.54	5.29	5.97
	East	NB	Ave Delay (sec)	135	127	131
			Max Delay (sec)	344	266	344
			Ave Queue (veh)	6	6	12
			Max Queue (veh)	14	13	27
			Average Delay per Queued Vehicle (sec/veh)	23.90	21.89	22.88
Summer	West	SB	Ave Delay (sec)	23	21	22
			Max Delay (sec)	105	86	105
			Ave Queue (veh)	3	3	6
			Max Queue (veh)	14	14	28
			Average Delay per Queued Vehicle (sec/veh)	7.34	6.37	6.85
	West	EB	Ave Delay (sec)	172	123	147
			Max Delay (sec)	401	305	401
			Ave Queue (veh)	27	23	50
			Max Queue (veh)	50	51	101
			Average Delay per Queued Vehicle (sec/veh)	6.26	5.29	5.82
	East	NB	Ave Delay (sec)	50	58	54
			Max Delay (sec)	231	158	231
			Ave Queue (veh)	3	3	6
			Max Queue (veh)	8	10	18
			Average Delay per Queued Vehicle (sec/veh)	18.85	18.97	18.91

By comparing the average delay per queued vehicle values of left lanes with right lanes in Table 5, we can see that all the right lanes have lower values than the left lanes, with the exception of NB in summer (i.e., both left and right lanes have approximately the same value). This finding is consistent with the fact that a right-lane vehicle can enter the roundabout on the outside circulating lane, but a left-lane vehicle usually need to cut

across the outside circulating lanes to get onto the inside lane of the roundabout. That is, during a same period of time, it is more likely for a right-lane vehicle to find a gap to enter than a left-lane vehicle. Thus, a vehicle on the left-lane queue is more likely to endure longer delay than one on the right-lane.

It is also interesting to note that the NB approach of the east roundabout has higher average delay per queued vehicle value than the other two entrance approaches. A potential reason for the higher delay at the NB approach is the higher circulating flow in front of the approach. We can also see that the NB approach has higher average delay per queued vehicle value in winter than in summer. The higher average delay per vehicle in winter at the NB approach was caused by an abnormal situation. According to our winter video records, the longest delay on the NB entrance approach in winter occurred in the 33rd minute (i.e., 5:18 pm) of our recording. Frame B in **Figure** 15 shows the arrival of the vehicle that endured the longest delay. Frame A in **Figure** 16 shows that the vehicle finally entered the roundabout. The duration between the vehicle's arrival and departure was approximately 347 seconds. The delay was measured at 344 seconds, which adjusts for 3 seconds of free flow travel time required to travel the short distance in the un-delayed condition.

Figure 15 Picture of the arrival of the vehicle (circled) enduring the longest delay on the NB approach of the east roundabout

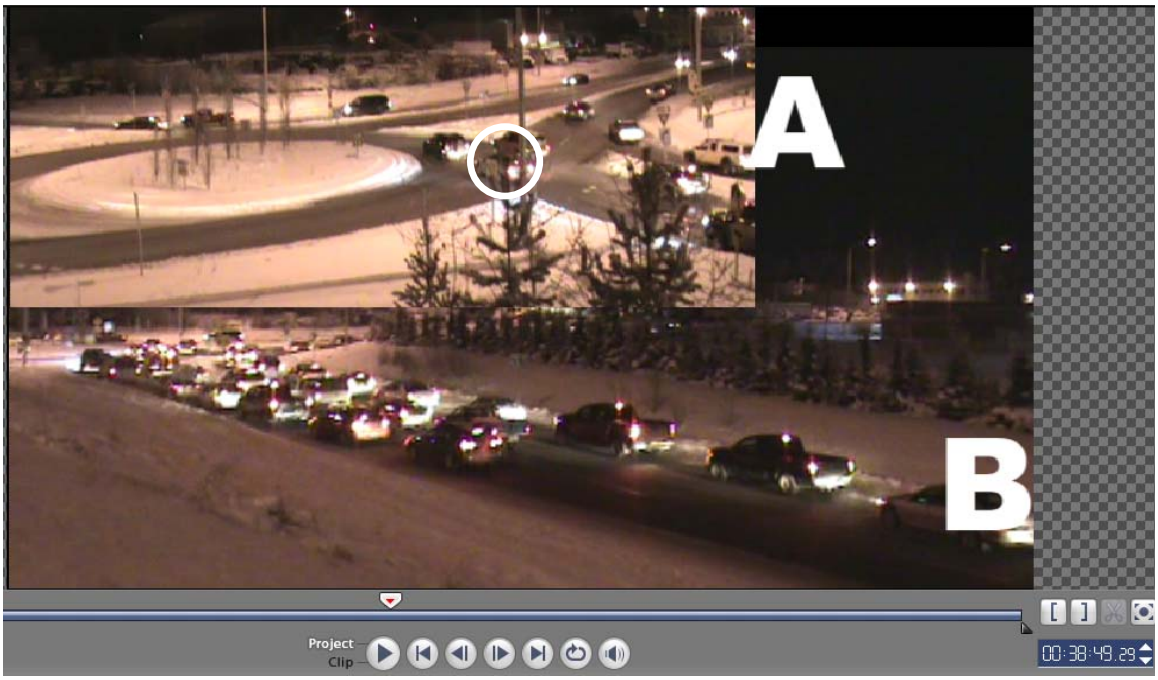

Figure 16 Picture of the departure of the vehicle (circled) enduring the longest delay on the NB approach of the east roundabout

4 PERFORMANCE COMPARISONS WITH ROUNDABOUTS IN OTHER COUNTRIES

Given the fact that roundabouts are relatively new to drivers in Alaska, it may be postulated that the full capacities of the roundabouts have not been realized because there may still be drivers who are not used to the roundabouts. Comparisons of the observed data of the Dowling roundabouts with data from countries where modern roundabouts have been used extensively may help shed light on the postulation.

There is abundant foreign research on models for predicting the entry capacity for multilane roundabouts. However, very few published studies included field flow measurements for comparison. Moreover, it is difficult to find data from two-lane roundabouts that are directly comparable to the Dowling road case. The comparisons presented three cases from the U.K., Germany, and Australia that have similar characteristics like the Dowling roundabouts.

4.1 UK

For studies that use linear regressions to develop the capacity models, field data in terms of capacities and circulating flows are usually presented in scatter plots that serve to show the goodness of fit for the models. Capacity of an approach is typically measured for a period of time when there are queues for the entire period. Simmens et al. (1980) reported capacities and circulating flows from a roundabout (see **Figure** 17) in Wincheap, Canterbury, UK. The Arm 2 of this roundabout shares the same characteristics with the Dowling roundabouts in that it has two entry lanes and two inside circulating lanes (i.e., driving on the left hand side). The published plot of entry flows vs. circulating flows for Arm 2 is shown in **Figure** 18. To facilitate further analysis of the data, the plot of the numbers of average entry flows and circulating flows were entered into a spreadsheet. The plot is recreated with the spreadsheet without information on standard deviations, whose scale was too small to be correctly retrieved from the original plot. The recreated plot with the regression equation of the best fit model is shown in **Figure** 19.

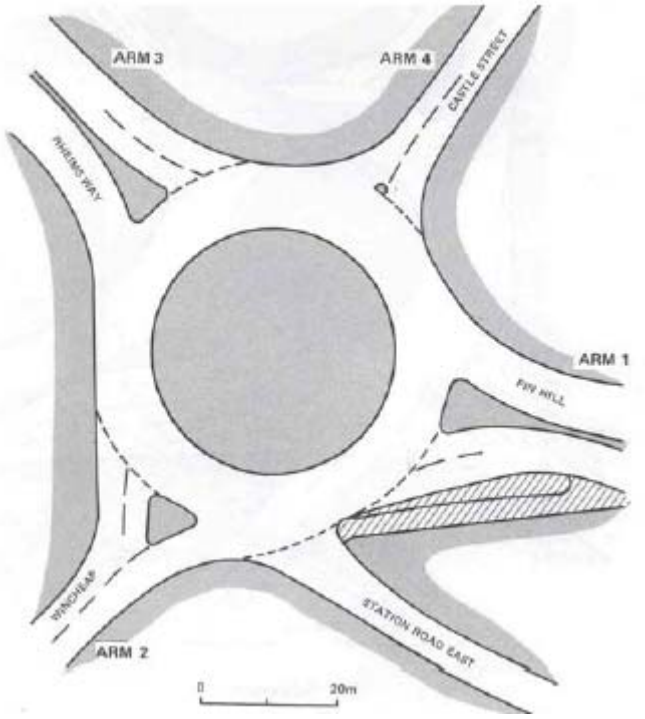

Figure 17 The Scheme of the Roundabout in Wincheap, Canterbury, UK.

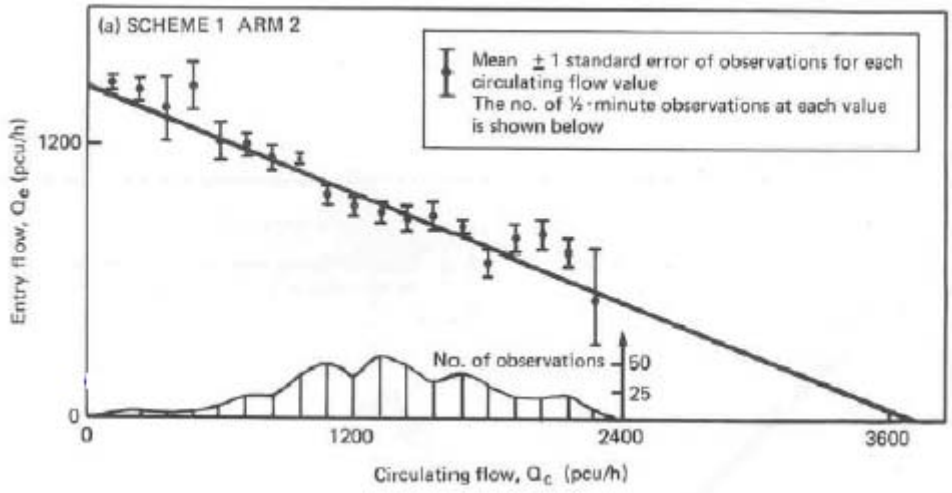

Figure 18 Entry Flow vs. Circulating Flow for the Wincheap Roundabout (pcu: passenger car unit)

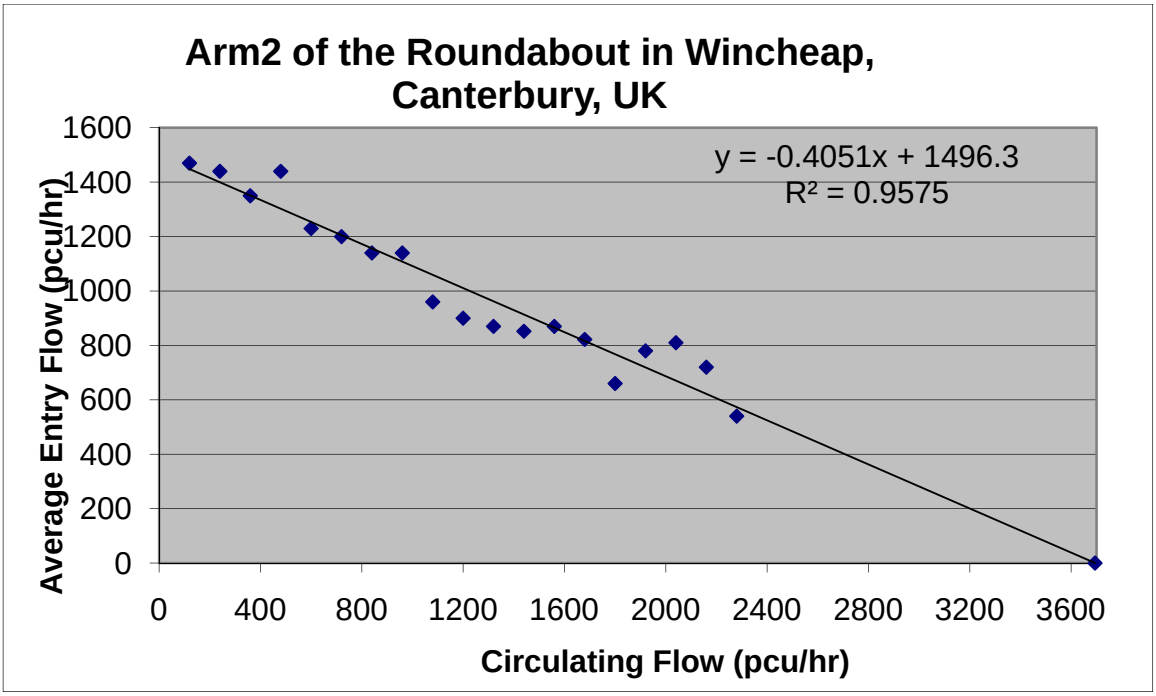

Figure 19 Recreated Average Entry Flow vs. Circulating Flow Plot for the Wincheap Roundabout

To be compared to the UK numbers, the capacity and circulating flow measurements at the EB entrance (i.e., the approach with sufficient number of data points for analysis) of the Dowling roundabouts are prepared in the same way as the UK numbers in **Figure** 18. That is, average capacities (i.e., entry flow when there is persistent queue for the entire period) were calculated for varying circulating flow groups. The results are presented in Table 6 and **Figure** 20.

Table 6 Average Entry Flow for Circulating Flow Groups at the EB entrance

Circulating Flow (Veh/hr)*	Average Entry Flow/Capacity (Veh/hr)*	Standard Deviation (Veh/hr)	Number of Observations
720	1200		1
780	1380		1
840	1320	127	5
900	1020	85	2
960	1100	223	6
1020	1110	159	4
1080	1030	353	6
1140	1020	255	2
1200	1380		1
1260	1020	170	2
1320	630	42	2
1440	855	274	4
1500	870	127	2
1560	480	255	2
1740	720		1
1860	600		1
2160	540		1

*The numbers include heavy vehicles. No passenger car unit (pcu) equivalency was sought for the heavy vehicles, because the number of heavy vehicle observed was very small.

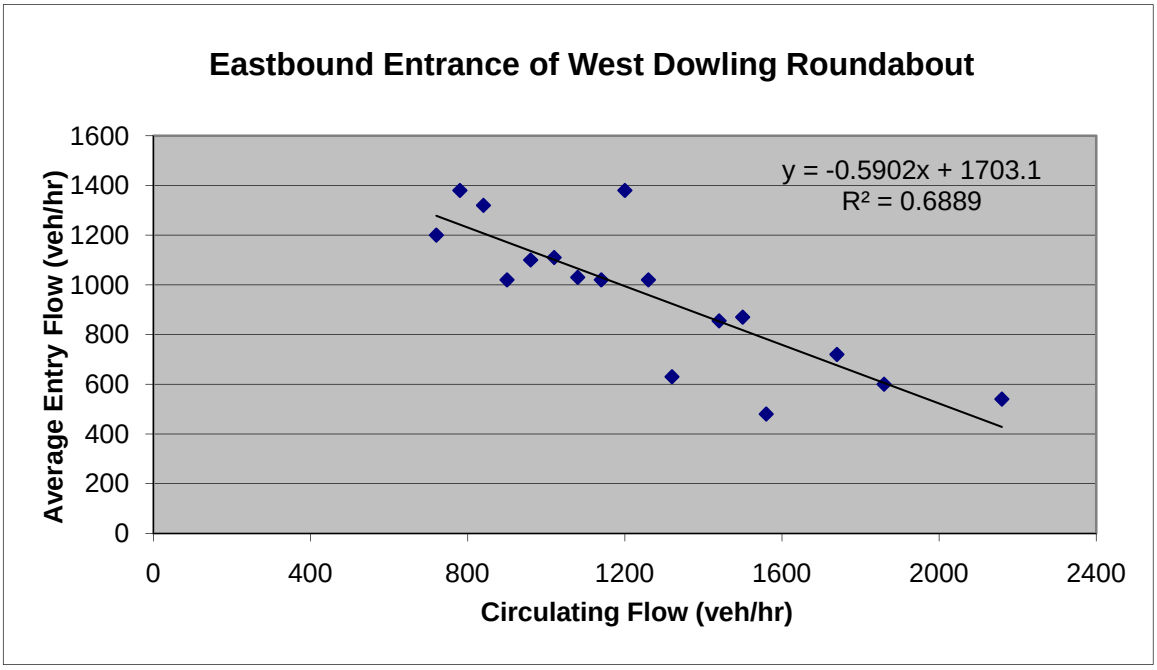

Figure 20 Circulating Flow vs. Average Entry Flow at the EB entrance of the West Dowling Roundabouts

By comparing **Figure** 19 with **Figure** 20, it appears that the EB entrance of the Dowling roundabout has a steeper descending slope of entry flow per circulating flow than the

Wincheap roundabout. At low to medium (i.e., <= 1200 pcu/hr) circulating flow rate, the Dowling roundabout has higher entry flow than Wincheap. At circulating flow rate of 1600 pcu/hr and above, the Wincheap roundabout seems to have slightly higher entry flows than the Dowling roundabout. However, the pattern in the high circulating flow range is not likely to be significant as both sets of data show high level of variation in this range.

4.2 Germany

Brilon (2005) presented capacity and circulating flow rate data (see **Figure** 21) collected from roundabouts in Germany. The data were derived from a large selection of roundabouts that have different general design and lane configurations in both urban and rural areas. Each of the data points in the plot on the left hand side of **Figure** 21 represents an one-minute observation at a roundabout. Each observation was multiplied by 60 to arrive at the pcu/hr number. The plot on the right hand side shows the average capacity values for various circulating flow groups. This plot is comparable to the plot for the roundabout in Wincheap, UK. We retrieved the values of the average capacities in the plot and entered them into a spreadsheet. The recreated plot is shown in **Figure** 22.

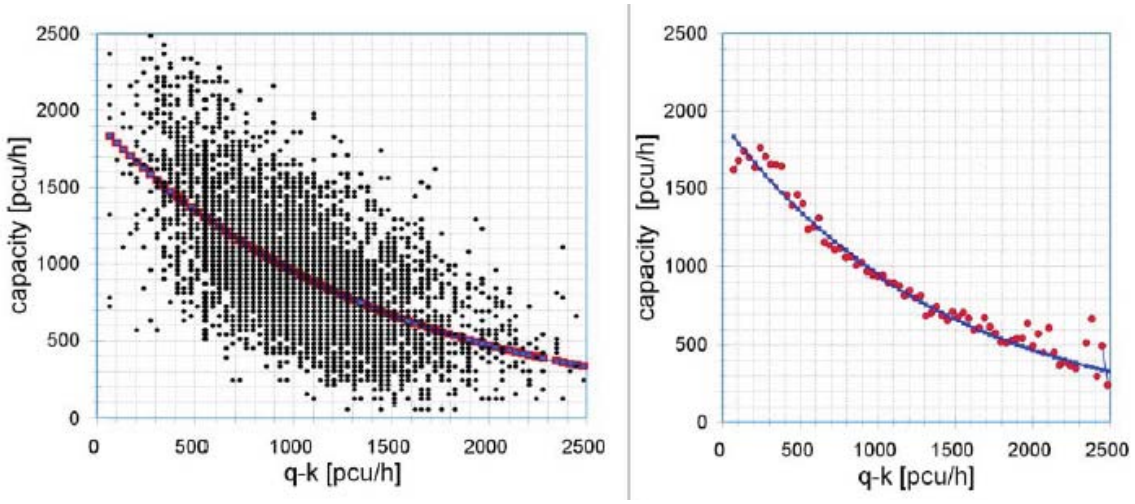

Figure 21 Capacity vs. Circulating Flow Rate Data from Roundabouts in Germany (Source: Brilon, W., 2005)

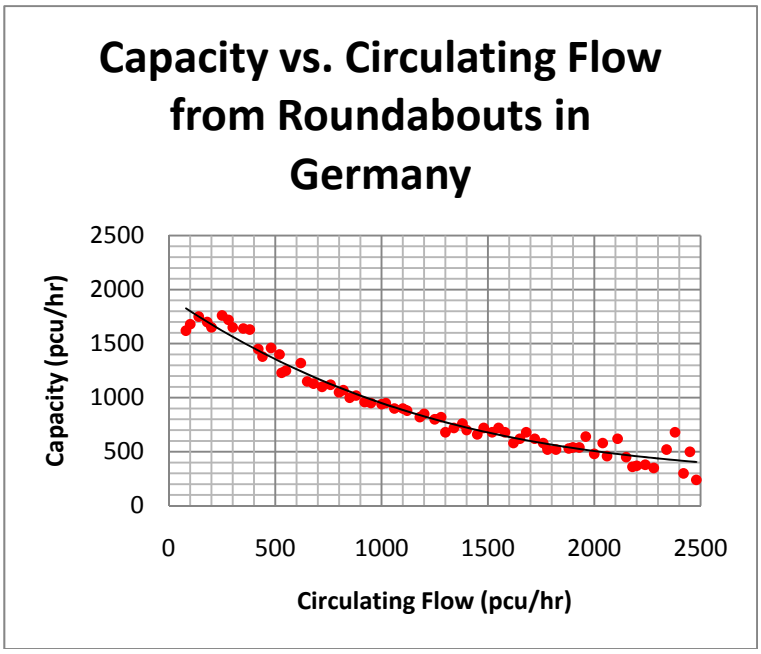

Figure 22 Recreated Plot for the Average Entry Flow Plot from Roundabouts in Germany

The pattern of average entry flow vs. circulating flow of the German data appears to be a curve. To facilitate comparison with the UK and the Dowling data, we tabulated the average entry flows based on three general circulating flow groups (see **Table** 7).

Table 7 Comparison of Average Entry Flow: Dowling, Germany, and UK

	Dowling EB		Germany		UK	
Circulating Flow Category (pcu/hr)	**Average**	**# of Obs.**	**Average**	**# of Obs.**	**Ave**	**# of Obs.**
900<=	1230	4	1397	25	1324	7
>900 and <=1200	1128	5	906	9	1000	3
>1200 and <=1500	844	4	733	8	861	2
>1500	585	4	526	28	743	8
Overall Average	957		909		1010	

We can see that the Dowling roundabout has higher average entry flows than German roundabouts for circulating flow rates greater than 900 pcu/hr. It is noted that the German numbers were average values of data from roundabouts of either one or two lanes. It is likely that the data for average capacity for circulating flow less than 900 pcu/hr were mostly from small single-lane roundabouts.

Another indication that the Dowling roundabout may have performed better than average German roundabouts is in the capacity vs. circulating flow relationships (see **Figure** 23) recommended in HBS 2001, which is German equivalent to the US Highway Capacity Manual. For roundabouts with 2 entry and 2 circulating lanes and a circulating flow greater than 1200 pcu/hr, German engineers would expect entry flows lower than those occurring at the Dowling roundabouts.

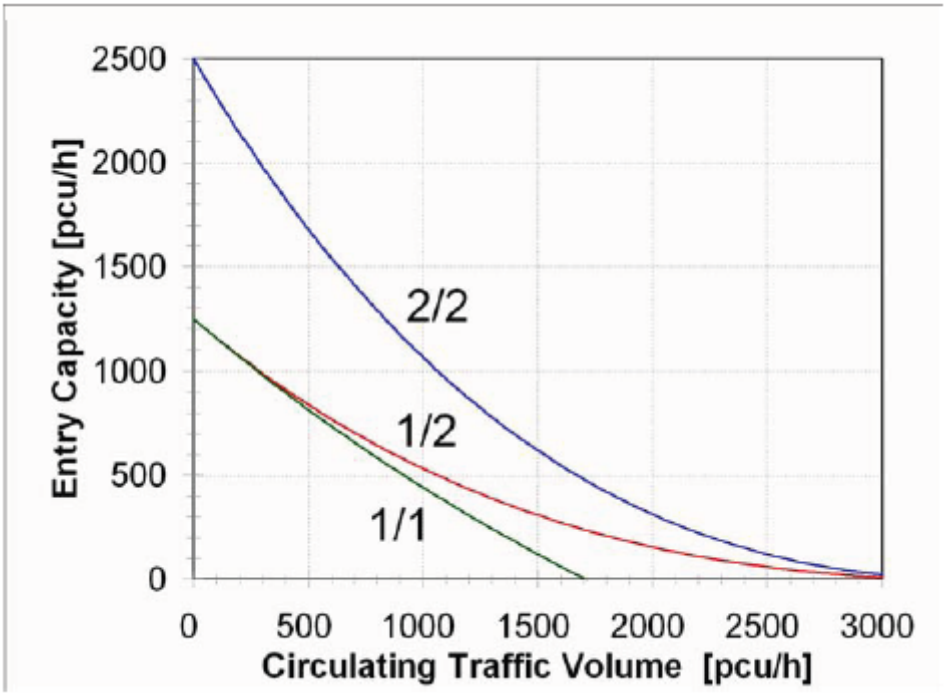

Figure 23 Entry Capacity of Roundabouts with Varying Lane Configurations (Entry/Circulating) According to HBS 2001 (Source: Brilon, 2005)

Table 1 also shows that the performance difference between the Dowling roundabout and the Wincheap roundabout is most significant for circulating flow greater than 1500 pcu/hr. The Wincheap roundabout has higher entry flow than Dowling for circulating flow greater than 1500. The group also has more observations than those from the Dowling roundabout.

4.3 Australia

Although roundabouts have been extensively used and researched in Australia, there is a lack of field performance data from Australia to be compared to roundabouts in other countries. The main reason for the lack of comparable data from Australia is that researchers in Australia use gap-acceptance theory to develop roundabout operation models. Such models are not built upon the relationship between capacity and circulating flow. As a result, published data about roundabout performance in Australia may not have taken on the same definitions as those in the studies that use regression to model capacity such as the UK approach presented earlier.

For example, Akcelik (2005) stated that capacity according to the aaSIDRA method is measured as "the departure flow rates during saturated (queued) portions of unblocked periods of gap-acceptance cycles and the associated portion of time available for queue discharge". As a result, the Australia data (see **Table** 8) used for the calibration of the aaSIDRA roundabout model have larger capacity numbers than the circulating flow numbers. This is not the same definition of capacity used in the regression approach.

Table 8 Data from Roundabouts in Australia used for the Development of the aaSIDRA model*

	Total entry width (ft)	No. of entry lanes	Average entry lane width (ft)	Circul. width (ft)	Inscribed Diameter (ft)	Entry radius (ft)	Conflict angle (°)
Minimum	12	1	10	21	52	13	0
Maximum	41	3	18	39	722	∞	80
Average	27	2	13	31	183	128	29
15th percentile	21	2	11	26	93	33	0
85th percentile	34	3	15	39	230	131	50
Count	55	55	55	55	55	55	55

	Follow-up Headway (s)	Critical Gap (s)	Crit. Gap / Fol. Hw Ratio	Circul. flow (veh/h)	Total entry flow (veh/h)	Dominant lane flow (veh/h)	Subdom. lane flow (veh/h)
Minimum	0.80	1.90	1.09	225	369	274	73
Maximum	3.55	7.40	3.46	2648	3342	2131	1211
Average	2.04	3.45	1.75	1066	1284	796	501
15th percentile	1.32	2.53	1.26	446	690	467	224
85th percentile	2.65	4.51	2.31	1903	1794	1002	732
Count	55	55	55	55	55	55	55

Source: Akcelik, R. (2005) Roundabout Model Calibration Issues and a Case Study Paper presented at the 2005 Transportation Research Board Roundabout Conference in Vail, Colorado.

We managed to find an individual case study in Australia (Akcelik, 2004) that may be comparable to the Dowling roundabout. For the roundabout in **Figure** 24, the Moreshead Drive approach was observed with long queue due to the large circulating flow from Parkes Way.

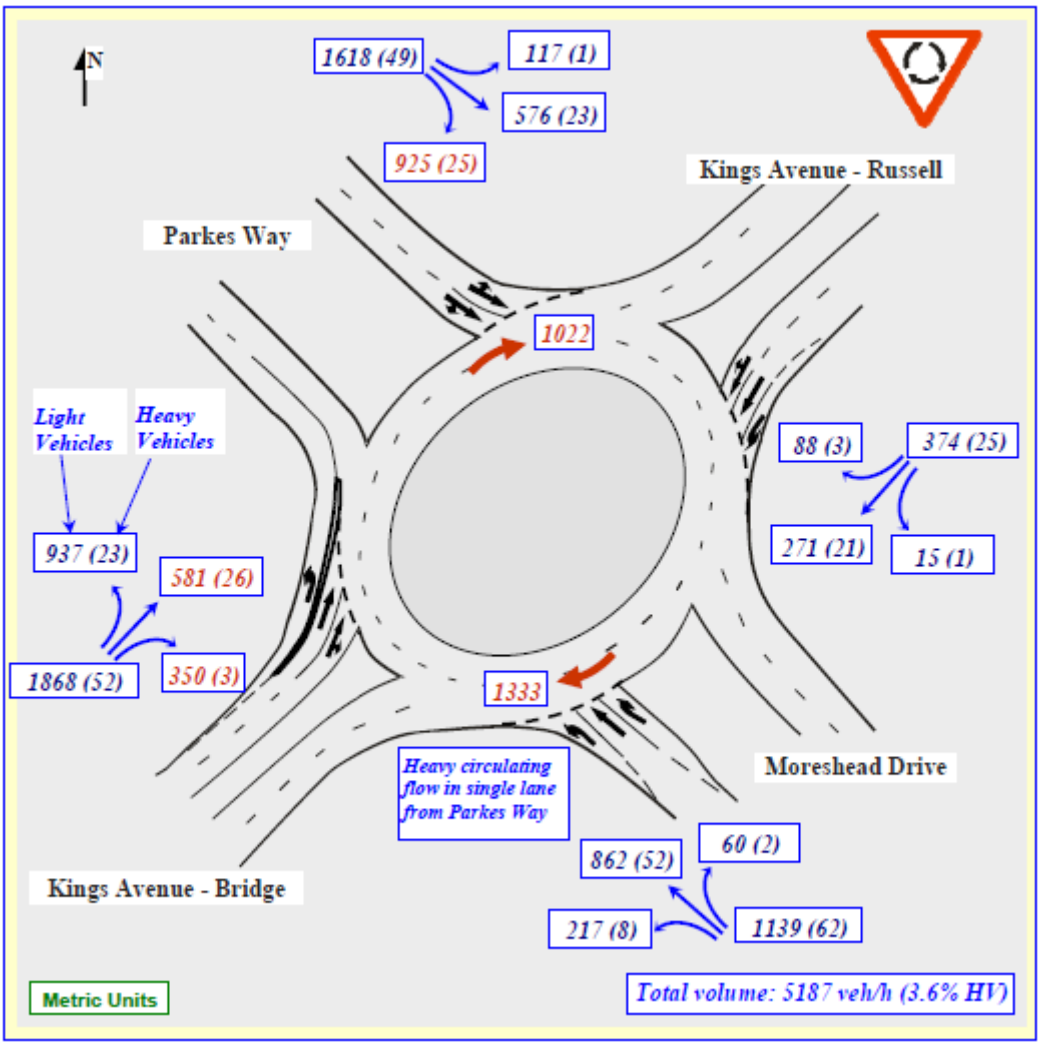

Figure 24 Peak Hour Flow Pattern at the Moreshead Roundabout in Canberra, Australia

Source: Akcelik, R. (2004) Roundabouts with Unbalaned Flow Patterns. Paper presented at the Institute of Transportation Engineers 2004 Annual Meeting, Lake Buena Vista, Florida, USA. August 1-4, 2004.

Table 9 shows the hourly circulating flow and entry flow extracted for the four approaches of the Moreshead Drive roundabout. We compare the numbers from the three queued approaches of the Dowling roundabout with the Moreshead drive, which is only known approach reportedly with queue. From the Dowling data, we selected those one-minute periods, when converted to hourly numbers, that have about 1300 vehicles per hour. **Table** 10 show the numbers for the three Dowling approaches. It shows that the three queued approaches of the Dowling roundabout allowed much lower entry flow than the Moreshead roundabout when the circulating flow level is at approximately 1300 veh/hr.

Table 9 Flow Numbers from the Moreshead Roundabout

Approach	Entry Flow (vehicles/hr)	Circulating Flow (vehicles/hr)	Ratio of Entry Flow to Circulating Flow
Moreshead Drive	**1201**	**1333**	**0.90**
Kings Avenue-Bridge	1920	1062	1.81
Parkes Way	1667	1022	1.63
Kings Avenue-Bridge	399	1902	0.21
Average	**1297**	**1330**	**0.98**

Table 10 Dowling Roundabout Entry Flow Numbers with Circulating Flow at 1300 veh/hr

Approach	Entry Flow (veh/min)	Circulating Flow (veh/min)	Entry Flow (vehicles/hr)	Circulating Flow (vehicles/hr)	Ratio of Entry Flow to Circulating Flow
EB	15	21	900	1260	0.71
EB	19	21	1140	1260	0.90
EB	10	22	600	1320	0.45
EB	11	22	660	1320	0.50
EB Average	**14**	**22**	**825**	**1290**	**0.64**
NB	**13**	**21**	**780**	**1260**	**0.62**
SB	**6**	**22**	**360**	**1320**	**0.27**

In summary, after comparing our field data with those from roundabouts in the UK, Germany, and Australia, we found that the performance of the Dowling roundabout in terms of entry flow and circulating flow are slightly lower than those in the UK and Australia. But, the Dowling numbers are slightly higher than those from Germany. In the future, applying the Dowling data using the Germany models may be tested to see if the model produce better results than those used in the UK and Australia.

5 RODEL ANALYSIS

After data were properly extracted from the video records, the data were entered into the software RODEL. To ensure the correctness of the analysis results, the analysis was done in conjunction with RODEL Software Ltd. (RSL), the maker of the RODEL software. RSL provided instructions for entering the input variables, and eventually reviewed the model outputs. Note that the RODEL models were not calibrated. The purpose of the RODEL analysis is to investigate how well RODEL and SIDRA can predict, in the project planning stage, the eventual field conditions. All the input variables entered into RODEL for the analysis are included in Appendix I.

5.1 RODEL Approach Capacity

Figure 25 to **Figure** 30 summarize the results of RODEL analysis on approach capacity. The approach capacity is the maximum entering flow rate when there are persistent queues of more than 5 vehicles on each lane of the approach during an entire analysis time period. The circulating flow rates in front of the approach are the sum of flow rates passing the approach from upstream approaches. Note that the winter capacity predicted by RODEL is applied with a 5% reduction factor to reflect the winter condition. The reduction was an instruction from RSL.

It is noted that the RODEL's estimate of capacity is in the form of a regression equation, with the capacity being the dependent variable and the circulating flow the independent variable. The output equation facilitates the plotting of the RODEL capacity estimates for different circulating flow in each figure. To be compared with field-measured capacity, both the RODEL outputs and the capacity measurement were converted to the conventional capacity unit of vehicles per hour. The field capacity was originally measured at vehicles per minute and the original RODEL outputs at vehicles per 5 minutes.

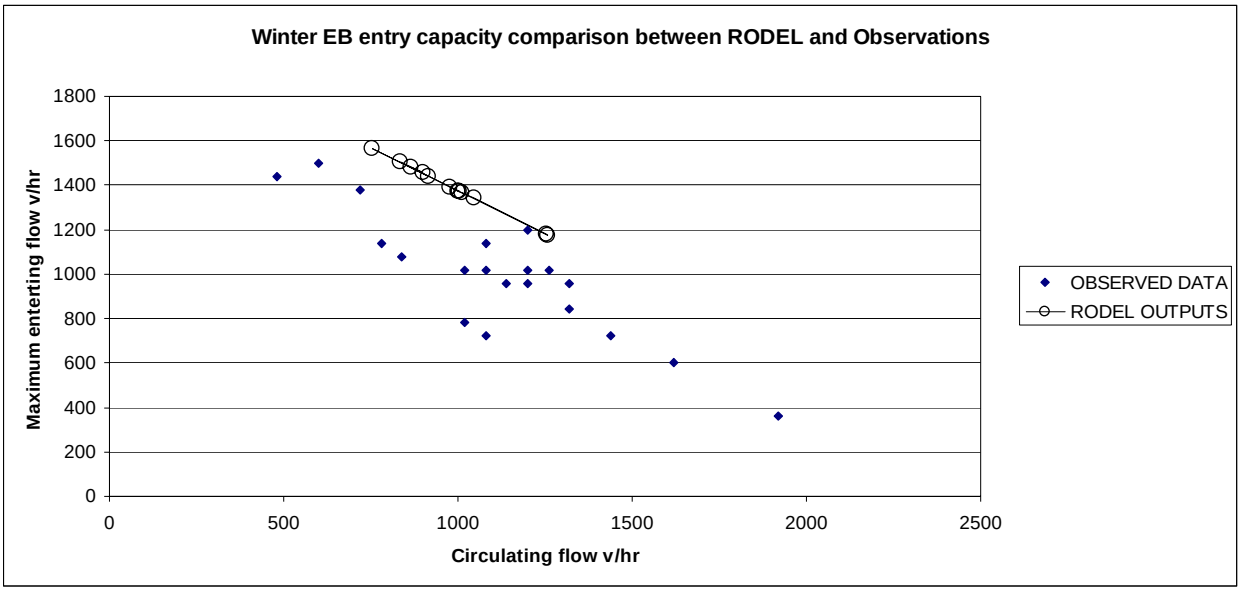

Figure 25 Winter Comparison between RODEL Capacity Estimates and Field Observations for EB Approach of the West Roundabout

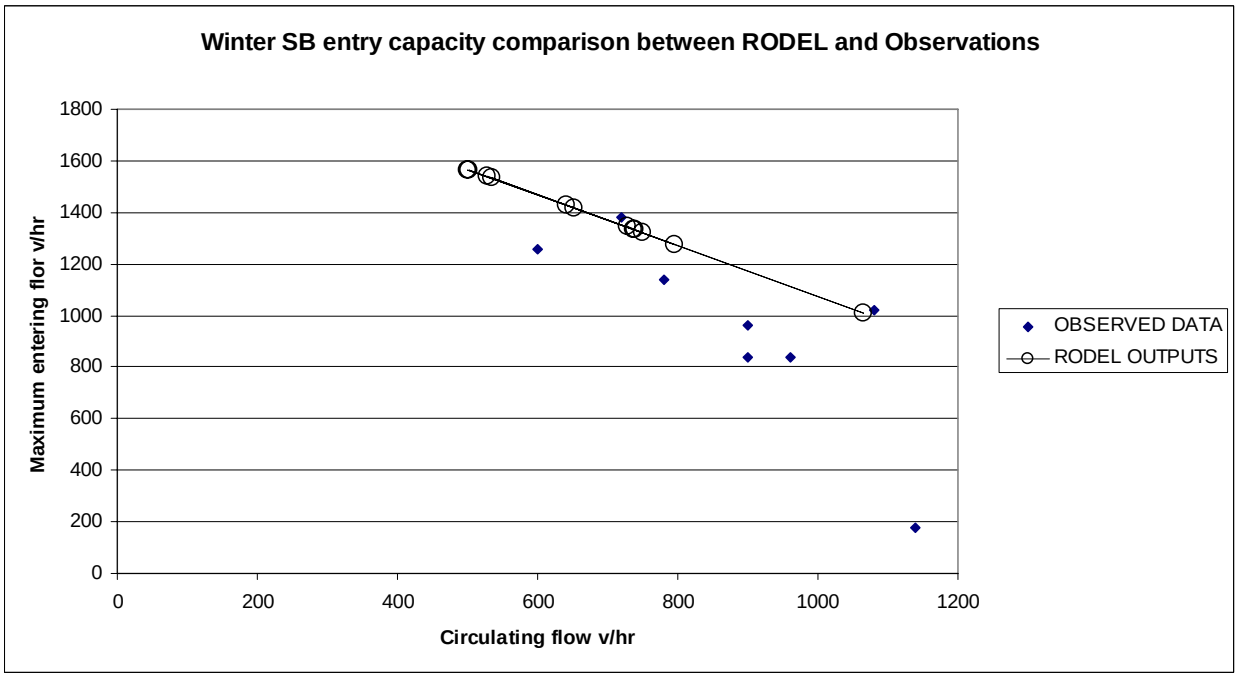

Figure 26 Winter Comparison between RODEL Capacity Estimates and Field Observations for SB Approach of the West Roundabout

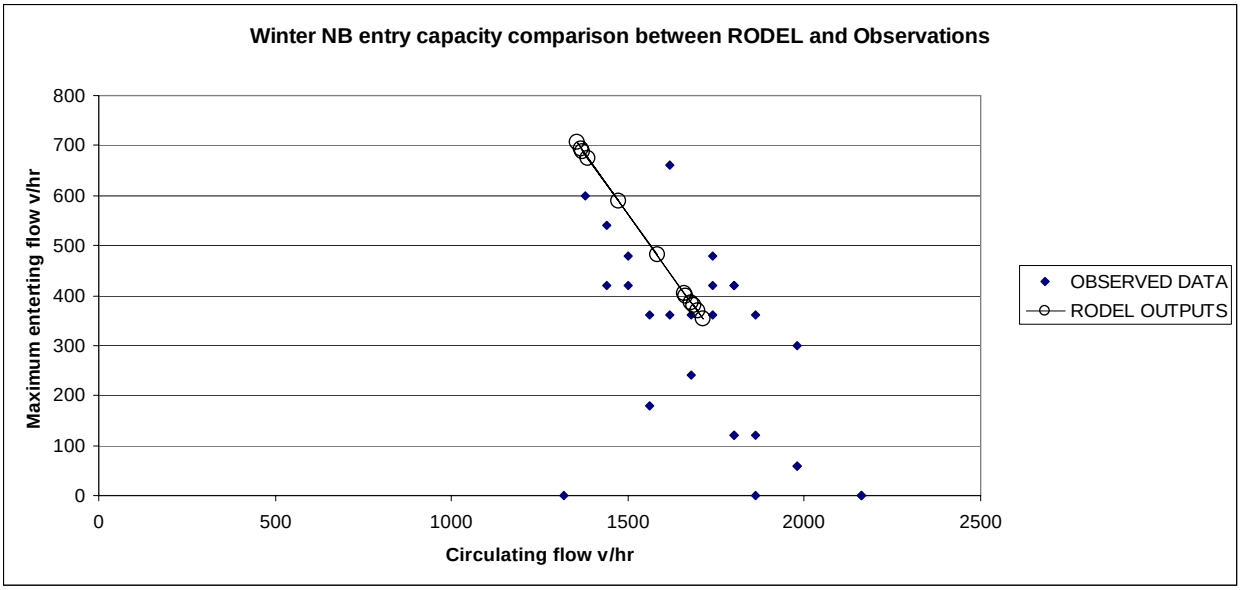

Figure 27 Winter Comparison between RODEL Capacity Estimates and Field Observations for NB Approach of the East Roundabout

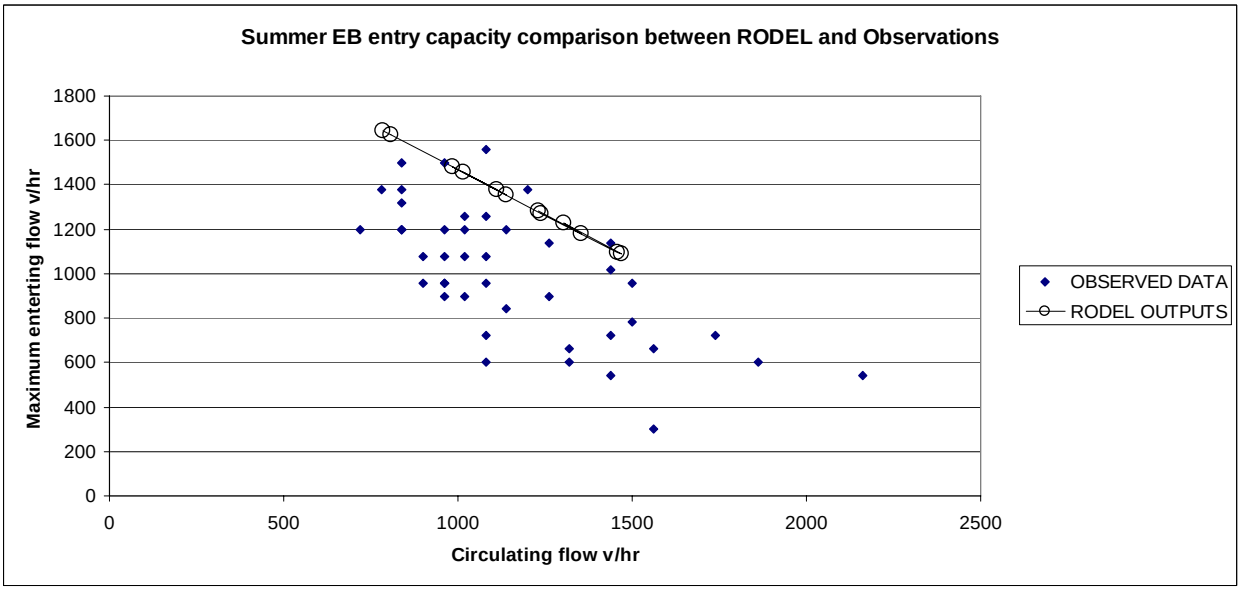

Figure 28 Summer Comparison between RODEL Capacity Estimates and Field Observations for EB Approach of the West Roundabout

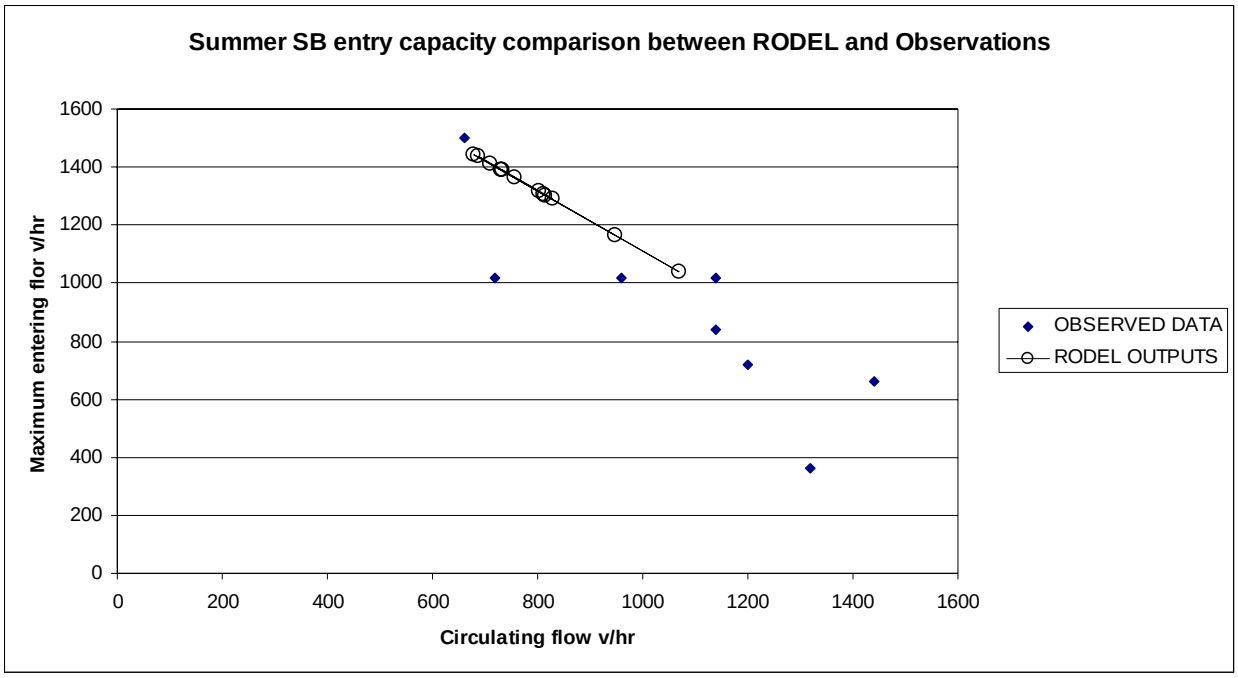

Figure 29 Summer Comparison between RODEL Capacity Estimates and Field Observations for SB Approach of the West Roundabout

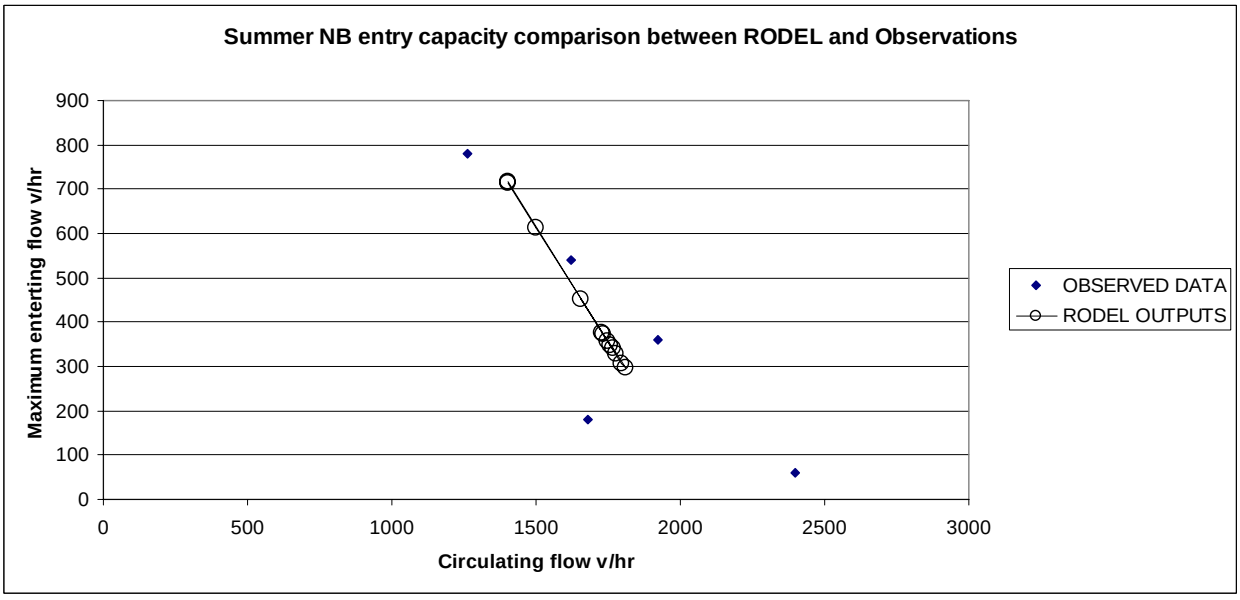

Figure 30 Summer Comparison between RODEL Capacity Estimates and Field Observations for SB Approach of the West Roundabout

In each of the above figures, the RODEL model line has higher capacity values than the field measured capacity for the given circulating flow range, indicating that RODEL overestimates the approach capacity. The finding is consistent with NCHRP report 572, which also reported the capacity overestimation by RODEL. However, the slope of the RODEL model approximately parallels the decreasing pattern of the field-measured data,

indicating that RODEL can reasonably predict the rate of capacity reduction for each unit of circulating flow increase.

In order to assess the accuracy of RODEL's capacity estimates, the Root Mean Square Errors (RMSE) between field measured capacities and corresponding RODEL estimates are calculated with the following equation:

$$RMSE = \sqrt{\frac{\sum_{i=1}^{n}(R_i - F_i)^2}{n}}$$

R_i = RODEL capacity estimates for circulating flow i
F_i = Field measured capacity at circulating flow i
n = number of field data point available for an approach

Table 11 summarizes the RMSE calculation for all three capacity-saturated approaches:

Table 11 RMSE of RODEL Capacity Estimates

Date	Roundabout	Approach	Average Field Circulating Flow (Vehicles/Hour)	Capacity Estimates RMSE
12/18/2008	East	NB	1,724	200.7
	West	SB	885	330.7
	West	EB	1,116	321.8
05/13/2009	East	NB	1,776	221.5
	West	SB	1,072	221.4
	West	EB	1,165	402.5

Considering both the winter and summer data, RODEL capacity estimates for the NB entrance of the east roundabout appears to be the most accurate among the three approaches. The reason for the NB approach's higher accuracy is unknown. The geometry and circulating flow of an approach are two well-recognized factors associated with the capacity of the approach. Geometry-wise, the NB approach of the east roundabout is essentially the mirror image of the SB approach of the west roundabout. But, the RMSE values for the two approaches are similar in summer yet very different in winter. In terms of circulating flows, we also could not identify a consistent pattern between the RMSE values and the average circulating flows.

5.2 RODEL Queue Length and Delay

There are four right-turn channels at the Dowling Roundabouts (i.e., EB right-turn and SB right-turn at the west roundabouts and the WB right-turn and NB right-turn at the east roundabout). Following the terminologies used in RODEL documents, the right-turn flows that exit the roundabout through the right turn channels are referred to as bypass traffic and the flows that enter the roundabouts are called non-bypass traffic. Version 1.0

of RODEL cannot model the queue length and delay of roundabouts in presence of bypass traffic. Following the instruction of RSL, a special procedure was applied to model the operation of the two Dowling roundabouts, each with two right-turn channels. The procedure essentially models queue and delay due to the roundabout circulating flow, and queue and delay due to the right turn channels separately. The final result combines the queue and delay caused by both the roundabout and the right-turn channels.

To combine the queue length and delay for each entrance approach with right turn channel, the following steps were taken:

1 Model each roundabout as one that has no right turn channels. Only non-bypass flows that eventually enter the roundabouts are analyzed. This step estimates the queue length and delay due exclusively to the entering flow, assuming no right turn traffic exists.

2 Model the roundabout as one in which the approach has only right-turn flow. That is, the number of bypass flows (i.e., right turn vehicles) and the lane width of the right turn channel are entered into the model as the approach's entering flow and entry width. This step essentially estimates the queue length and delay caused by the conflicts created by the right turn traffic from this approach.

3 Combine the queue length and delay estimates from steps 1 and 2. The combined values represent the total queue length and delay for the entrance approach with right-turn channel.

The combined average delay for an approach is estimated using the following equation:

> Combined average delay = (average delay per non-bypass vehicle * number of non-bypass vehicles + average delay per bypass vehicle * number of bypass vehicles) / the sum of non-bypass and bypass vehicles

The combined maximum delay for an approach is larger between the non-bypass and bypass delays. The combined average queue length for an approach is the sum of average queue length caused by both the non-bypass and bypass traffic. The combined maximum queue length for an approach is the sum of maximum queue lengths in non bypass and bypass model.

Table 12 summarizes RODEL's queue length and delay prediction for the three entrance approaches that had queues. It is noted that RODEL's predictions of delay and queue length are approach-based. The approach-based field measurements introduced in Table 5 are used to compare with the RODEL predictions.

Table 12 RODEL Estimated and Field-observed Delays and Queue Lengths

Date	Roundabout	Approach	Measurements	RODEL estimates			Approach-based field measurement
				Non bypass	Bypass	Combined	
12/18/2008	West	SB	Ave Delay (sec)	7.3	15.1	8.24	17.5
			Max Delay (sec)	16.3	56.1	56.1	88
			Ave Queue (veh)	1.7	0.5	2.2	5
			Max Queue (veh)	4.1	2	6.1	21
	West	EB	Ave Delay (sec)	128.8	21	113.81	43
			Max Delay (sec)	366.1	98.6	366.1	171
			Ave Queue (veh)	44.1	1.2	45.3	15
			Max Queue (veh)	138.5	6.6	145.1	44
	East	NB	Ave Delay (sec)	149	NA	NA	131
			Max Delay (sec)	344.7	NA	NA	344
			Ave Queue (veh)	17.7	NA	NA	12
			Max Queue (veh)	50	NA	NA	27
05/13/2009	West	SB	Ave Delay (sec)	23.3	21.3	23.06	22
			Max Delay (sec)	59.1	78.3	78.3	105
			Ave Queue (veh)	6.1	0.8	6.9	6
			Max Queue (veh)	19.5	2.9	22.4	28
	West	EB	Ave Delay (sec)	525.9	38.7	466.72	147
			Max Delay (sec)	886.3	162.1	886.3	401
			Ave Queue (veh)	241.9	2.4	244.3	50
			Max Queue (veh)	376.5	7.4	383.9	101
	East	NB	Ave Delay (sec)	151.3	NA	NA	54
			Max Delay (sec)	289.9	NA	NA	231
			Ave Queue (veh)	17.4	NA	NA	6
			Max Queue (veh)	35.7	NA	NA	18

For the NB approach of the east roundabout, after entering all the required inputs based on RSL's instructions, no value is produced for the bypass model. It is noted that both the right turn movements and the circulating flow at the approach are relative high. When the single right-turn lane is used in the bypass model as the entry flow to the

roundabout, it is likely that the high right turn volumes and high circulating flow exceed the value range required for RODEL to generate reasonable capacity estimates.

By comparing the combined RODEL estimates with field measurements, we can see that RODEL highly overestimated the delay and queue for the EB approach of the west roundabout for both the winter and summer data. We cannot identify a clear pattern for the SB approach.

According to the RODEL outputs, the right turn movements at the SB approach of the west roundabout appears to incur more delay than the entering flow. The high delay is likely due to the fact that the bypass model is modeled as one lane and the non-bypass model as two lanes. However, the bypass and non-bypass models of the EB approach of the west roundabout were also modeled in the same way, but the bypass delay appears to be much lower than that of the non-bypass model. Based on these results, we can not be sure that the bypass model can reasonably represent the additional delay and queue caused by the right turn movements through the right turn channels. Thus, RODEL's ability to accurately estimate the delay and queue length for a multilane roundabout with right turn channels is limited.

6. SIDRA ANALYSIS

The extracted field data were also analyzed with the software SIDRA with assistance from SIDRA's technical support. Note that the SIDRA models were not calibrated for the same reason that the RODEL models were not calibrated. All the input variables entered into SIDRA for the analysis are included in Appendix II.

6.1 SIDRA Capacity Analysis

Unlike RODEL, SIDRA does not produce regression equations for graphing the relationship between capacities and circulating flows. In order to produce capacity estimates at different circulating flow levels, SIDRA technical support instructed us to apply different flow scales to the turning movements at the entrance approaches of the roundabouts. A flow scale is essentially an arbitrary ratio used to proportionally adjust the turning movements for the purposes of forecasting future traffic growth and/or sensitivity analysis. By applying an appropriate range of flow scales to all turning movements, capacity estimates at different circulating flow rate levels can be obtained. Table 13 shows an example of capacity estimates and the corresponding circulating flow rates for the NB entrance approach with flow scales ranging from 60% to 140%.

Table 13 Example of Varying Capacity with Different Flow Scales

Date	Roundabout	Approach	Flow scale	Demand flow rate (veh/h)	Capacity (veh/h)	Circulating flow rate (veh/h)
05/13/2008	East	NB	60%	268	1242	1119
			70%	313	1139	1306
			80%	358	1044	1492
			90%	402	951	1679
			100%	447	858	1865
			110%	492	765	2052
			120%	536	671	2239
			130%	581	576	2425
			140%	626	477	2612

The capacities estimated by SIDRA for all entrance approaches of the two roundabouts are shown in **Figure** 31to **Figure** 36. Note that the WB approach of the east roundabout is not considered, because it did not have at least 5 queued vehicles in any one-minute period. The ranges of flow scales applied to generate the capacity estimates in SIDRA were based on the range of field-observed capacities. The selection of flow scale ranges facilitates comparison with field-measured capacities for the entrance approaches.

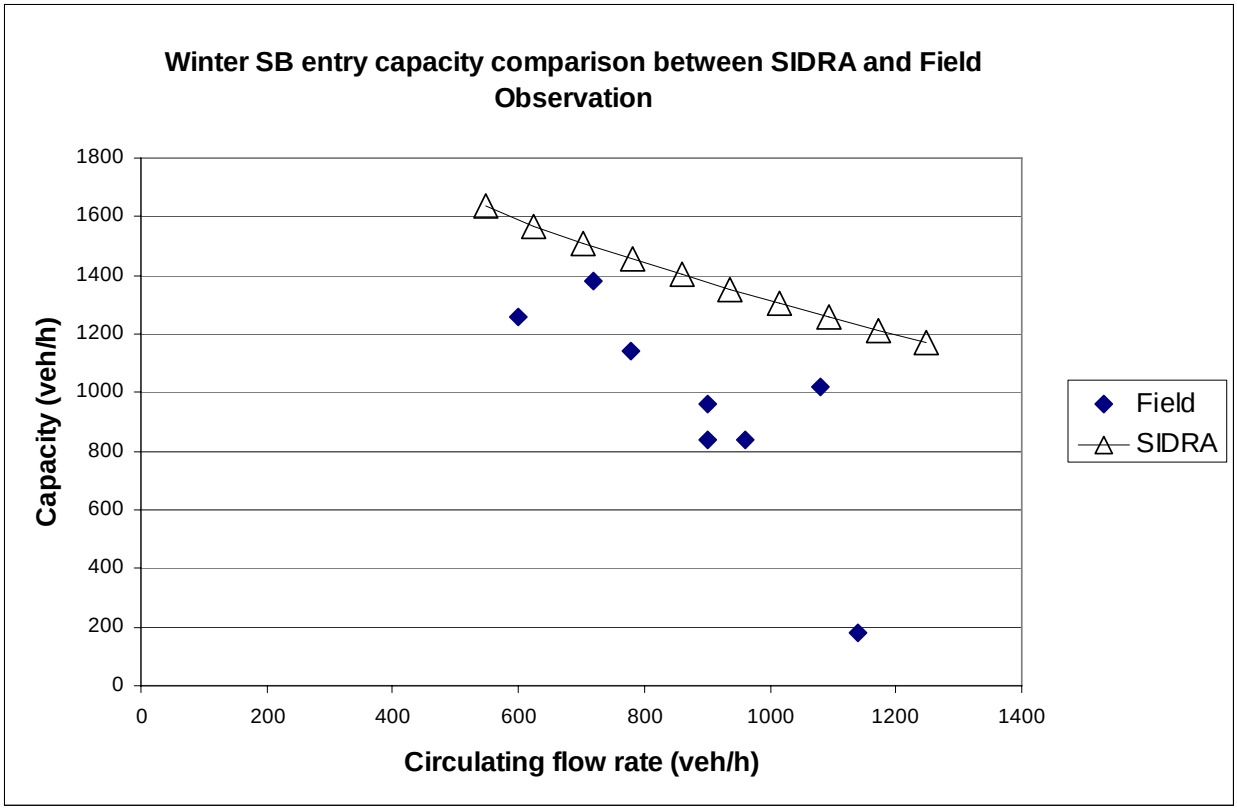

Figure 31 Winter Comparison between SIDRA Capacity Estimates and Field Observations for SB Approach of the West Roundabout

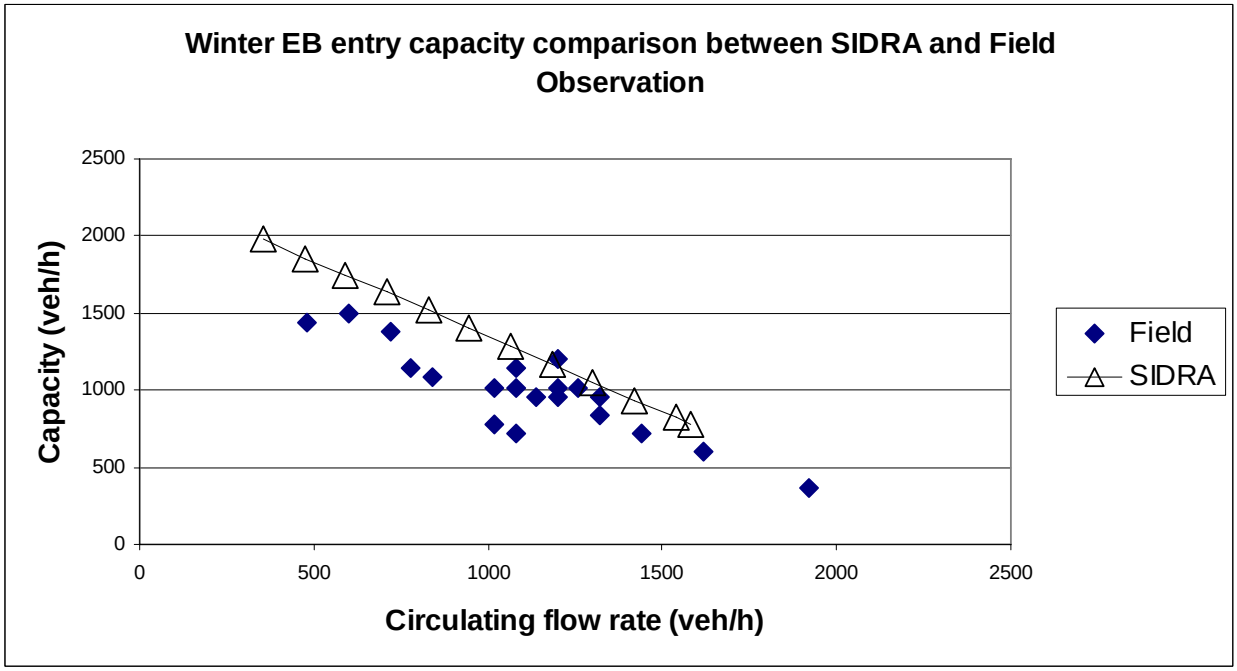

Figure 32 Winter Comparison between SIDRA Capacity Estimates and Field Observations for EB Approach of the West Roundabout

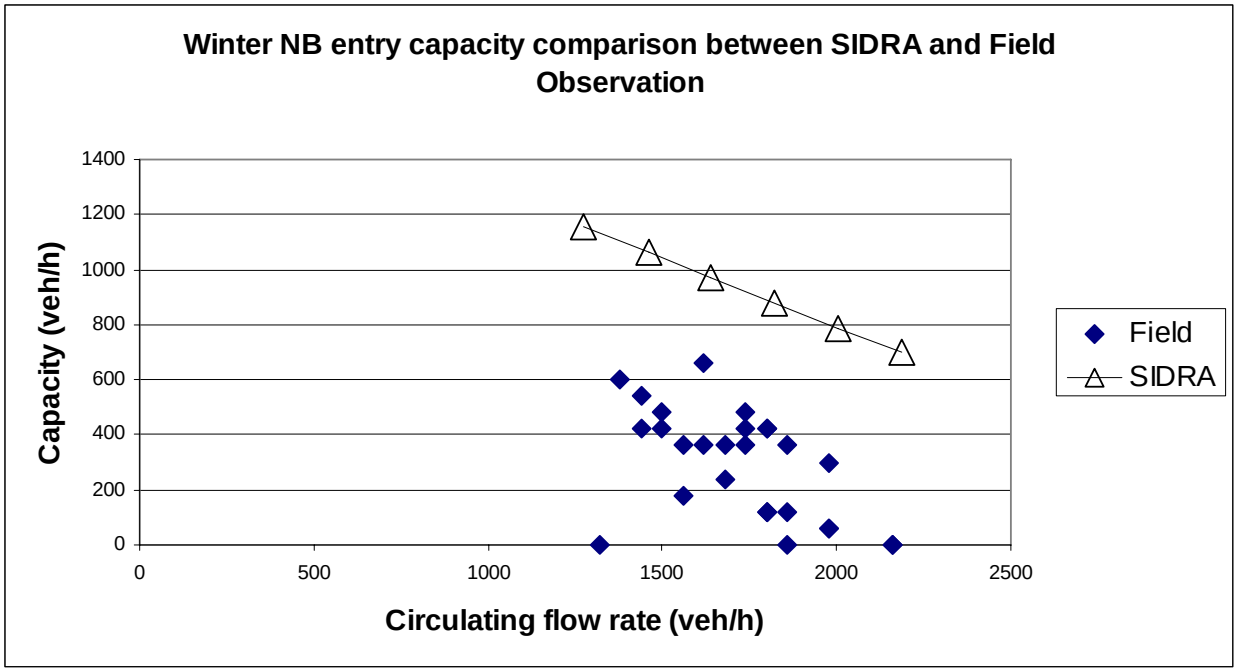

Figure 33 Winter Comparison between SIDRA Capacity Estimates and Field Observations for NB Approach of the East Roundabout

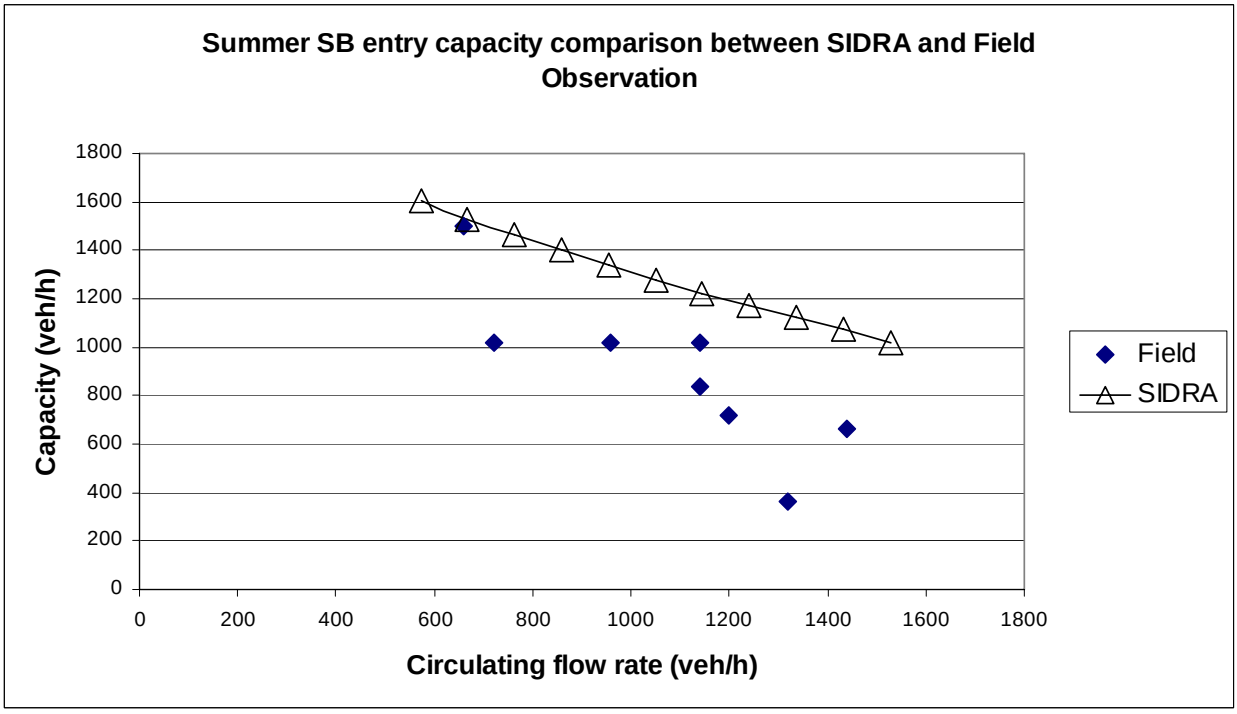

Figure 34 Summer Comparison between SIDRA Capacity Estimates and Field Observations for SB Approach of the West Roundabout

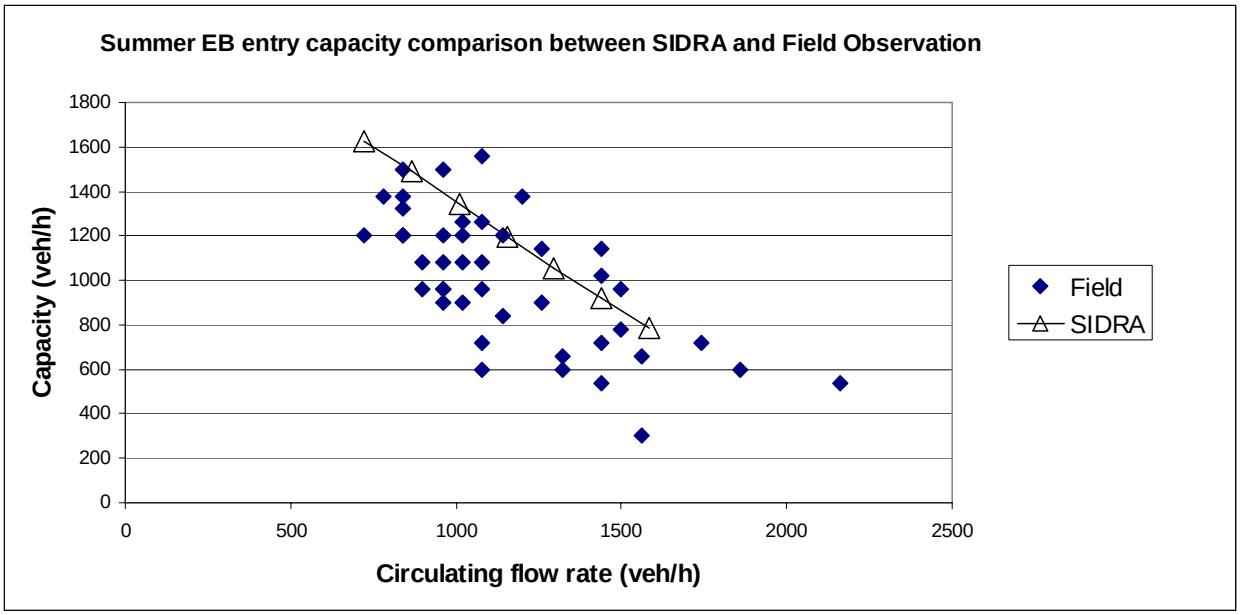

Figure 35 Summer Comparison between SIDRA Capacity Estimates and Field Observations for EB Approach of the West Roundabout

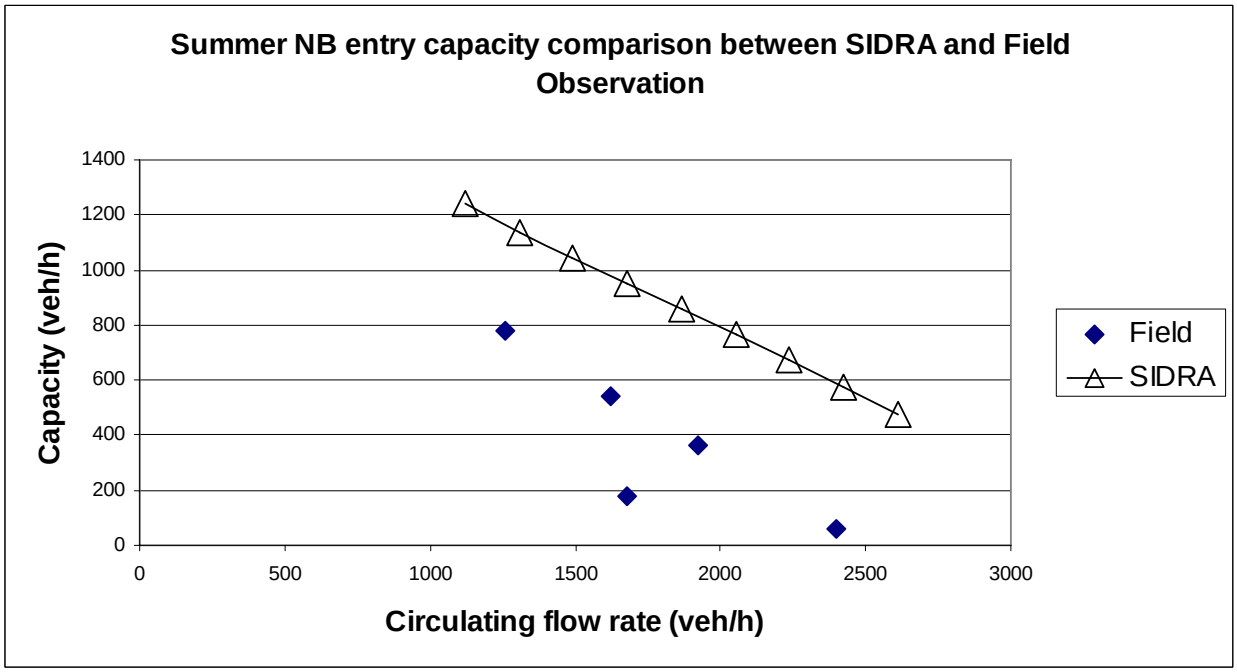

Figure 36 Summer Comparison between SIDRA Capacity Estimates and Field Observations for NB Approach of the East Roundabout

The figures show that SIDRA overestimates the capacity for all three entrance approaches. SIDRA's capacity estimates for the EB approach of the west roundabout is better than those for the other two approaches. To quantitatively assess the accuracy of the SIDRA estimates, RMSE calculation was performed for the SIDRA estimates. Because that SIDRA capacity estimates are indeed a series of point estimates created

with varying flow scales, we first created a best-fitting regression line for the SIDRA estimates of each approach. RMSE values between values on this regression line and the field measurements are then calculated using the same RMSE equation used for RODEL.

Table 14 shows the RMSE of the SIDRA capacity estimates.

Table 14 RMSE of SIDRA Capacity Estimates

Date	Roundabout	Approach	Average Field Circulating Flow (Vehicles/Hour)	Capacity Estimates RMSE
12/18/2008	East	NB	1,724	657.5
	West	SB	885	486.2
	West	EB	1,116	287.7
05/13/2009	East	NB	1,776	536.6
	West	SB	1,072	398.4
	West	EB	1,165	306.7

The EB approach of the west roundabout has the smallest RMSE value, followed by the SB approach of the same about. The NB approach of the east roundabout has the highest RMSE value. The order of RMSE values of the three approaches is consistent for both the winter and summer data.

It appears that the NB entrance approach of the east roundabout has both the highest RMSE and circulating flow values among the three approaches. But, we can not observe a clear pattern for the association between circulating flow and RMSE for the SB and EB approaches of the west roundabout.

6.2 SIDRA Queue and Delay

The SIDRA estimated delays and queue lengths by lane are shown in **Table** 15. Unlike RODEL, right turn channels can be entered into SIDRA. SIDRA estimates of delay and queue lengths thus take into accounts of delay and queues caused by the right turn movements. SIDRA does not produce maximum delay estimate. For queue length, SIDRA estimates the 95^{th} percentile queue lengths instead of maximum queue length.

Table 15 SIDRA-estimated Delay and Queue Length

Date	Roundabout	Approach	Lane [1]	Measurement [2]	SIDRA estimates	Field Data	Error
12/18/2008	East	NB	Left	Ave Delay (sec)	24.3	135	-82%
				Ave Queue (veh)	0.6	6	-90%
				95% Queue (veh)	2.8	11	-75%
			Right	Ave Delay (sec)	19.3	127	-85%
				Ave Queue (veh)	0.6	6	-90%
				95% Queue (veh)	3.0	12	-75%
	West	EB	Left	Ave Delay (sec)	21.5	51	-58%
				Ave Queue (veh)	3.6	8	-55%
				95% Queue (veh)	10.7	18	-41%
			Right	Ave Delay (sec)	21	35	-40%
				Ave Queue (veh)	3.7	7	-47%
				95% Queue (veh)	10.9	18	-39%
	West	SB	Left	Ave Delay (sec)	18.3	17	8%
				Ave Queue (veh)	2	2	0%
				95% Queue (veh)	6	7	-14%
			Right	Ave Delay (sec)	16.7	18	-7%
				Ave Queue (veh)	2	3	-33%
				95% Queue (veh)	6	8	-25%
05/13/2009	East	NB	Left	Ave Delay (sec)	26.7	50	-47%
				Ave Queue (veh)	1.1	3	-63%
				95% Queue (veh)	3.5	6	-42%
			Right	Ave Delay (sec)	21.4	58	-63%
				Ave Queue (veh)	1.2	3	-60%
				95% Queue (veh)	3.7	6	-38%
	West	SB	Left	Ave Delay (sec)	26.6	23	16%
				Ave Queue (veh)	3.8	3	27%
				95% Queue (veh)	11.2	13	-14%
			Right	Ave Delay (sec)	25.0	21	19%
				Ave Queue (veh)	3.8	3	27%
				95% Queue (veh)	11.3	11	3%
	West	EB	Left	Ave Delay (sec)	113.4	172	-34%
				Ave Queue (veh)	15.0	27	-44%
				95% Queue (veh)	39.2	47	-17%
			Right	Ave Delay (sec)	112.4	123	-9%
				Ave Queue (veh)	16.2	23	-30%
				95% Queue (veh)	41.9	43	-3%

Table 15 shows that SIDRA underestimates delays and queue length on the NB approach of the east roundabout and the EB approach of the west roundabout. The underestimation in delay and queue length for these two approaches may be attributed to SIDRA's overestimation of the capacities. However, SIDRA's estimates of the delay and queue length for the SB approach of the west roundabout are close to the field values. Thus, the accuracy of SIDRA's capacity estimates may not be the most critical factor determining how well queue length and delay are predicted.

Table 16 shows the approach average of SIDRA's delay and queue length estimates with field measured circulating flow. The approach average values are the average of the left lane and right lane values. The winter values show a clear pattern between circulating

flow and estimation error. The lower the circulating flow is the smaller the error is for the delay and queue estimate.

For the summer data, the pattern does not apply to all approaches. The error for the NB approach, which has the largest circulating flow, is slightly smaller than those of the EB approach. However, the SB approach, which has the smallest circulating flow, does have the smallest errors among all three approaches.

Table 16 Approach Average of SIDRA-estimated Queue Length and Delay

Season	Roundabout	Approach	Circulating Flow	Measurement	SIDRA Approach Average	Field Values	Error
Winter	East	NB	1,724	Ave Delay (sec)	21.56	131	-84%
				Ave Queue (veh)	1.2	12	-90%
				95% Queue (veh)	5.8	3	93%
	West	SB	885	Ave Delay (sec)	17.5	17.5	0%
				Ave Queue (veh)	4	5	-20%
				95% Queue (veh)	12	18	-33%
	West	EB	1,116	Ave Delay (sec)	21.24	43	-51%
				Ave Queue (veh)	7.3	15	-51%
				95% Queue (veh)	21.6	8	170 %
Summer	East	NB	1,776	Ave Delay (sec)	23.8	54	-56%
				Ave Queue (veh)	2.3	6	-62%
				95% Queue (veh)	7.2	6	20%
	West	SB	1,072	Ave Delay (sec)	25.8	22	17%
				Ave Queue (veh)	7.6	6	27%
				95% Queue (veh)	22.5	13	73%
	West	EB	1,165	Ave Delay (sec)	112.88	147	-23%
				Ave Queue (veh)	31.2	50	-38%
				95% Queue (veh)	81.1	47	73%

7. COMPARISON BETWEEN RODEL AND SIDRA

7.1 Capacity Estimates Comparison

The graphs comparing the capacity estimates between RODEL and SIDRA are shown in **Figure** 37 to **Figure** 42.

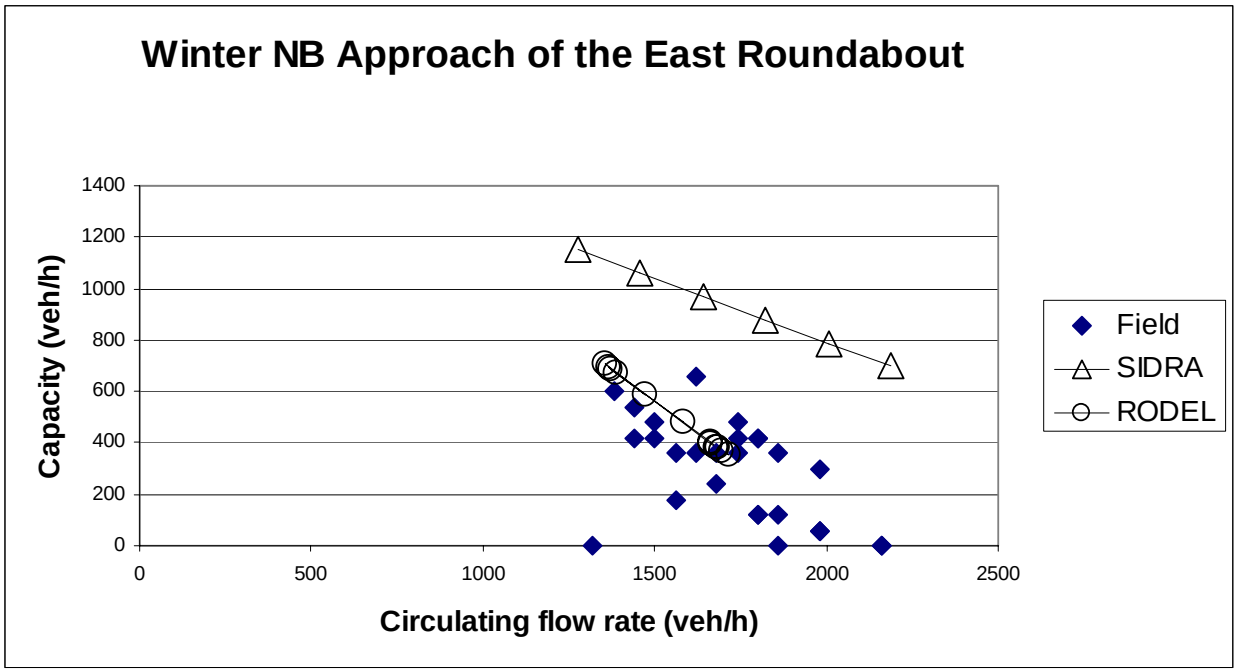

Figure 37 Winter Comparison of Capacity Estimates between RODEL and SIDRA for the NB Approach of the East Roundabout

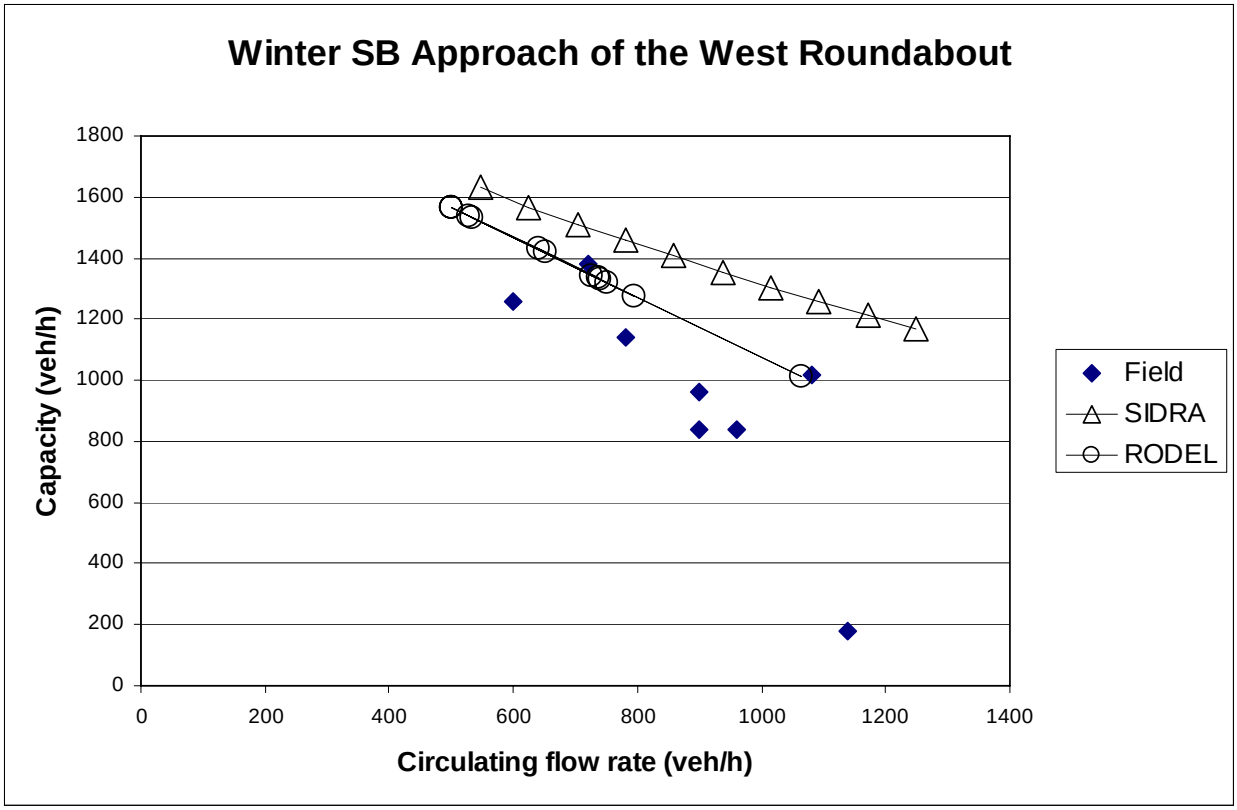

Figure 38 Winter Comparison of Capacity Estimates between RODEL and SIDRA for the SB Approach of the West Roundabout

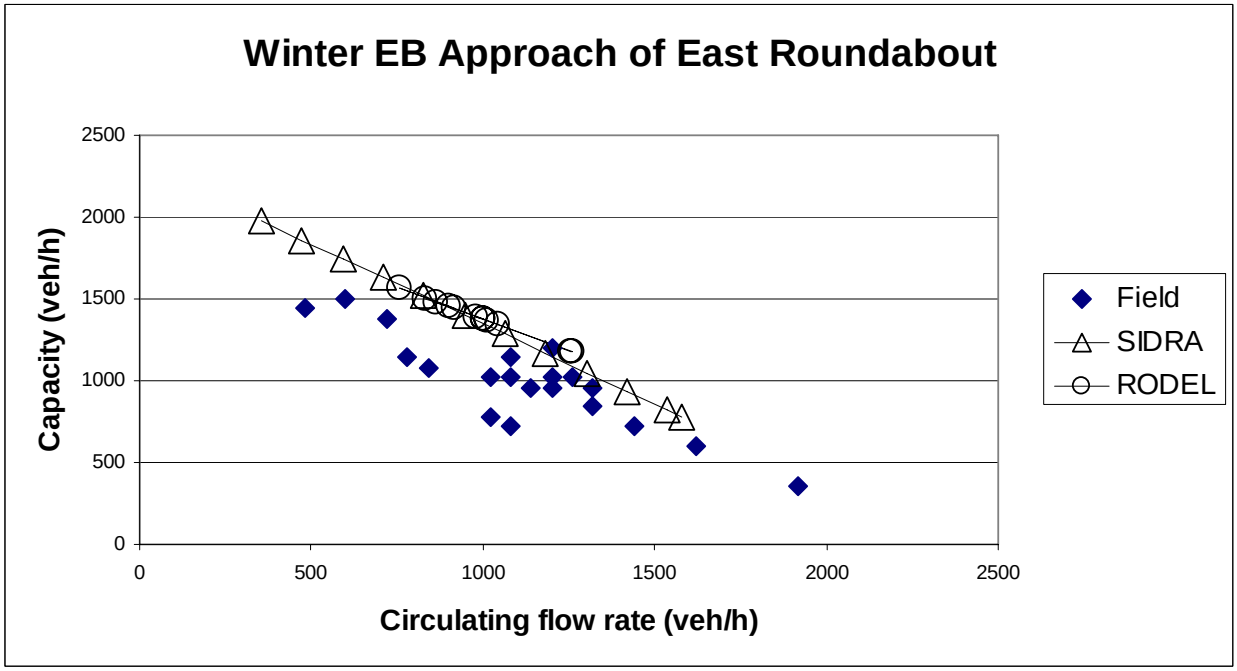

Figure 39 Winter Comparison of Capacity Estimates between RODEL and SIDRA for the EB Approach of the West Roundabout

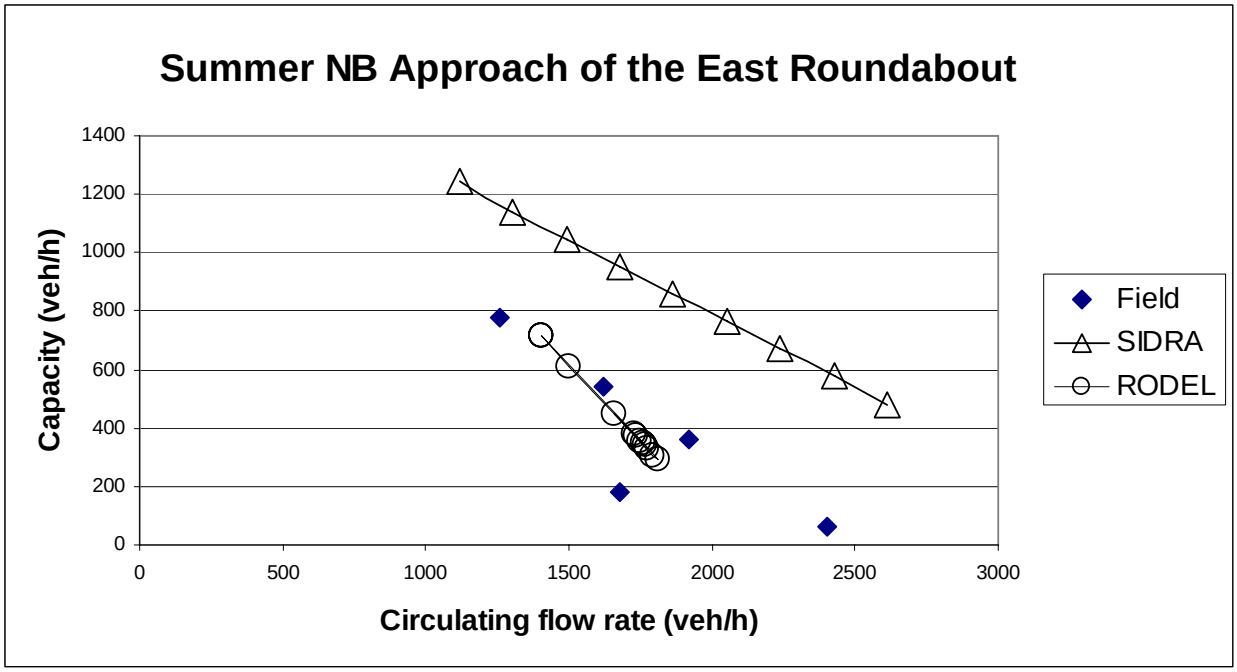

Figure 40 Summer Comparison of Capacity Estimates between RODEL and SIDRA for the NB Approach of the East Roundabout

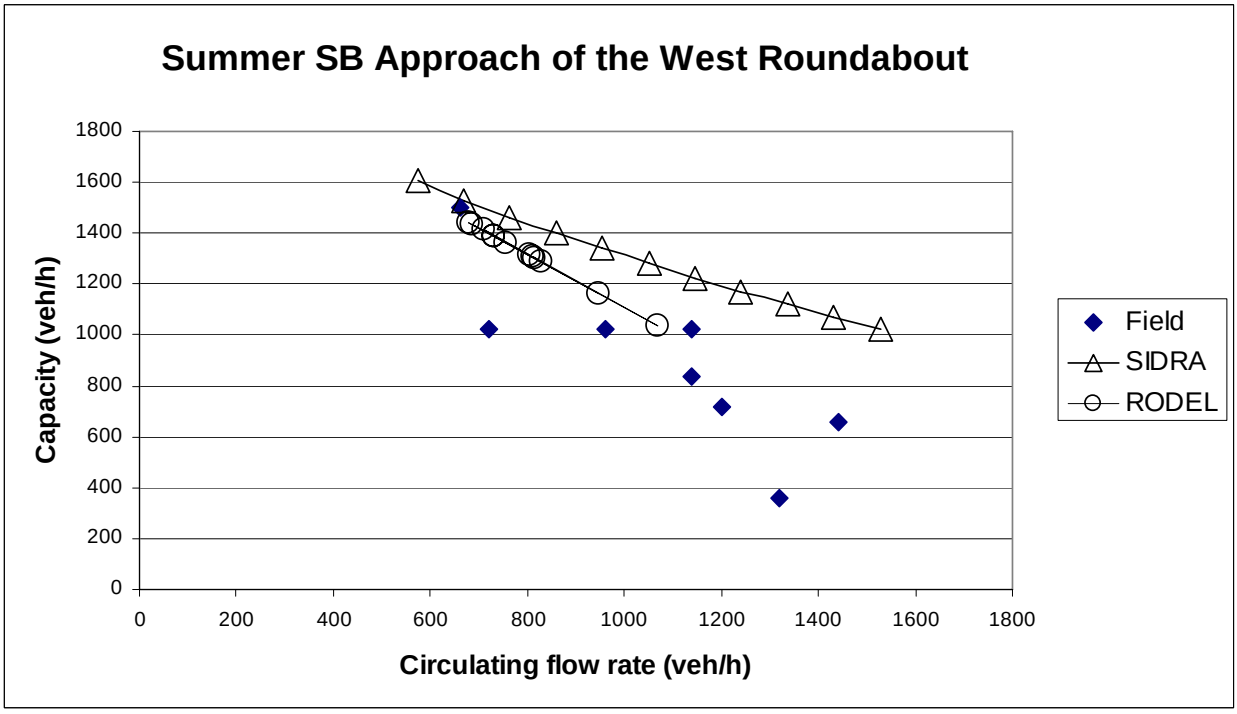

Figure 41 Summer Comparison of Capacity Estimates between RODEL and SIDRA for the SB Approach of the West Roundabout

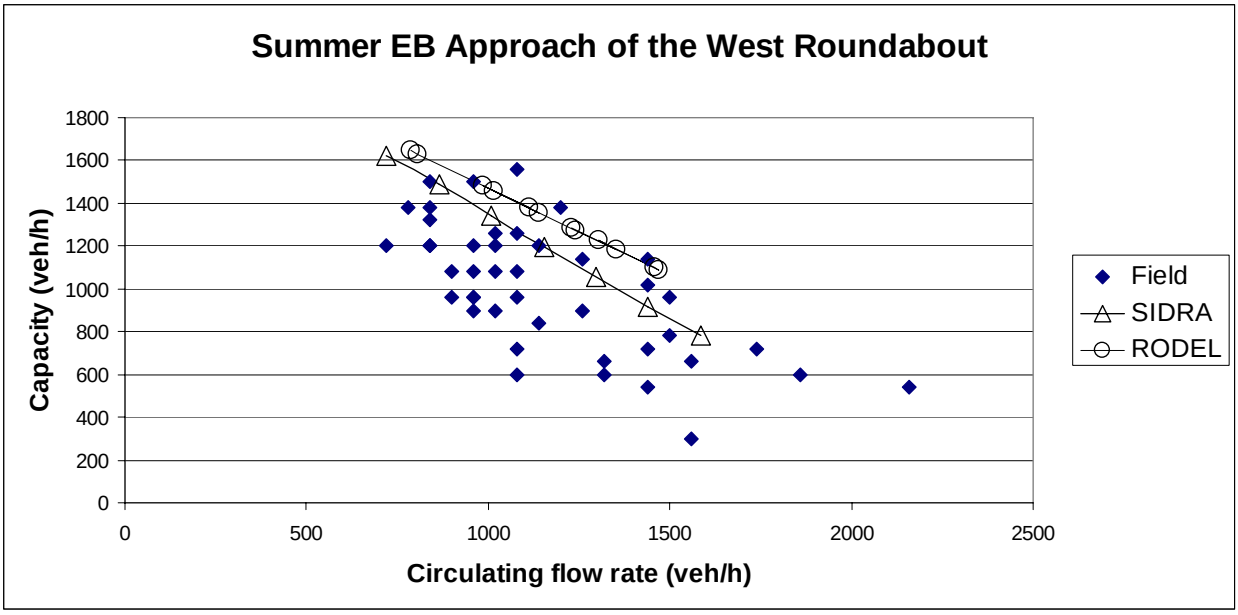

Figure 42 Summer Comparison of Capacity Estimates between RODEL and SIDRA for the EB Approach of the West Roundabout

The above figures show that with the exception of the EB approach of the west roundabout, RODEL's capacity estimates are closer to the field values than SIDRA's. The finding is confirmed with a comparison of the RMSE values between model estimates and field values (see Table 17).

Table 17 RMSE of Capacity Estimates of RODEL and SIDRA

Date	Roundabout	Approach	Average Field Circulating Flow (Vehicles/Hour)	RODEL Capacity RMSE	SIDRA Capacity RMSE
12/18/2008	East	NB	1,724	200.7	657.5
	West	SB	885	330.7	486.2
	West	EB	1,116	321.8	287.7
05/13/2009	East	NB	1,776	221.5	536.6
	West	SB	1,072	221.4	398.4
	West	EB	1,165	402.5	306.7
			Average	283.1	445.5

The predicted delays and queue lengths of RODEL and SIDRA comparing to field observations are shown in **Table** 18, which shows that RODEL overestimated delays and queue lengths for most approaches. In contrast, SIDRA underestimated delays and queue lengths. Note that the RODEL estimates do not include the delay and queue length caused by the right turn channels, because RODEL does not produce delay and queue length values for the NB approach of the east roundabout. Thus, if the delay and queue caused by the right turn movements were to be combined, RODEL's overestimation would be higher for most approaches than the values shown in **Table** 18.

Table 18 Comparison of Delay and Queue Length Estimates between RODEL and SIDRA

Season	Roundabout	Approach	Measurement [1]	RODEL estimates [2]	SIDRA estimates	Field	RODEL dev from field [3]	SIDRA dev from field [3]
Winter	East	NB	Ave Delay (sec/veh)	149	21.56	131	14%	-84%
			Ave Queue (veh)	17.7	1.2	12	48%	-90%
	West	SB	Ave Delay (sec/veh)	7.3	17.5	17.5	-58%	0%
			Ave Queue (veh)	1.7	4	5	-66%	-20%
	West	EB	Ave Delay (sec/veh)	128.8	21.24	43	200%	-51%
			Ave Queue (veh)	44.1	7.3	15	194%	-51%
Summer	East	NB	Ave Delay (sec/veh)	151.3	23.8	54	180%	-56%
			Ave Queue (veh)	17.4	2.3	6	190%	-62%
	West	SB	Ave Delay (sec/veh)	23.3	25.8	22	6%	17%
			Ave Queue (veh)	6.1	7.6	6	2%	27%
	West	EB	Ave Delay (sec/veh)	525.9	112.88	147	258%	-23%
			Ave Queue (veh)	241.9	31.2	50	384%	-38%
			Total	1314.5	276.4	508.5	259%	54%

It was discussed previously that SIDRA's estimation error can be related to the circulating flow (see **Table** 14). An approach with a small circulating flow can result in a small prediction error for delay and queue length estimates in SIDRA. However, RODEL's prediction errors of delays and queue lengths do not show particular patterns.

8. VISSIM ANALYSIS

In addition to the analyses performed with RODEL and SIDRA, we also created a VISSIM simulation model to investigate the mechanism of queue formation on the EB approach of the west roundabout. In addition to the two roundabouts, the VISSIM model also includes the upstream traffic signal at the intersection between Old Seward highway and Dowling road (see **Figure** 43). The simulation model enables us to identify and test measures designed to reduce the delay and queue length on the EB entrance approach of the west roundabout.

Figure 43 VISSIM Simulation

The VISSIM model was created by first entering the field-measured geometric and flow rates data collected in the summer, for which we have complete recordings of both the roundabout and the upstream signalized intersection operation. Numerous calibration runs were then carried out to adjust model parameters such that the queue length and delay values produced by the simulation resemble the corresponding field-measured values.

8.1 Delay and Queue Calibration

Table 19 shows the calibration results. The approach-based VISSIM queue and delay values were derived by averaging the values of 20 simulation runs.

Table 19 VISSIM Delay and Queue Length Estimates

Season	Roundabout	Approach	Measurement	VISSIM Approach Values	Field Values	Error*
Summer	East	NB	Ave Delay (sec)	63	54	9
			Ave Queue (veh)	8	6	-2
			Max Queue (veh)	32	18	14
	West	SB	Ave Delay (sec)	14	22	-8
			Ave Queue (veh)	3	6	-3
			Max Queue (veh)	36	28	12
	West	EB	Ave Delay (sec)	152	147	5
			Ave Queue (veh)	65	50	15
			Max Queue (veh)	129	101	28
*Error = VISSIM Value – Field Value						

The values in **Table** 19 show that the calibrated baseline model is able to reasonably replicate the delay at the roundabouts. The errors of the VISSIM-estimated delay and the corresponding field values are within 10 seconds. The error for maximum queue length in vehicles is larger than that for average queue length. This is in part due to the fact that the VISSIM queue length estimates are provided in distance. Estimation of the number of vehicles over a certain distance is likely to result in larger error as the distance increases. Thus, the errors of maximum queue (i.e., longer distance than average queue) in vehicles appear to be larger than the errors for the average queue.

8.2 VISSIM Capacity Estimation

The approach capacities produced by the VISSIM base model capacities are extracted in the same way by which the field capacities were extracted. The method extracts field capacities as field entering flow rates per queued minute during which the consecutive queues on each lane contain no less than 5 vehicles. Because VISSIM outputs are approach-based, each approach with a persistent queue of at least 10 vehicles (i.e., 5 vehicles per lane) is considered capacity-saturated. The entering flow during a capacity-saturated minute is considered the capacity of the approach.

The graphs of VISSIM-predicted and field capacities and circulating flow rates are shown in **Figure** 44 to **Figure** 46. Note that for the SB approach of the west roundabout, the VISSIM model only produced one minute of persistent queue for which the 10 vehicles threshold is met. In order to produce sufficient number of data points for the capacities versus circulating flow plot, we included data points from minutes that have at least 7 vehicles per approach. In Figure 38, the number of vehicles per minute is noted on each data point.

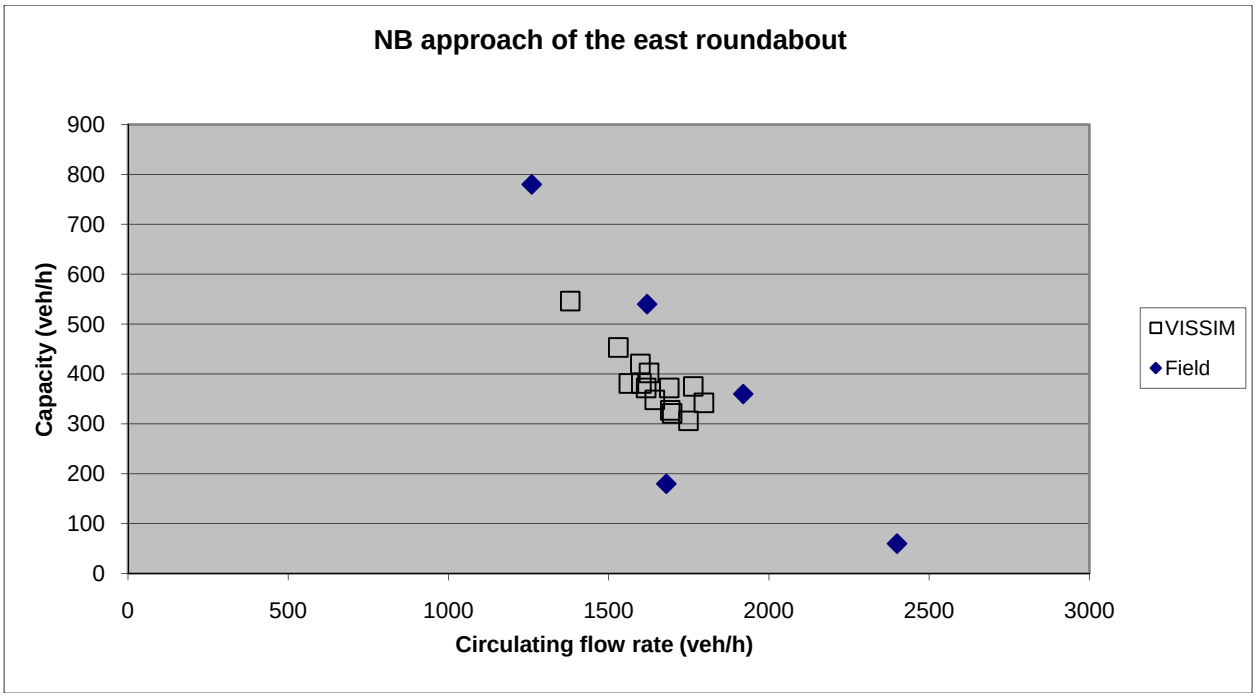

Figure 44 VISSIM Capacity and Circulating Flow Estimates for the NB Approach of East Roundabout

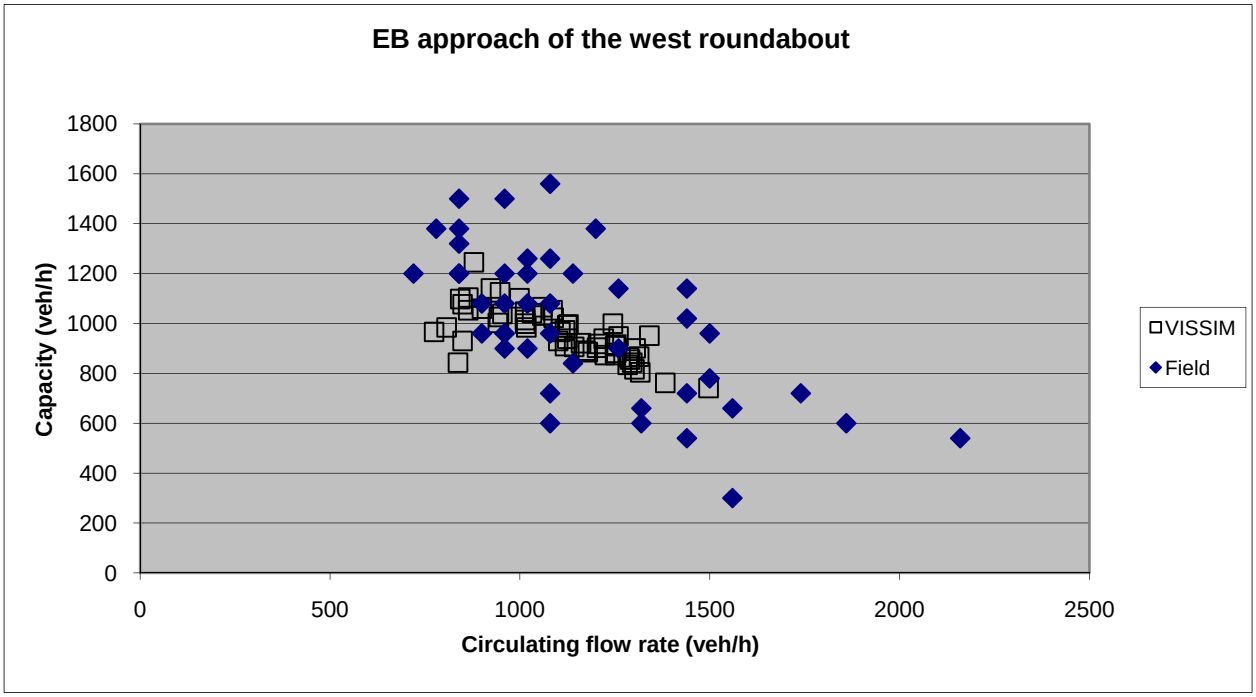

Figure 45 VISSIM Capacity and Circulating Flow Estimates for the NB Approach of West Roundabout

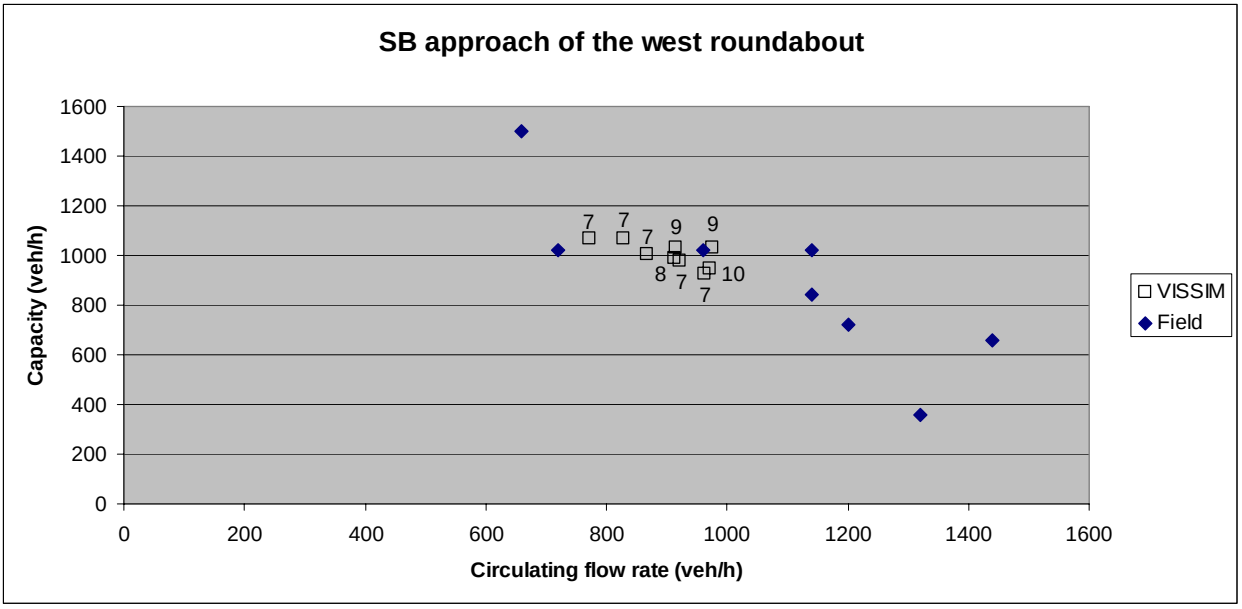

Figure 46 VISSIM Capacity and Circulating Flow Estimates for the SB Approach of West Roundabout

As can be seen from the figures, the VISSIM model is able to produce capacity estimates that are located within the center of the field data clusters. The tendency is most obvious for the EB approach, for which RODEL and SIDRA estimates are located on the upper edge of the field data cluster (see **Figure** 42).

8.3 Simulation for Potential Mitigation Measures

Based on the results of our study, we identify that the reason for the excessive queue on the EB approach is mainly due to the large number of vehicles that enter the EB entrance approach in a 15 to 20 minute period during the evening peak hour. Thus, mitigation measures intended for the reduction of the EB queue length need to reduce the flow rate that enters the EB entrance approach on Dowling road.

8.3.1 Reduction of Upstream Flow on Eastbound Dowling Road

The Alaska Department of Transportation and Public Facilities has plan of constructing a pair of new roundabouts at another Seward Highway ramp terminal southerly of the Dowling roundabouts. Once completed, the new ramp terminal will take some vehicles away from the Dowling roundabouts, resulting in reduced vehicle flow for the EB approach of the west roundabout We designed a series of VISSIM simulation runs to study how much reduction in vehicle flow on the EB entrance approach will result in an acceptable level of delay and queue on this approach.

We tested a total of eight simulation runs. For each run, the total EB upstream flow (i.e., the sum of the three movements indicated by the flow arrows in Figure 47) entering the eastbound Dowling road from the signalized intersection at Old Seward and Dowling is a proportion of the original flow. For example, the total EB upstream flow for the second simulation run is 90% of the original total flow. The 10% reduction in total flow (i.e., 117 vehicles) is deducted from the three movements that made up the total EB upstream flow, based on the ratio of a movement's volume to the total flow.

We began the simulation runs at 100% total EB upstream flow and ended the simulation at a run whose EB upstream flow is 30% of the original flow. When the EB upstream flow is reduced to 30% of its original flow, the average EB queue length is reduced to 0. Table 20 shows the results of the simulation runs. Note that for each volume reduction level, the queue length and delay value are the average values of 20 simulation runs.

Figure 47 EB Dowling Road Upstream Movements (Source: Google Maps®)

Table 20 Results of VISSIM Simulation Runs with Reduced EB Upstream Flows

	100% Volume	90% Volume	80% Volume	70% Volume	60% Volume	50% Volume	40% Volume	30% Volume
Total flow entering EB Dowling road from the upstream signal (veh)	1170	1053	936	819	702	585	468	351
WR EB average delay (sec)	152	86	41	23	17	12	10	7
WR EB average queue (veh)	32	16	6	3	2	1	1	0
WR EB max queue (veh)	65	49	28	18	12	9	7	5
WR SB average delay (sec)	14	15	15	16	16	16	16	17
WR SB average queue (veh)	2	2	2	2	2	2	2	2
WR SB max queue (veh)	18	18	18	17	18	19	17	19
ER NB average delay (sec)	63	41	29	22	18	14	11	9
ER NB average queue (veh)	4	2	2	1	1	1	0	0
ER NB max queue (veh)	16	11	9	8	8	7	6	5

Table 20 shows that with each incremental reduction of the upstream flow on the EB approach, the average delay on the EB entrance approach of the west roundabout can be effectively reduced. From 100% to 70%, each 10% reduction in the EB upstream flow can reduce the average delay of the EB entrance approach at the roundabout by 50%. When the flow reduction is lower than 70%, each 10% reduction in the EB upstream flow continue to reduce the EB average delay, although at a reduction rate smaller than 50%.

The simulation results show that a reduction of the EB upstream flow at 70% of the original flow can result in an acceptable level of delay and queue length. The maximum EB queue length during the peak 15 minutes is approximately 18 vehicles. This is a substantial reduction from its current value at 65 vehicles, which reach and block the upstream signal.

The simulation runs also show that the reduction in the upstream EB flow on Dowling road can help reduce the delay at the NB entrance approach of the east roundabout. The NB approach of the east roundabout currently incurs long delay due to high circulating flows that come from the upstream EB Dowling road. If the EB upstream flow were to be reduced, the delay at the NB approach of the east roundabout could also be reduced for the corresponding lower circulating flow. However, the reduction of the NB approach delay comes with small amount of increase for delay at the SB approach of the west roundabout. The delay increase at the SB approach is due to the increased circulating flow coming from the NB approach of the east roundabout.

8.3.2 No Turn on Red from Old Seward Highway to E. Dowling Road

Using the VISSIM simulation model, we experimented with another potential mitigation measure. In the simulation, we set up the signal at the intersection between Old Seward Highway and Dowling Road to prohibit right turn on red from NB Old Seward Highway to EB Dowling Road (see movement arrow #3 in Figure 39).

We tested two No Turn On Red (NTOR) options: 1) the NB right turn movement is only allowed concurrently with the NB through movement, and 2) in addition to its concurrently movement with NB through, the NB right turn movement also overlaps the EB/WB left turn movement.

Table 21 shows the simulation results of the two NTOR options. The numbers reported for each option is again the average of 20 simulation runs.

Table 21 NTOR VISSIM Simulation Results

	Base Model	NTOR 1	NTOR 2
Signal NBR average delay (sec)	35.13	95.22	74.50
Signal NBR average queue (veh)	4.23	8.31	6.66
Signal NBR max queue (veh)	19.82	27.52	26.25
West Roundabout EB average delay (sec)	151.28	142.10	143.64
West Roundabout EB average queue (veh)	63.98	59.30	60.74
West Roundabout EB max queue (veh)	128.94	125.95	128.26
West Roundabout SB average delay (sec)	14.68	14.43	13.98
West Roundabout SB average queue (veh)	3.21	3.13	2.89
West Roundabout SB max queue (veh)	36.34	32.25	31.10
East Roundabout NB average delay (sec)	59.46	58.02	60.2
East Roundabout NB average queue (veh)	7.77	7.63	7.78
East Roundabout NB max queue (veh)	31.73	31.56	30.88

The results show that NTOR can reduce the delay and queue length at the EB approach of the west roundabout, although the reduction is fairly minimal. The small amount of reduction for the queue length and delay at the EB approach of the wet roundabout comes with the cost of significant amount of delay increase for the NB right turn movement at the Old Seward/Dowling intersection.

Option 2 has slightly longer queue length and delay than option 1, because option 2 allows more right turn vehicles to enter EB Dowling Road than option 1 through the overlap phase with EB/WB left turn.

Based on the simulation, NTOR does not appear to be an effective measure to reduce the queue length and delay at the EB approach of the west roundabout. The minimal amount of delay reduction can not justify for the large amount of increase in delay that the NB right turn movement at the Old Seward/Dowling would suffer, if turning on red from this approach were to be prohibited.

The results of our simulation runs demonstrated the advantage of the VISSIM simulation over analytical tools such as RODEL and SIDRA in that a VISSIM model enables the evaluation of two roundabout set and the upstream signal as an integrated system. Mitigation measures designed to change a particular approach of the roundabouts or the signal will have impacts on other element of the system.

9 PEDESTRIAN SAFETY ANALYSIS

The original research plan for this part of the project intends to study issues related to pedestrian safety at the roundabouts by quantifying drivers' yielding behavior. The plan called for the deployment of investigators acting as pedestrians attempting to use crosswalks at the Dowling roundabouts during summer evening peak hours. The investigators were not to cross the street, but to wait for drivers' response. The attempt was to be made at every roundabout entrance and exit that has a cross walk. The purpose of the attempt was to find out how many drivers would yield to pedestrians at the roundabout.

The NCHRP 527 report on roundabouts in the US includes a section on pedestrian safety analysis that used the videos collected for operational studies to analyze drivers' yielding behavior to pedestrians crossing the streets of the roundabouts. For this part of the study, prior to the field work, we expected to produce similar results for comparison with the NCHRP project results.

The field investigation was indeed carried out as intended. However, the traffic conditions in the field were very different from expected, making the original research plan invalid. The field work continued for approximately 30 to 40 minutes before being forced to stop by a near-crash involving a vehicle yielding to the investigator acting as a pedestrian.

Although we didn't manage to collect data for quantitative analysis, the field experience still offers much needed qualitative information about pedestrian safety at the Dowling roundabouts. We used the information to contrast and generalize findings from the pedestrian safety study in the NCHRP 527 report, which was assessed quantitatively. This section of the report begins with a brief summary of the NCHRP pedestrian study. We then describe our field experience, before validating and contrasting our findings with the NCHRP results.

9.1. NCHRP Report 527 Findings on Roundabout Pedestrian Safety Issues

The NCHRP Report 527: Roundabouts in the United States documents the process and results of a comprehensive study examining many aspects of roundabout applications in the US. Central to this study is a data collection effort that used video cameras to capture roundabout operations, including pedestrian crossing, at various roundabouts in different states. It has been noted earlier that the data collection took part in 2003 and 2004, before the completion of the Dowling roundabouts.

The part of the study on pedestrian safety used the video records collected from 7 of the study roundabouts to analyze various aspects of pedestrian safety issues at the roundabouts. One of the aspects analyzed is driver yielding (to pedestrians) behavior. Three types of driver yielding behavior were defined:

- Active Yield: Drivers slowed or stopped for a crossing pedestrian or a pedestrian waiting on the curb or the middle island to cross. The pedestrian was the only reason the driver stopped or slowed.
- Passive Yield: The driver yielded to the pedestrians, but prior to the yield he/she had already stopped for another reason such as queuing to enter the roundabout or stopping for a prior pedestrian crossing.
- Did Not Yield: The motorist did not yield to a crossing pedestrian or a pedestrian waiting on the curb or splitter island to cross.

Results of the yielding behavior analysis depend on where the pedestrians were before crossing and the number of circulating lanes of the roundabouts. **Figure** 48 shows the results for the cases when the pedestrians started the crossing from the roundabout entry leg. The results are separated into driver yielding to pedestrians on the entry leg and yielding on the exit leg. Figure 49 shows the results for cases when pedestrians began crossing on the exit legs of the roundabouts.

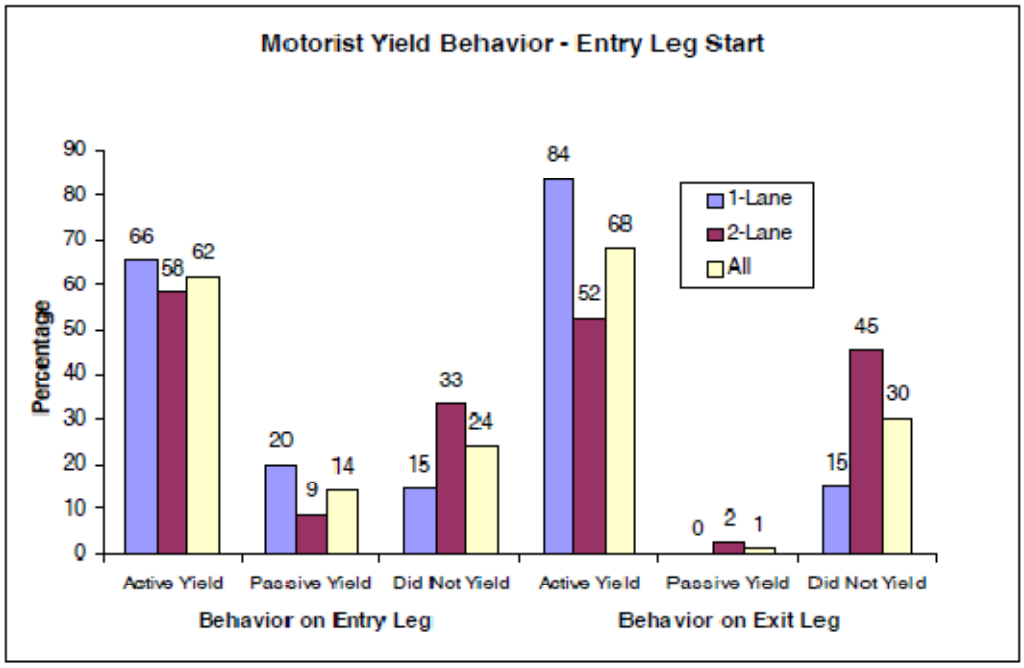

Figure 48 NCHRP Report 527 Findings on Driver Yielding Behavior-Pedestrians started on the Entry Legs

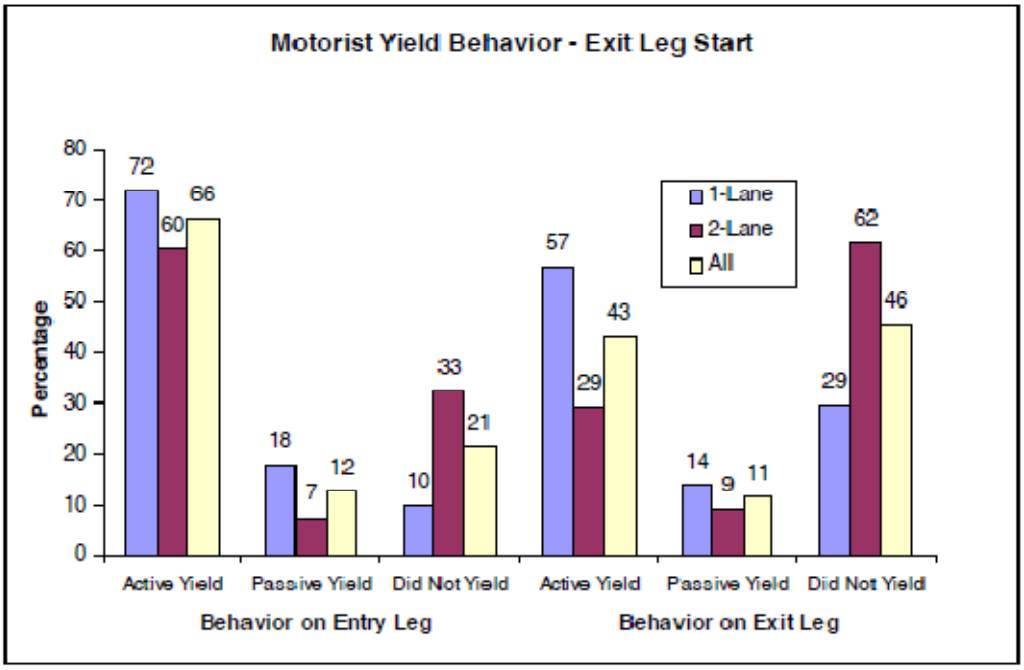

Figure 49 NCHRP Report 527 Findings on Driver Yielding Behavior-Pedestrians started on the Exit Legs

The two figures show that there was a higher percentage of did-not-yield behavior observed on two-lane roundabouts than one-lane roundabouts for all four types of crossing situations. Exit legs have higher percentage of did-not-yield behavior. In addition, drivers were less likely to yield to pedestrians who started crossing at the exit legs. For two-lane roundabouts, there was a 62 percentage of did-not-yield on the exit legs, when pedestrians started crossing on the exit legs. Once the pedestrians moved onto the entry legs, the active-yield percentage increased and the did-not-yield percentage decreased dramatically.

9.2 Field Observation

During most of the evening peak hour, three of the four entrance approaches had extensive lengths of stopped vehicle queues. We observed that the types of drivers' yielding to pedestrians depend largely to where the queues were located. **Figure** 50 shows the layout of the crosswalks and the locations of the entry legs with queues.

Based on the location of the crossing legs, we can characterize our observation at the roundabouts into four groups of behavior:

1. On the entry legs that had queues, we observed passive-yield and did-not-yield.
2. Active-yield on the entry legs was only observed when queue length was reduced after the peak traffic condition.
3. On the exit legs, it was predominantly did-not-yield, which occurred almost exclusively, regardless of the traffic volume.
4. On the WB entry leg and the right-turn channels where there were no queue, active yield did occurr sparingly.

Figure 50 Locations of Crosswalks and Queued Approaches on the Dowling Roundabouts

On three of the four entry legs that had extensive queues, the queues of stopped vehicles at the yield lines already created gaps for the pedestrians and the drivers expect the pedestrians to take the gaps. As soon as a driver became the first in the queue, it appeared that all of his/her attention was on spotting the next available gap to enter. If the pedestrians stood on the curb and did not cross the entry leg actively, most drivers at the yield line would move across the yield line to take the gap, because a gap in the vehicle stream was not easy to come by and was expected to close quickly.

An interesting observation we had is that after a long wait in the queue, drivers that finally got to the first few positions at the queue may become impatient for any further hold up at the yield line. Drivers of the first two to three vehicles in the queue, as long as their views into the circulating flow were not blocked, would all be looking for gaps, even if he/she is yet to be the first vehicle at the yield line. If when a gap appeared and the first vehicle did not move immediately (e.g., yielding to a pedestrian), the risk for rear-end collision could increase because the second vehicle saw the gap too and expected to move.

During the investigation, we encountered a near-crash because a driver yielded to the investigator and ironically created a conflicting situation with the vehicle that trailed behind. The pictures in Figure 51 to Figure 53 show the sequence of events that led to the near-collision. The right turning vehicle queue shown in Figure 51 had been waiting for a gap for over two minutes prior to this point. After a gap appeared, the first truck gestured the investigator to walk through. While the investigator ran across the street, the gap was about the close and the SUV that trailed the first truck attempted to overtook the truck and nearly hit the truck from behind. The truck driver immediately got off the car

to confront the driver of the SUV. Fortunately, no altercation ensured as the SUV soon fled the scene and avoided the confrontation. The investigation was promptly stopped after the incidence.

Figure 51 The truck yielded to the investigator (circled)

Figure 52 The SUV (circled) attempted to overtake the truck

Figure 53 The truck driver (circled) confronted the SUV driver

For yielding on the exit legs, we found that if the investigators stayed on the curb or the middle island without actively taking gaps, no drivers yielded to the investigators. The traffic condition that made it difficult for the drivers to yield actively at the exit leg is the small headways between two circulating vehicles. Yielding to pedestrians or any other unexpected situations can create dangerous situation for the following vehicles. Our field observation indicated that vehicles in such a dense traffic stream appeared to be aware of the cars that trailed closely behind, and would carry on its course without suddenly slowing down or stopping for a pedestrian, unless the pedestrian was already on the crosswalk.

Based on our experience in the field, we found that high traffic volume combined with long vehicle queue and delays at the entrance approaches made it difficult for drivers to actively yield to pedestrians crossing the roundabouts. Under such situations, pedestrians actively sought gaps to cross streets without expecting drivers to yield to them. Drivers would be forced to slow down for pedestrians who had already on the crosswalk in motion. But, very rarely would drivers react to pedestrians who stood still by the side of the road. It is thus difficult for the investigators to generate data for quantitatively analysis with investigators waiting as pedestrians, but not actively crossing the road.

We also performed the same field experiment at the signalized intersection of Lake Otis and Tudor Road. Our experience at the crosswalks of the signalized intersection was very similar to that at the roundabouts. Drivers would slow down or stop for pedestrians already stepped onto the crosswalks. Drivers rarely responded to people who stood by the side of the road.

Our field study suggests that observational studies that capture the behavior of real pedestrians should be better suited for the purpose of assessing pedestrian safety at the roundabouts. Qualitative analysis based on the observation can help us understand the behavior of real pedestrians and the interaction between pedestrians and vehicles using the roundabouts. A study attempting to quantitatively assessing pedestrian safety will only be successfully after we can clearly define the situations dangerous to pedestrians.

9.3 Comparing the Dowling Experience with the NCHRP Findings

One of the most important differences between roundabouts in the NCHRP study and the Dowling roundabouts is that there were very few roundabouts in the NCHRP study that were operating at capacity. There was little to no queue at the entry legs of the NCHRP roundabouts and the active-yield behavior was more likely to happen because there was sufficient headway between vehicles. However, we do find areas of consistency in terms of findings between our observations and those of NCHRP.

In the followings, we list the three major findings of NCHRP and provide our comments after each one of them.

NCHRP: Exit lanes appear to place crossing pedestrians at a greater risk than entry lanes. Motorists were less likely to yield to pedestrians on the exit side (38% of the time) compared to the entry side (23% of the time).

> We agree with this finding and offer a rationale for the tendency of non-yielding on exit legs. Upon approaching the crosswalks of the entry legs, drivers were being slowed down by the geometric and operational features of the roundabouts, and active yielding could occur more safely and naturally. One the contrary, we observed that, upon approaching the crosswalk of the exit legs, vehicles had picked up speed of up to 35 mph and the headway between vehicles could be as small as 5 seconds. With such speed and tense headway, it is much more difficult for drivers to slow down and yield to pedestrians on the exit legs.

NCHRP: Two-lane legs are more difficult for pedestrians to cross than one-lane legs, primarily because of the non-yielding behaviors of motorists. On two-lane legs, the non-yielding percentage was 43%. The lack of yielding was perhaps reflected in the observed pedestrian behaviors. Single-lane legs resulted in hesitation crossings 24% of the time, while two-lane legs produced hesitations 33% of the time.

> Based on our observation, we believe that the increased tendency for non-yielding on two-lane legs was mainly due to traffic volume. Two-lane roundabouts are designed to carry larger traffic volume than their one-lane counterparts. Prior to the forming of long queue during the peak traffic conditions, we had observed active yielding on the queue-less entry legs and the right turn exit channels. The tendency for active yielding was all but disappear once the extensive queue began to form. Some natural consequences of larger traffic volume that contribute to

non-yielding are smaller headways between vehicles and more intense stress on the drivers.

NCHRP: Roundabouts result in the type of behaviors expected when compared to other types of intersections and levels of traffic control. Roundabouts, which are under yield control, produced motorist and pedestrian behaviors that were between the behaviors observed at crossings with no traffic control and those observed at crossings with signal or stop control.

Although we do not have quantitative data from our observation to comment on this finding, our observation at both the roundabouts and a busy signalized intersection show that drivers' yielding behavior depends very much on the existence of queue, traffic volume (i.e., resulting in smaller headways and driver stress), and vehicle speed approaching the crosswalks. The three factors appear to have work on roundabouts and signalized intersections.

In summary, we find that during the peak traffic conditions (i.e., 15 to 20 minutes during the evening peak hour) when there are extensive queues on the entry legs of the roundabouts, there appear to be realistic safety concerns for pedestrians crossing the Dowling roundabouts. During the time, pedestrians have to actively seek gaps in traffic stream due to the non-existence of active yielding.

Consistent with the NCHRP findings and recommendations, we recommend that an emphasis be placed on designing exit lanes to facilitate active yielding for pedestrians in the design of roundabouts in the future. The NCHRP report lists three specific countermeasures for this purpose:

1. Changes in design: Design changes could include reduction in the exit lane radius, reduction in circulating lane widths, and/or relocation of the crosswalks.
2. Changes in operations: Operational changes may include warning signs and warning devices that are activated when a pedestrian is present (e.g., pedestrian push buttons). We also recommend placing speed limit on the circulating lanes as one of the countermeasures.
3. Targeted enforcement and education: Enforcement and education should focus on improving user compliance with existing rules of using the roundabouts.

10. ANALYSIS OF CRASH EVENTS BEFORE AND AFTER THE ROUNDABOUT CONSTRUCTION

To analyze crash tendencies associated with the roundabouts, we obtained crash statistics at the two ramp terminals of Seward Highways and Dowling Road. The roundabouts began operation in August of 2004. Prior to the construction of the roundabouts, the two terminals were controlled by two traffic signals. Tables 22 and 23 show the crash statistics of the SB terminal and the NB terminal from 1998 to 2007. The data were obtained from Alaska Department of Transportation and Public Facilities.

Table 22 Summary of SB Ramp Terminal Crash Events

YEAR	PROPERTY DAMAGE ONLY	MINOR INJURY	MAJOR INJURY	FATALITY	TOTAL	COMPUTED AVG AADT	COMPUTED ACCIDENT RATE
1998	4	4	0	0	8	24751	0.885
1999	7	0	0	0	7	24590	0.779
2000	2	3	0	0	5	25680	0.553
2001	8	0	0	0	8	27192	0.806
2002	7	2	1	0	10	24782	1.105
2003	12	2	0	0	14	24690	1.553
2004	6	2	0	0	8	21800	1.005
2005	29	5	0	0	34	23716	3.927
2006	14	6	0	0	20	23348	2.346
2007	6	1	0	0	7	24436	0.784

Table 23 Summary of NB Ramp Terminal Crash Events

YEAR	PROPERTY DAMAGE ONLY	MINOR INJURY	MAJOR INJURY	FATALITY	TOTAL	COMPUTED AVG AADT	COMPUTED ACCIDENT RATE
1998	9	2	0	0	11	24218	1.244
1999	12	5	0	0	17	24145	1.928
2000	9	4	0	0	13	25065	1.420
2001	9	1	0	0	10	26190	1.046
2002	3	2	0	0	5	25141	0.544
2003	8	5	0	0	13	23640	1.506
2004	20	7	0	0	27	22329	3.312
2005	30	8	0	0	38	23685	4.395
2006	26	8	0	0	34	23614	3.944
2007	22	6	0	0	28	24355	2.924

Comparing the numbers before 2004 and after 2004, we can see that there were more events in every crash category (i.e., Property damage only, minor injury, and major injury) after the roundabouts were in operation. But, we can see that the crash rates had been decreasing every year after 2004, suggesting that drivers were learning to safely negotiate the roundabouts. Because we have only three years of data after the roundabout operation, we need to wait for a few more years before a fair assessment of roundabout crash rate in comparison with traffic signals can be made.

11. CONCLUSIONS

We successfully collected video records of the operation of the two roundabouts, including the turning movements and the extended vehicle queues on three of the four entrance approaches. Based on the data extracted from the video records, we can see that the extended queue on the EB approach of the west roundabout is the result of the unbalanced flow pattern at the roundabouts, in which the EB entering flow rate was substantially higher than the other three entrance approaches. The unbalanced flow pattern also created a high circulating flow in front of the NB approach of the east roundabout. The high circulating flow for the NB approach explains why this approach of the east roundabout had low capacity and high delay and queue values.

We also identify that the overall turning movements at the roundabouts are higher in the summer than winter. The higher total numbers of movements in summer explains why we observed longer queues on the EB approach of the west roundabout in summer than winter. After comparing our field data with those from roundabouts in the UK, Germany, and Australia, we found that the performance of the Dowling roundabout in terms of entry flow and circulating flow are slightly lower than those in the UK and Australia. But, the Dowling numbers are slightly higher than those from Germany. In the future, applying the Dowling data using the Germany models may be tested to see if the model produces better results than those used in the UK and Australia.

We then analyzed the data with RODEL, SIDRA, and VISSIM. It is noted that our RODEL and SIDRA models were un-calibrated. But, the VISSIM model was calibrated to the field-measured delay and queue length. The results of our analysis show that the un-calibrated RODEL and SIDRA models both overestimate the capacities for the queued approaches. RODEL's capacity estimates are closer to the field measurements than SIDRA's.

For queue length and delay estimation, version 1.0 of RODEL cannot model the queue length and delay of roundabouts in presence of right-turn channels. Following the instruction of RSL, a special procedure was applied to model the operation of the two Dowling roundabouts, each with two right-turn channels. However, the procedure does not generate reasonable results for the Dowling roundabouts. When only the delay and queue caused by the entering flow (without the right turn movements) are considered, RODEL overestimated delays and queue lengths for most approaches.

SIDRA's estimation of queue length and delay appears to be more reasonable than RODEL's. However, when compared with field values, SIDRA underestimates the delay and queue length for the two roundabouts.

The VISSIM model was calibrated to field queue length and delay. The calibrated model produced capacity estimates that are closer to the field values than the un-calibrated RODEL and SIDRA models. We designed a series of VISSIM simulation runs to study

how much reduction in vehicle flow on the EB entrance approach will result in an acceptable level of delay and queue on this approach.

The simulation results show that a reduction of the EB upstream flow at 70% of the original flow can result in an acceptable level of delay and queue length at the EB approach of the west roundabout. The maximum EB queue length during the peak 15 minutes is approximately 18 vehicles. This is a substantial reduction from its current value at 65 vehicles, which reach and block the upstream signal.

We also simulated the effect of No Turn On Red (NTOR) from the NB Old Seward Highway to EB Dowling Road. The results of the simulation show that NTOR does not appear to be an effective measure to reduce the queue length and delay at the EB approach of the west roundabout. The minimal amount of delay reduction can not justify for the large amount of increase in delay that the NB right turn movement at the Old Seward/Dowling would suffer, if turning on red from this approach were to be prohibited.

The results of the VISSIM simulation runs demonstrated the advantage of the VISSIM simulation over analytical tools such as RODEL and SIDRA in that a VISSIM model enables the evaluation of two roundabout set and the upstream signal as an integrated system. Mitigation measures designed to change a particular approach of the roundabouts or the signal will have impacts on other element of the system.

We also carried out the driver yielding study as intended. However, the traffic conditions in the field were different from the expected. Our investigation ended after involving in a near collision. Based on our experience in the field, we found that the high traffic volume combined with long vehicle queue and delays at the entrance created realistic risk for pedestrians crossing the roundabouts during the peak traffic conditions (i.e., 15 to 20 minutes during the evening peak hour). We found that drivers would slow down for pedestrians who had already on the crosswalk in motion. But, very rarely would drivers react to pedestrians who stood still by the side of the road. We recommend that an emphasis be placed on designing exit lanes to facilitate active yielding for pedestrians in the design of roundabouts in the future.

Based on the crash statistics of the SB terminal and the NB terminal from 1998 to 2007, we found that there were more events in every crash category (i.e., Property damage only, minor injury, and major injury) after the roundabouts were in operation. But, we also found that the crash rates had been decreasing every year after 2004, suggesting that drivers were learning to safely negotiate the roundabouts. Because we have only three years of data after the roundabout operation, we need to wait for a few more years before a fair assessment of roundabout crash rate in comparison with traffic signals can be made.

REFERENCES

1. Akcelik, R. (2005) Roundabout Model Calibration Issues and a Case Study Paper presented at the 2005 Transportation Research Board Roundabout Conference in Vail, Colorado.
2. *Roundabouts in the United States.* NCHRP Reports 572. Transportation Research Board, Washington, D.C., 2007.
3. *Highway Capacity Manual*. TRB, National Research Council, Washington, DC, 2000.
4. *Roundabouts: An Informational Guide.* Report FHWA-RD-00-067. FHWA, U.S. Department of Transportation, June 2000.
5. *SIDRA INTERSECTION User Guide.* Akcelik & Associates Pty Ltd. July, 2007.
6. *RODEL 1 Interactive Roundabout Design* RODEL Software Ltd.
7. Brilon, W. Roundabouts: A State of the Art in Germany. paper presented at the National Roundabout Conference, Vail, Colorado; May 22 – 25, 2005

APPENDIX I RODEL INPUT VARIABLES

RODEL Inputs

RODEL required inputs in 8 fields shown in Figure 54. The input window of direct flows (Field 8 in Figure 54) would show by pressing F7 key in the main screen. The direct flows input window was shown in Figure 55.

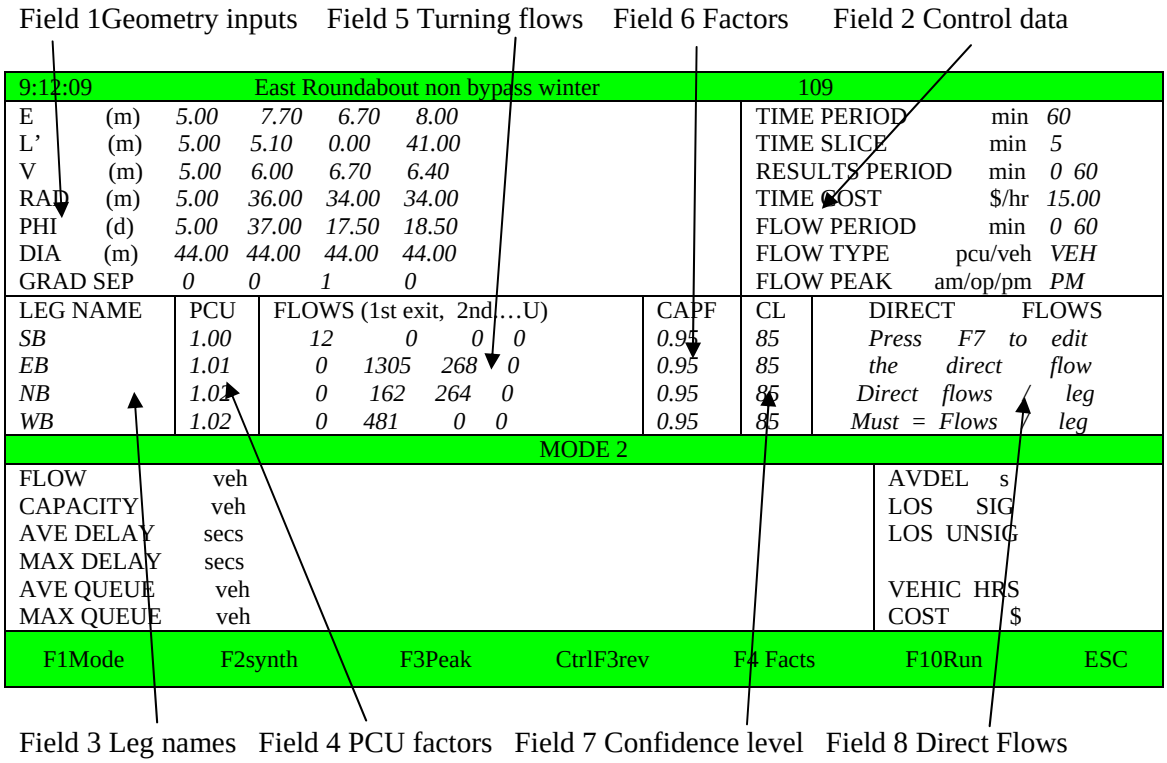

Figure 54: Example of RODEL main screen

9:12:09 East Roundabout non bypass winter 109

PM Peak 12 Time Slices

1	0 - 5	1	144	31	31
2	5 - 10	1	108	36	47
3	10 - 15	1	126	30	33
4	15 - 20	1	114	39	51
5	20 - 25	1	153	33	27
6	25 - 30	1	150	45	44
7	30 - 35	1	143	44	44
8	35 - 40	1	155	27	39
9	40 - 45	1	134	40	41
10	45 - 50	1	118	44	38
11	50 - 55	1	111	33	44
12	55 - 60	1	117	24	42

F7/F8 scroll F9 print ESC

Figure 55: Example of RODEL direct flow input screen

Winter Non-bypass Model of the East Roundabout

RODEL inputs of the model were illustrated in Table 0.1 to Table 0.8.

Table 0.1: Field 1 Geometry inputs

Variable name	Abbreviation	Unit	SB	EB	NB	WB
Entry width	E	meters	5	7.7	6.7	8
Flare Length	L`	meters	5	5.1	0	41
Half width	V	meters	5	6	6.7	6.4
Entry radius	R	meters	5	36	34	34
Entry angle	PHI	degrees	5	37	17.5	18.5
Diameter	D	meters	44	44	44	44
Grade separation	GS	0 or 1	0	0	1	0

Table 0.2: Field 2 Control data

Variable name	Unit	
TIME PERIODS	minutes	60
TIME SLICE	minutes	5
RESULT PERIOD	minutes	0 60
TIME COST	$/hour	15
FLOW PERIOD	minutes	0 60
FLOW TYPE	pcu or veh	VEH
FLOW PEAK	AM OP or PM	PM

Table 0.3: Field 3 Leg names

	Leg name
Leg1	SB
Leg2	EB
Leg3	NB
Leg4	WB

Table 0.4: Field 4 PCU factors

Leg name	PCU factor
SB	1.00
EB	1.01
NB	1.02
WB	1.02

Table 0.5: Field 5 Turning flows

Leg name	1st exit	2nd exit	3rd exit	u-turn
SB	12	0	0	0
EB	0	1305	268	0
NB	0	162	264	0
WB	0	481	0	0

Table 0.6: Field 6 Factors

Leg name	Capacity factor
SB	0.95
EB	0.95
NB	0.95
WB	0.95

Table 0.7: Field 7 Confidence level

Leg name	Confidence level
SB	85
EB	85
NB	85
WB	85

Table 0.8: Field 8 Direct flows

Time slice	PM Peak	Unit	SB	EB	NB	WB
1	0-5	veh	1	144	31	31
2	5-10	veh	1	108	36	47
3	10-15	veh	1	126	30	33
4	15-20	veh	1	114	39	51
5	20-25	veh	1	153	33	27
6	25-30	veh	1	150	45	44
7	30-35	veh	1	143	44	44
8	35-40	veh	1	155	27	39
9	40-45	veh	1	134	40	41
10	45-50	veh	1	118	44	38
11	50-55	veh	1	111	33	44
12	55-60	veh	1	117	24	42

Winter NB Bypass Model of the East Roundabout

RODEL inputs of the model were illustrated in Table 0.1 to Table 0.8.

Table 0.1: Field 1 Geometry inputs

Variable name	Abbreviation	Unit	SB	EB	NB RT	WB
Entry width	E	meters	5	7.7	4	8
Flare Length	L`	meters	5	5.1	0	41
Half width	V	meters	5	6	3.3	6.4
Entry radius	R	meters	5	36	34	34
Entry angle	PHI	degrees	5	37	17.5	18.5
Diameter	D	meters	44	44	44	44
Grade separation	GS	0 or 1	0	0	1	0

Table 0.2: Field 2 Control data

Variable name	Unit	
TIME PERIODS	minutes	60
TIME SLICE	minutes	5
RESULT PERIOD	minutes	0 60
TIME COST	$/hour	15
FLOW PERIOD	minutes	0 60
FLOW TYPE	pcu or veh	VEH
FLOW PEAK	AM OP or PM	PM

Table 0.3: Field 3 Leg names

	Leg name
Leg1	SB
Leg2	EB
Leg3	NB RT
Leg4	WB

Table 0.4: Field 4 PCU factors

Leg name	PCU factor
SB	1.00
EB	1.01
NB RT	1.00
WB	1.02

Table 0.5: Field 5 Turning flows

Leg name	1st exit	2nd exit	3rd exit	u-turn
SB	12	0	0	0
EB	0	1279	263	0
NB RT	235	0	0	0
WB	0	481	0	0

Table 0.6: Field 6 Factors

Leg name	Capacity factor
SB	0.95
EB	0.95
NB RT	0.95
WB	0.95

Table 0.7: Field 7 Confidence level

Leg name	Confidence level
SB	85
EB	85
NB RT	85
WB	85

Table 0.8: Field 8 Direct flows

Time slice	PM Peak	Unit	SB	EB	NB RT	WB
1	0-5	veh	1	141	24	31
2	5-10	veh	1	105	20	47
3	10-15	veh	1	123	19	33
4	15-20	veh	1	111	16	51
5	20-25	veh	1	150	17	27
6	25-30	veh	1	147	19	44
7	30-35	veh	1	140	16	44
8	35-40	veh	1	153	22	39
9	40-45	veh	1	132	32	41
10	45-50	veh	1	116	24	38
11	50-55	veh	1	109	15	44
12	55-60	veh	1	115	11	42

Winter Non-bypass Model of the West Roundabout

RODEL inputs of the model were illustrated in Table 0.1 to Table 0.8.

Table 0.1: Field 1 Geometry inputs

Variable name	Abbreviation	Unit	NB	WB	SB	EB
Entry width	E	meters	5	7.7	6.7	8
Flare Length	L`	meters	5	5.1	0	65
Half width	V	meters	5	6	6.7	6.4
Entry radius	R	meters	5	36	34	34
Entry angle	PHI	degrees	5	37	17.5	18
Diameter	D	meters	44	44	44	44
Grade separation	GS	0 or 1	0	0	1	0

Table 0.2: Field 2 Control data

Variable name	Unit	
TIME PERIODS	minutes	60
TIME SLICE	minutes	5
RESULT PERIOD	minutes	0 60
TIME COST	$/hour	15
FLOW PERIOD	minutes	0 60
FLOW TYPE	pcu or veh	VEH
FLOW PEAK	AM OP or PM	PM

Table 0.3: Field 3 Leg names

	Leg name
Leg1	NB
Leg2	WB
Leg3	SB
Leg4	EB

Table 0.4: Field 4 PCU factors

Leg name	PCU factor
NB	1.00
WB	1.02
SB	1.01
EB	1.03

Table 0.5: Field 5 Turning flows

Leg name	1st exit	2nd exit	3rd exit	u-turn
NB	12	0	0	0
WB	0	495	180	0
SB	0	150	674	0
EB	0	1232	0	0

Table 0.6: Field 6 Factors

Leg name	Capacity factor
NB	0.95
WB	0.95
SB	0.95
EB	0.95

Table 0.7: Field 7 Confidence level

Leg name	Confidence level
NB	85
WB	85
SB	85
EB	85

Table 0.8: Field 8 Direct flows

Time slice	PM Peak	Unit	NB	WB	SB	EB
1	0-5	veh	1	44	60	105
2	5-10	veh	1	66	59	95
3	10-15	veh	1	41	62	83
4	15-20	veh	1	89	63	103
5	20-25	veh	1	43	76	121
6	25-30	veh	1	54	94	178
7	30-35	veh	1	62	91	138
8	35-40	veh	1	41	72	95
9	40-45	veh	1	53	69	80
10	45-50	veh	1	61	69	65
11	50-55	veh	1	61	47	104
12	55-60	veh	1	60	62	65

Winter SB bypass Model of the West Roundabout

RODEL inputs of the model were illustrated in Table 0.1 to Table 0.8.

Table 0.1: Field 1 Geometry inputs

Variable name	Abbreviation	Unit	NB	WB	SB RT	EB
Entry width	E	meters	5	7.7	4	8
Flare Length	L`	meters	5	5.1	0	65
Half width	V	meters	5	6	3.3	6.4
Entry radius	R	meters	5	36	34	34
Entry angle	PHI	degrees	5	37	17.5	18
Diameter	D	meters	44	44	44	44
Grade separation	GS	0 or 1	0	0	1	0

Table 0.2: Field 2 Control data

Variable name	Unit	
TIME PERIODS	minutes	60
TIME SLICE	minutes	5
RESULT PERIOD	minutes	0 60
TIME COST	$/hour	15
FLOW PERIOD	minutes	0 60
FLOW TYPE	pcu or veh	VEH
FLOW PEAK	AM OP or PM	PM

Table 0.3: Field 3 Leg names

	Leg name
Leg1	NB
Leg2	WB
Leg3	SB RT
Leg4	EB

Table 0.4: Field 4 PCU factors

Leg name	PCU factor
NB	1.00
WB	1.02
SB RT	1.02
EB	1.03

Table 0.5: Field 5 Turning flows

Leg name	1st exit	2nd exit	3rd exit	u-turn
NB	12	0	0	0
WB	0	500	182	0
SB RT	113	0	0	0
EB	0	1232	0	0

Table 0.6: Field 6 Factors

Leg name	Capacity factor
NB	0.95
WB	0.95
SB RT	0.95
EB	0.95

Table 0.7: Field 7 Confidence level

Leg name	Confidence level
NB	85
WB	85
SB RT	85
EB	85

Table 0.8: Field 8 Direct flows

Time slice	PM Peak	Unit	NB	WB	SB RT	EB
1	0-5	veh	1	45	12	105
2	5-10	veh	1	67	13	95
3	10-15	veh	1	42	11	83
4	15-20	veh	1	90	11	103
5	20-25	veh	1	44	9	121
6	25-30	veh	1	55	9	178
7	30-35	veh	1	63	8	138
8	35-40	veh	1	41	11	95
9	40-45	veh	1	53	9	80
10	45-50	veh	1	61	12	65
11	50-55	veh	1	61	4	104
12	55-60	veh	1	60	4	65

Winter EB bypass Model of the West Roundabout

RODEL inputs of the model were illustrated in Table 0.1 to Table 0.8**Table 0.8**.

Table 0.1: Field 1 Geometry inputs

Variable name	Abbreviation	Unit	NB	WB	SB	EB RT
Entry width	E	meters	5	7.7	6.7	4
Flare Length	L`	meters	5	5.1	0	65
Half width	V	meters	5	6	6.7	4
Entry radius	R	meters	5	36	34	34
Entry angle	PHI	degrees	5	37	17.5	18
Diameter	D	meters	44	44	44	44
Grade separation	GS	0 or 1	0	0	1	0

Table 0.2: Field 2 Control data

Variable name	Unit	
TIME PERIODS	minutes	60
TIME SLICE	minutes	5
RESULT PERIOD	minutes	0 60
TIME COST	$/hour	15
FLOW PERIOD	minutes	0 60
FLOW TYPE	pcu or veh	VEH
FLOW PEAK	AM OP or PM	PM

Table 0.3: Field 3 Leg names

	Leg name
Leg1	NB
Leg2	WB
Leg3	SB
Leg4	EB RT

Table 0.4: Field 4 PCU factors

Leg name	PCU factor
NB	1.00
WB	1.02
SB	1.01
EB RT	1.02

Table 0.5: Field 5 Turning flows

Leg name	1st exit	2nd exit	3rd exit	u-turn
NB	12	0	0	0
WB	0	495	180	0
SB	0	149	665	0
EB RT	199	0	0	0

Table 0.6: Field 6 Factors

Leg name	Capacity factor
NB	0.95
WB	0.95
SB	0.95
EB RT	0.95

Table 0.7: Field 7 Confidence level

Leg name	Confidence level
NB	85
WB	85
SB	85
EB RT	85

Table 0.8: Field 8 Direct flows

Time slice	PM Peak	Unit	NB	WB	SB	EB RT
1	0-5	veh	1	44	59	20
2	5-10	veh	1	66	58	9
3	10-15	veh	1	41	61	22
4	15-20	veh	1	89	62	11
5	20-25	veh	1	43	75	17
6	25-30	veh	1	54	93	30
7	30-35	veh	1	62	90	15
8	35-40	veh	1	41	71	20
9	40-45	veh	1	53	68	12
10	45-50	veh	1	61	68	8
11	50-55	veh	1	61	47	17
12	55-60	veh	1	60	62	18

Summer Non-bypass Model of the East Roundabout

RODEL inputs of the model were illustrated in Table 0.1 to Table 0.8.

Table 0.1: Field 1 Geometry inputs

Variable name	Abbreviation	Unit	SB	EB	NB	WB
Entry width	E	meters	5	7.7	6.7	8
Flare Length	L`	meters	5	5.1	0	41
Half width	V	meters	5	6	6.7	6.4
Entry radius	R	meters	5	36	34	34
Entry angle	PHI	degrees	5	37	17.5	18.5
Diameter	D	meters	44	44	44	44
Grade separation	GS	0 or 1	0	0	1	0

Table 0.2: Field 2 Control data

Variable name	Unit	
TIME PERIODS	minutes	60
TIME SLICE	minutes	5
RESULT PERIOD	minutes	0 60
TIME COST	$/hour	15
FLOW PERIOD	minutes	0 60
FLOW TYPE	pcu or veh	VEH
FLOW PEAK	AM OP or PM	PM

Table 0.3: Field 3 Leg names

	Leg name
Leg1	SB
Leg2	EB
Leg3	NB
Leg4	WB

Table 0.4: Field 4 PCU factors

Leg name	PCU factor
SB	1.00
EB	1.01
NB	1.01
WB	1.01

Table 0.5: Field 5 Turning flows

Leg name	1st exit	2nd exit	3rd exit	u-turn
SB	12	0	0	0
EB	0	1370	306	0
NB	0	128	279	0
WB	0	568	0	0

Table 0.6: Field 6 Factors

Leg name	Capacity factor
SB	1.00
EB	1.00
NB	1.00
WB	1.00

Table 0.7: Field 7 Confidence level

Leg name	Confidence level
SB	85
EB	85
NB	85
WB	85

Table 0.8: Field 8 Direct flows

Time slice	PM Peak	Unit	SB	EB	NB	WB
1	0-5	veh	1	120	38	56
2	5-10	veh	1	160	31	43
3	10-15	veh	1	146	37	63
4	15-20	veh	1	144	26	59
5	20-25	veh	1	148	32	48
6	25-30	veh	1	159	28	44
7	30-35	veh	1	142	30	43
8	35-40	veh	1	125	29	50
9	40-45	veh	1	151	40	34
10	45-50	veh	1	153	37	44
11	50-55	veh	1	111	44	37
12	55-60	veh	1	117	35	47

Summer NB Bypass Model of the East Roundabout

RODEL inputs of the model were illustrated in Table 0.1 to Table 0.8.

Table 0.1: Field 1 Geometry inputs

Variable name	Abbreviation	Unit	SB	EB	NB RT	WB
Entry width	E	meters	5	7.7	4	8
Flare Length	L`	meters	5	5.1	0	41
Half width	V	meters	5	6	3.3	6.4
Entry radius	R	meters	5	36	34	34
Entry angle	PHI	degrees	5	37	17.5	18.5
Diameter	D	meters	44	44	44	44
Grade separation	GS	0 or 1	0	0	1	0

Table 0.2: Field 2 Control data

Variable name	Unit	
TIME PERIODS	minutes	60
TIME SLICE	minutes	5
RESULT PERIOD	minutes	0 60
TIME COST	$/hour	15
FLOW PERIOD	minutes	0 60
FLOW TYPE	pcu or veh	VEH
FLOW PEAK	AM OP or PM	PM

Table 0.3: Field 3 Leg names

	Leg name
Leg1	SB
Leg2	EB
Leg3	NB RT
Leg4	WB

Table 0.4: Field 4 PCU factors

Leg name	PCU factor
SB	1.00
EB	1.01
NB RT	1.04
WB	1.01

Table 0.5: Field 5 Turning flows

Leg name	1st exit	2nd exit	3rd exit	u-turn
SB	12	0	0	0
EB	0	1370	306	0
NB RT	226	0	0	0
WB	0	568	0	0

Table 0.6: Field 6 Factors

Leg name	Capacity factor
SB	1.00
EB	1.00
NB RT	1.00
WB	1.00

Table 0.7: Field 7 Confidence level

Leg name	Confidence level
SB	85
EB	85
NB RT	85
WB	85

Table 0.8: Field 8 Direct flows

Time slice	PM Peak	Unit	SB	EB	NB RT	WB
1	0-5	veh	1	120	17	56
2	5-10	veh	1	160	9	43
3	10-15	veh	1	146	24	63
4	15-20	veh	1	144	22	59
5	20-25	veh	1	148	11	48
6	25-30	veh	1	159	24	44
7	30-35	veh	1	142	25	43
8	35-40	veh	1	125	17	50
9	40-45	veh	1	151	16	34
10	45-50	veh	1	153	22	44
11	50-55	veh	1	111	25	37
12	55-60	veh	1	117	14	47

Summer Non-bypass Model of the West Roundabout

RODEL inputs of the model were illustrated in Table 0.1 to Table 0.8.

Table 0.1: Field 1 Geometry inputs

Variable name	Abbreviation	Unit	NB	WB	SB	EB
Entry width	E	meters	5	7.7	6.7	8
Flare Length	L`	meters	5	5.1	0	65
Half width	V	meters	5	6	6.7	6.4
Entry radius	R	meters	5	36	34	34
Entry angle	PHI	degrees	5	37	17.5	18
Diameter	D	meters	44	44	44	44
Grade separation	GS	0 or 1	0	0	1	0

Table 0.2: Field 2 Control data

Variable name	Unit	
TIME PERIODS	minutes	60
TIME SLICE	minutes	5
RESULT PERIOD	minutes	0 60
TIME COST	$/hour	15
FLOW PERIOD	minutes	0 60
FLOW TYPE	pcu or veh	VEH
FLOW PEAK	AM OP or PM	PM

Table 0.3: Field 3 Leg names

	Leg name
Leg1	NB
Leg2	WB
Leg3	SB
Leg4	EB

Table 0.4: Field 4 PCU factors

Leg name	PCU factor
NB	1.00
WB	1.02
SB	1.02
EB	1.02

Table 0.5: Field 5 Turning flows

Leg name	1st exit	2nd exit	3rd exit	u-turn
NB	12	0	0	0
WB	0	581	217	0
SB	0	157	785	0
EB	0	1584	0	0

Table 0.6: Field 6 Factors

Leg name	Capacity factor
NB	1.00
WB	1.00
SB	1.00
EB	1.00

Table 0.7: Field 7 Confidence level

Leg name	Confidence level
NB	85
WB	85
SB	85
EB	85

Table 0.8: Field 8 Direct flows

Time slice	PM Peak	Unit	NB	WB	SB	EB
1	0-5	veh	1	80	86	111
2	5-10	veh	1	56	97	148
3	10-15	veh	1	90	99	164
4	15-20	veh	1	67	104	158
5	20-25	veh	1	69	98	137
6	25-30	veh	1	57	75	159
7	30-35	veh	1	61	65	164
8	35-40	veh	1	61	79	148
9	40-45	veh	1	63	67	133
10	45-50	veh	1	67	75	94
11	50-55	veh	1	59	50	87
12	55-60	veh	1	68	47	81

Summer SB bypass Model of the West Roundabout

RODEL inputs of the model were illustrated in Table 0.1 to Table 0.8.

Table 0.1: Field 1 Geometry inputs

Variable name	Abbreviation	Unit	NB	WB	SB RT	EB
Entry width	E	meters	5	7.7	4	8
Flare Length	L`	meters	5	5.1	0	65
Half width	V	meters	5	6	3.3	6.4
Entry radius	R	meters	5	36	34	34
Entry angle	PHI	degrees	5	37	17.5	18
Diameter	D	meters	44	44	44	44
Grade separation	GS	0 or 1	0	0	1	0

Table 0.2: Field 2 Control data

Variable name	Unit	
TIME PERIODS	minutes	60
TIME SLICE	minutes	5
RESULT PERIOD	minutes	0 60
TIME COST	$/hour	15
FLOW PERIOD	minutes	0 60
FLOW TYPE	pcu or veh	VEH
FLOW PEAK	AM OP or PM	PM

Table 0.3: Field 3 Leg names

	Leg name
Leg1	NB
Leg2	WB
Leg3	SB RT
Leg4	EB

Table 0.4: Field 4 PCU factors

Leg name	PCU factor
NB	1.00
WB	1.02
SB RT	1.06
EB	1.02

Table 0.5: Field 5 Turning flows

Leg name	1st exit	2nd exit	3rd exit	u-turn
NB	12	0	0	0
WB	0	604	225	0
SB RT	128	0	0	0
EB	0	1584	0	0

Table 0.6: Field 6 Factors

Leg name	Capacity factor
NB	1.00
WB	1.00
SB RT	1.00
EB	1.00

Table 0.7: Field 7 Confidence level

Leg name	Confidence level
NB	85
WB	85
SB RT	85
EB	85

Table 0.8: Field 8 Direct flows

Time slice	PM Peak	Unit	NB	WB	SB RT	EB
1	0-5	veh	1	83	10	111
2	5-10	veh	1	59	15	148
3	10-15	veh	1	93	11	164
4	15-20	veh	1	70	10	158
5	20-25	veh	1	72	9	137
6	25-30	veh	1	60	8	159
7	30-35	veh	1	64	12	164
8	35-40	veh	1	64	14	148
9	40-45	veh	1	67	6	133
10	45-50	veh	1	68	9	94
11	50-55	veh	1	60	10	87
12	55-60	veh	1	69	14	81

Summer EB bypass Model of the West Roundabout

RODEL inputs of the model were illustrated in Table 0.1 to Table 0.8**Table 0.8**.

Table 0.1: Field 1 Geometry inputs

Variable name	Abbreviation	Unit	NB	WB	SB	EB RT
Entry width	E	meters	5	7.7	6.7	4
Flare Length	L`	meters	5	5.1	0	65
Half width	V	meters	5	6	6.7	4
Entry radius	R	meters	5	36	34	34
Entry angle	PHI	degrees	5	37	17.5	18
Diameter	D	meters	44	44	44	44
Grade separation	GS	0 or 1	0	0	1	0

Table 0.2: Field 2 Control data

Variable name	Unit	
TIME PERIODS	minutes	60
TIME SLICE	minutes	5
RESULT PERIOD	minutes	0 60
TIME COST	$/hour	15
FLOW PERIOD	minutes	0 60
FLOW TYPE	pcu or veh	VEH
FLOW PEAK	AM OP or PM	PM

Table 0.3: Field 3 Leg names

	Leg name
Leg1	NB
Leg2	WB
Leg3	SB
Leg4	EB RT

Table 0.4: Field 4 PCU factors

Leg name	PCU factor
NB	1.00
WB	1.02
SB	1.02
EB RT	1.01

Table 0.5: Field 5 Turning flows

Leg name	1st exit	2nd exit	3rd exit	u-turn
NB	12	0	0	0
WB	0	581	217	0
SB	0	155	776	0
EB RT	219	0	0	0

Table 0.6: Field 6 Factors

Leg name	Capacity factor
NB	1.00
WB	1.00
SB	1.00
EB RT	1.00

Table 0.7: Field 7 Confidence level

Leg name	Confidence level
NB	85
WB	85
SB	85
EB RT	85

Table 0.8: Field 8 Direct flows

Time slice	PM Peak	Unit	NB	WB	SB	EB RT
1	0-5	veh	1	80	85	24
2	5-10	veh	1	56	96	28
3	10-15	veh	1	90	98	24
4	15-20	veh	1	67	103	7
5	20-25	veh	1	69	97	20
6	25-30	veh	1	57	74	20
7	30-35	veh	1	61	64	11
8	35-40	veh	1	61	78	22
9	40-45	veh	1	63	66	19
10	45-50	veh	1	67	74	13
11	50-55	veh	1	59	49	11
12	55-60	veh	1	68	47	20

APPENDIX II SIDRA INPUT VARIABLES

Appendix II: SIDRA Inputs

Leg arrangement of both the east and west roundabout was shown in Figure 56.

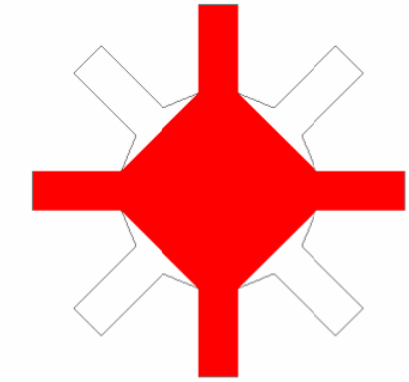

Figure 56: Leg arrangement of both the east and west roundabout

Lane configuration of the two roundabouts was shown in Figure 57.

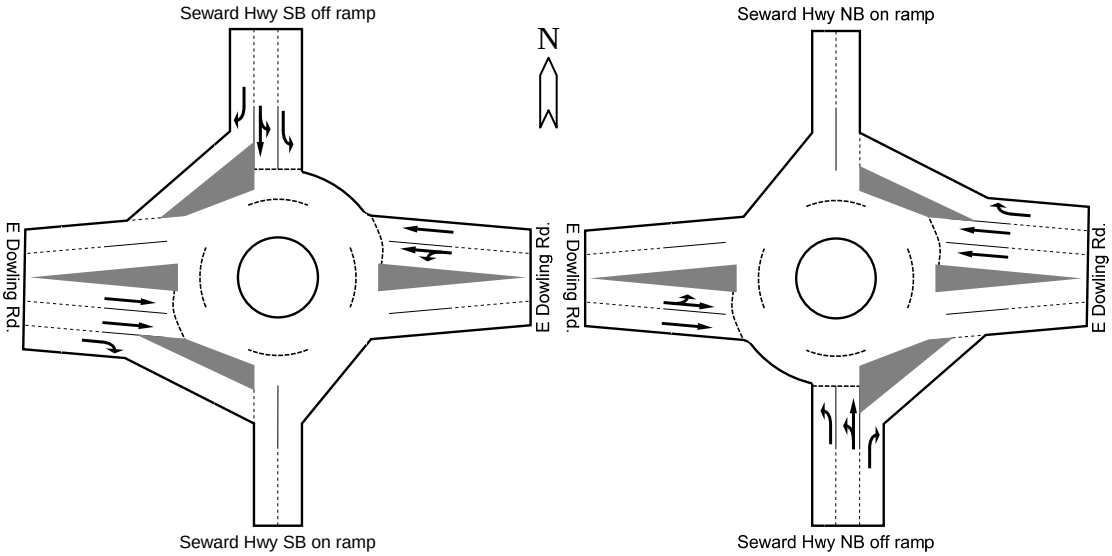

Figure 57: Lane configuration of the east and west roundabout

Winter Model of the East Roundabout

SIDRA inputs of the model were illustrated in Table 0.1 to Table 0.6. It is noted that the table names were the names of the input sections in SIDRA. In Table 0.1, the lane side (i.e., left, middle, right) in an entry/exit is defined along the direction which vehicles traveled forward.

Table 0.1: Approach & Lanes

Approach	Lane	Entry/Exit	Lane discipline	Lane type	Lane width (ft)	Lane length (ft)	Grade (%)	Median (ft)	Short lane
SB	Left	Exit			13.12	1600	2	0	None
	Right	Exit			13.12				
EB	Left	Entry	Left/Through	Normal	11.808	235	1.65	6	
	Right	Entry	Through	Normal	7.872				
	Left	Exit			11.808	235	-1.65		
	Right	Exit			7.872				
NB	Left	Entry	Left	Normal	11.152	1600	-1.5	0	
	Middle	Entry	Left/Through	Normal	10.824				
	Right	Slip Entry	Right	Slip	13.12	200			
WB	Left	Entry	Through	Normal	13.448	1600	-1.65	11	
	Middle	Entry	Through	Normal	17.056				
	Right	Slip Entry	Right	Slip	13.12	179			
	Left	Exit			13.12	1600	1.65		
	Right	Exit			13.448				

Table 0.2: Roundabout

Variable name	Value
Central island diameter (ft)	72
Circulating lane width (ft)	36
Number of circulating lanes	2
Extra bunching (%)	0
Environmental factor	1.2
Entry/Circulating flow adjustment	Medium

Table 0.3: Definitions & Path Data

Approach	Movement	Turn designation	Approach cruise speed (mph)	Exit Cruise Speed (mph)	Approach travel distance (ft)

Approach	Movement	Turn designation	Approach cruise speed (mph)	Exit Cruise Speed (mph)	Approach travel distance (ft)
EB	LT	Left	30	40	235
	TH	Through	30	45	235
	U-turn	Movement banned			
NB	LT	Left	40	30	1600
	TH	Through	40	40	1600
	RT	Right	40	45	1600
WB	TH	Through	45	30	1600
	RT	Right	45	40	1600
	U-turn	Movement banned			

Table 0.4: Volumes

Unit time for volumes (min)	Peak Flow Period (min)	Approach	Movement	LV	HV	PHF (%)	Vehicle Occupancy
60	15	EB	LT	267	1	93	1.2
			TH	1293	12	85	1.2
		NB	LT	189	5	77	1.2
			TH	117	2	85	1.2
			RT	212	1	81	1.2
		WB	TH	462	8	90	1.2
			RT	199	5	82	1.2

Table 0.5: Movement Data

Approach	Movement	LV queue space (ft)	HV queue space (ft)	Movement ID	Movement type	Sign control
EB	LT	25	45	5L	Normal	
	TH	25	45	2T	Normal	
NB	LT	25	45	3L	Normal	
	TH	25	45	8T	Normal	
	RT	25	45	8R	Slip lane (Unsig)	Give way/yield
WB	TH	25	45	6T	Normal	
	RT	25	45	6R	Slip lane (Unsig)	Give way/yield

Table 0.6: Gap-Acceptance Data

Approach	Movement	Minimum departures	Exiting flow effect (%)	Heavy vehicle equivalent
EB	LT	2.5	0	2
	TH	2.5	0	2
NB	LT	2.5	0	2
	TH	2.5	0	2
	RT	2.5	0	2
WB	TH	2.5	0	2
	RT	2.5	0	2

Winter Model of the West Roundabout

SIDRA inputs of the model were illustrated in Table 0.1 to Table 0.6. It is noted that the table names were the names of the input sections in SIDRA. In Table 0.1, the lane side (i.e., left, middle, right) in an entry/exit is defined along the direction which vehicles traveled forward.

Table 0.1: Approach & Lanes

Approach	Lane	Entry/Exit	Lane discipline	Lane type	Lane width (ft)	Lane length (ft)	Grade (%)	Median (ft)	Short lane
NB	Left	Exit			13.12	1600	3	0	
	Right	Exit			13.12				
WB	Left	Entry	Left/Through	Normal	11.808	235	-0.534	6	
	Right	Entry	Through	Normal	7.872				
	Left	Exit			11.808	235	0.534		
	Right	Exit			7.872				
SB	Left	Entry	Left	Normal	11.152	1600	-2.5	0	None
	Middle	Entry	Left/Through	Normal	10.824				
	Right	Slip Entry	Right	Slip	13.12	192			
EB	Left	Entry	Through	Normal	13.448	1600	0.534	11	
	Middle	Entry	Through	Normal	16.728				
	Right	Slip Entry	Right	Slip	13.12	149			
	Left	Exit			9.84	1600	-0.534		
	Right	Exit			9.84				

Table 0.2: Roundabout

Variable name	Value
Central island diameter (ft)	72
Circulating lane width (ft)	36
Number of circulating lanes	2
Extra bunching (%)	0
Environmental factor	1.2
Entry/Circulating flow adjustment	Medium

Table 0.3: Definitions & Path Data

Approach	Movement	Turn designation	Approach cruise speed (mph)	Exit Cruise Speed (mph)	Approach travel distance (ft)
WB	LT	Left	30	40	235

Approach	Movement	Turn designation	Approach cruise speed (mph)	Exit Cruise Speed (mph)	Approach travel distance (ft)
	TH	Through	30	45	235
	U-turn	Movement banned			
SB	LT	Left	40	30	1600
	TH	Through	40	40	1600
	RT	Right	40	45	1600
EB	TH	Through	45	30	1600
	RT	Right	45	40	1600
	U-turn	Movement banned			

Table 0.4: Volumes

Unit time for volumes (min)	Peak Flow Period (min)	Approach	Movement	LV	HV	PHF (%)	Vehicle Occupancy
60	15	WB	LT	177	3	78	1.2
			TH	483	12	90	1.2
		SB	LT	635	5	83	1.2
			TH	137	6	79	1.2
			RT	110	2	78	1.2
		EB	TH	896	26	89	1.2
			RT	189	3	74	1.2

Table 0.5: Movement Data

Approach	Movement	LV queue space (ft)	HV queue space (ft)	Movement ID	Movement type	Sign control
WB	LT	25	45	1L	Normal	
	TH	25	45	6T	Normal	
SB	LT	25	45	7L	Normal	
	TH	25	45	4T	Normal	
	RT	25	45	4R	Slip lane (Unsig)	Give way/yield
EB	TH	25	45	2T	Normal	
	RT	25	45	2R	Slip lane (Unsig)	Give way/yield

Table 0.6: Gap-Acceptance Data

Approach	Movement	Minimum departures	Exiting flow effect (%)	Heavy vehicle equivalent
WB	LT	2.5	0	2
	TH	2.5	0	2
SB	LT	2.5	0	2
	TH	2.5	0	2
	RT	2.5	0	2
EB	TH	2.5	0	2
	RT	2.5	0	2

Summer Model of the East Roundabout

SIDRA inputs of the model were illustrated in Table 0.1 to Table 0.6. It is noted that the table names were the names of the input sections in SIDRA. In Table 0.1, the lane side (i.e., left, middle, right) in an entry/exit is defined along the direction which vehicles traveled forward.

Table 0.1: Approach & Lanes

Approach	Lane	Entry/Exit	Lane discipline	Lane type	Lane width (ft)	Lane length (ft)	Grade (%)	Median (ft)	Short lane
SB	Left	Exit			13.12	1600	2	0	None
	Right	Exit			13.12				
EB	Left	Entry	Left/Through	Normal	11.808	235	1.65	6	
	Right	Entry	Through	Normal	7.872				
	Left	Exit			11.808	235	-1.65		
	Right	Exit			7.872				
NB	Left	Entry	Left	Normal	11.152	1600	-1.5	0	
	Middle	Entry	Left/Through	Normal	10.824				
	Right	Slip Entry	Right	Slip	13.12	200			
WB	Left	Entry	Through	Normal	13.448	1600	-1.65	11	
	Middle	Entry	Through	Normal	17.056				
	Right	Slip Entry	Right	Slip	13.12	179			
	Left	Exit			13.12	1600	1.65		
	Right	Exit			13.448				

Table 0.2: Roundabout

Variable name	Value
Central island diameter (ft)	72
Circulating lane width (ft)	36
Number of circulating lanes	2
Extra bunching (%)	0
Environmental factor	1.2
Entry/Circulating flow adjustment	Medium

Table 0.3: Definitions & Path Data

Approach	Movement	Turn designation	Approach cruise speed (mph)	Exit Cruise Speed (mph)	Approach travel distance (ft)

Approach	Movement	Turn designation	Approach cruise speed (mph)	Exit Cruise Speed (mph)	Approach travel distance (ft)
EB	LT	Left	30	40	235
	TH	Through	30	45	235
	U-turn	Movement banned			
NB	LT	Left	40	30	1600
	TH	Through	40	40	1600
	RT	Right	40	45	1600
WB	TH	Through	45	30	1600
	RT	Right	45	40	1600
	U-turn	Movement banned			

Table 0.4: Volumes

Unit time for volumes (min)	Peak Flow Period (min)	Approach	Movement	LV	HV	PHF (%)	Vehicle Occupancy
60	15	EB	LT	301	5	85	1.2
			TH	1351	19	91	1.2
		NB	LT	233	3	80	1.2
			TH	106	2	71	1.2
			RT	194	8	84	1.2
		WB	TH	548	8	85	1.2
			RT	195	1	89	1.2

Table 0.5: Movement Data

Approach	Movement	LV queue space (ft)	HV queue space (ft)	Movement ID	Movement type	Sign control
EB	LT	25	45	5L	Normal	
	TH	25	45	2T	Normal	
NB	LT	25	45	3L	Normal	
	TH	25	45	8T	Normal	
	RT	25	45	8R	Slip lane (Unsig)	Give way/yield
WB	TH	25	45	6T	Normal	
	RT	25	45	6R	Slip lane (Unsig)	Give way/yield

Table 0.6: Gap-Acceptance Data

Approach	Movement	Minimum departures	Exiting flow effect (%)	Heavy vehicle equivalent
EB	LT	2.5	0	2
	TH	2.5	0	2
NB	LT	2.5	0	2
	TH	2.5	0	2
	RT	2.5	0	2
WB	TH	2.5	0	2
	RT	2.5	0	2

Summer Model of the West Roundabout

SIDRA inputs of the model were illustrated in Table 0.1 to Table 0.6. It is noted that the table names were the names of the input sections in SIDRA. In Table 0.1, the lane side (i.e., left, middle, right) in an entry/exit is defined along the direction which vehicles traveled forward.

Table 0.1: Approach & Lanes

Approach	Lane	Entry/Exit	Lane discipline	Lane type	Lane width (ft)	Lane length (ft)	Grade (%)	Median (ft)	Short lane
NB	Left	Exit			13.12	1600	3	0	None
	Right	Exit			13.12				
WB	Left	Entry	Left/Through	Normal	11.808	235	-0.534	6	
	Right	Entry	Through	Normal	7.872				
	Left	Exit			11.808	235	0.534		
	Right	Exit			7.872				
SB	Left	Entry	Left	Normal	11.152	1600	-2.5	0	
	Middle	Entry	Left/Through	Normal	10.824				
	Right	Slip Entry	Right	Slip	13.12	192			
EB	Left	Entry	Through	Normal	13.448	1600	0.534	11	
	Middle	Entry	Through	Normal	16.728				
	Right	Slip Entry	Right	Slip	13.12	149			
	Left	Exit			9.84	1600	-0.534		
	Right	Exit			9.84				

Table 0.2: Roundabout

Variable name	Value
Central island diameter (ft)	72
Circulating lane width (ft)	36
Number of circulating lanes	2
Extra bunching (%)	0
Environmental factor	1.2
Entry/Circulating flow adjustment	Medium

Table 0.3: Definitions & Path Data

Approach	Movement	Turn designation	Approach cruise speed (mph)	Exit Cruise Speed (mph)	Approach travel distance (ft)
WB	LT	Left	30	40	235
	TH	Through	30	45	235
	U-turn	Movement banned			
SB	LT	Left	40	30	1600
	TH	Through	40	40	1600
	RT	Right	40	45	1600
EB	TH	Through	45	30	1600
	RT	Right	45	40	1600
	U-turn	Movement banned			

Table 0.4: Volumes

Unit time for volumes (min)	Peak Flow Period (min)	Approach	Movement	LV	HV	PHF (%)	Vehicle Occupancy
60	15	WB	LT	209	8	72	1.2
			TH	576	5	89	1.2
		SB	LT	727	6	78	1.2
			TH	137	9	73	1.2
			RT	116	8	86	1.2
		EB	TH	947	19	88	1.2
			RT	214	3	72	1.2

Table 0.5: Movement Data

Approach	Movement	LV queue space (ft)	HV queue space (ft)	Movement ID	Movement type	Sign control
WB	LT	25	45	1L	Normal	
	TH	25	45	6T	Normal	
SB	LT	25	45	7L	Normal	
	TH	25	45	4T	Normal	
	RT	25	45	4R	Slip lane (Unsig)	Give way/yield
EB	TH	25	45	2T	Normal	
	RT	25	45	2R	Slip lane (Unsig)	Give way/yield

Table 0.6: Gap-Acceptance Data

Approach	Movement	Minimum departures	Exiting flow effect (%)	Heavy vehicle equivalent
WB	LT	2.5	0	2
	TH	2.5	0	2
SB	LT	2.5	0	2
	TH	2.5	0	2
	RT	2.5	0	2
EB	TH	2.5	0	2
	RT	2.5	0	2